Corresponding author: Zeno Levy
e-mail: zlevy@usgs.gov
ORCID: https://orcid.org/0000-0003-4580-2309

Decadal Trends in the Quality of Groundwater Used for Public Drinking-Water Supply in California, 2004–2023, California Groundwater Ambient Monitoring and Assessment Program, Priority Basin Project

By Zeno F. Levy[1] and Andrew L. Soldavini[2]

[1]U.S. Geological Survey, California Water Science Center, 6000 J Street, Placer Hall, Sacramento, California 95819, USA.

[2]U.S. Geological Survey, California Water Science Center, 4165 Spruance Road, San Diego, California 95101, USA.

Prepared in cooperation with California State Water Resources Control Board

A product of the California Groundwater Ambient Monitoring and Assessment (GAMA) Program

Acknowledgments

Funding for this work was provided by the California State Water Resources Control Board Groundwater Ambient Monitoring and Assessment Program and U.S. Geological Survey Cooperative Matching Funds.

We especially thank the site owners and water purveyors for their cooperation in allowing the U.S. Geological Survey to collect samples from their sites.

Outline

Figures

be found in Levy and Soldavini (2026). Data summarized from Levy and Soldavini (2026). MTBE, methyl *tert*-butyl ether.

Figure 8. Decadal increases (top) and decreases (bottom) of relative concentration (concentration change divided by constituent benchmark) for inorganic water-quality constituents with non-regulatory, aesthetic-based benchmarks. Benchmarks used to calculate relative concentration changes for respective constituents can be found in Levy and Soldavini (2026). Data summarized from Levy and Soldavini (2026). TDS, total dissolved solids.

Figure 9. Decadal increases (top) and decreases (bottom) of relative concentration (concentration change divided by constituent benchmark) for inorganic water-quality constituents with non-regulatory, health-based benchmarks. Data summarized from Levy and Soldavini (2026).

Figure 10. Decadal increases (top) and decreases (bottom) for indicators of geochemical conditions. Data summarized from Levy and Soldavini (2026).

Figure 11. Decadal increases (top) and decreases (bottom) for indicators of groundwater source and age. Data summarized from Levy and Soldavini (2026). $\delta^{18}O$, oxygen-18.

Figure 12. Decadal increases (top) and decreases (bottom) for geochemical salinity indicators. Data summarized from Levy and Soldavini (2026). $\delta^{13}C$, carbon-13.

Figure 13. *A*, heatmap; and *B,* dendrogram of Spearman's correlations among decadal changes of focal water-quality constituents and geochemical indicators organized by hierarchical agglomerative clustering. Positive Spearman's rho values indicate direct correlation of decadal change values (constituents increasing or decreasing together) and negative Spearman's rho values indicate inverse correlation of change values (constituent concentrations changing in opposite directions). Black boxes in the heatmap (*A*) correspond to the two top-level cluster groups (split with maximum height value) defined in the dendrogram (*B*). Data summarized from Levy and Soldavini (2026). $\delta^{13}C$, carbon-13; $\delta^{18}O$, oxygen 18; d-excess, deuterium excess; DO, dissolved oxygen; TDS, total dissolved solids.

Figure 14. Panels showing significant (p-values less than 0.05) Spearman's correlations for censored differences of water-quality constituents to respective geochemical indicators. Positive Spearman's rho values indicate direct correlation of decadal change values (constituents increasing or decreasing together) and negative Spearman's rho values indicate inverse correlation of change values (constituent concentrations changing in opposite directions). Data summarized from Levy and Soldavini (2026). $\delta^{18}O$, oxygen 18; d-excess, deuterium excess; TDS, total dissolved solids.

Figure 15. Maps of California showing study sites that had significant decreases (top), significant increases (middle), and non-significant changes (bottom) for decadal comparisons of total dissolved solids (TDS). Change significance is indicated for initial and decadal concentration values with non-overlapping confidence intervals. Point sizes and colors are scaled to absolute and directional concentration changes, respectively. Directional differences ranged from -729 to 1818 milligrams per liter, but scales were symmetrically saturated at value of ±274 milligrams per liter to prevent outliers (less than 2 percent of change values statewide) from obscuring visualization of most change values. Data summarized from Levy and Soldavini (2026).

Figure 16. Count of sites with largest solute mass changes corresponding to significant total dissolved solids (TDS) increases and decreases for *A*, major cations; *B*, major anions; and *C*, major ion pairs. Data summarized from Levy and Soldavini (2026). Ca, calcium; K, potassium; Mg, magnesium; Na, sodium; Cl, chloride; HCO_3, bicarbonate; SO_4, sulfate.

Figure 17. Maps of California showing study sites that had significant decreases (top), significant increases (middle), and non-significant changes (bottom) for decadal comparisons of uranium (left) and alkalinity (right). Change significance is indicated for initial and decadal concentration values with non-overlapping confidence intervals. Point sizes and colors are scaled to absolute and directional concentration changes, respectively. Directional differences ranged from -40 to 93 micrograms per liter for

uranium and -145 to 100 milligrams per liter as calcium carbonate for alkalinity. Respective measurement scales for uranium and alkalinity were symmetrically saturated at values of ±16 micrograms per liter and ±75 milligrams per liter (as calcium carbonate) to prevent outliers (less than 2 percent of change values statewide) from obscuring visualization of most change values. Data summarized from Levy and Soldavini (2026).

Figure 18. Maps of California showing study sites that had significant decreases (top), significant increases (middle), and non-significant changes (bottom) for decadal comparisons of fluoride (left) and calcium (right). Change significance is indicated for initial and decadal concentration values with non-overlapping confidence intervals. Point sizes and colors are scaled to absolute and directional concentration changes, respectively. Directional differences ranged from -1.28 to 0.42 milligrams per liter for fluoride and -71 to 252 milligrams per liter for calcium. Respective measurement scales for fluoride and calcium were symmetrically saturated at values of ±0.44 milligrams per liter and ±48 milligrams per liter to prevent outliers (less than 2 percent of change values statewide) from obscuring visualization of most change values. Data summarized from Levy and Soldavini (2026).

Figure 19. Maps of California showing study sites that had significant decreases (top), significant increases (middle), and non-significant changes (bottom) for decadal comparisons of nitrate. Change significance is indicated for initial and decadal concentration values with non-overlapping confidence intervals. Point sizes and colors are scaled to absolute and directional concentration changes, respectively. Directional differences ranged from -5.2 to 28.5 milligrams per liter as nitrogen, but scales were symmetrically saturated at value of ±7 milligrams per liter as nitrogen to prevent outliers (less than 2 percent of change values statewide) from obscuring visualization of most change values. Data summarized from Levy and Soldavini (2026).

Figure 20. Maps of California showing study sites that had significant decreases (top), significant increases (middle), and non-significant changes (bottom) for decadal comparisons of arsenic. Change significance is indicated for initial and decadal concentration values with non-overlapping confidence intervals. Point sizes and colors are scaled to absolute and directional concentration changes, respectively. Directional differences ranged from -23 to 29 micrograms per liter, but scales were symmetrically saturated at value of ±14 micrograms per liter to prevent outliers (less than 2 percent of change values statewide) from obscuring visualization of most change values. Data summarized from Levy and Soldavini (2026).

Figure 21. Maps of California showing study sites that had significant decreases (top), significant increases (middle), and non-significant changes (bottom) for decadal comparisons of perchlorate. Change significance is indicated for initial and decadal concentration values with non-overlapping confidence intervals. Point sizes and colors are scaled to absolute and relative concentration changes, respectively. Directional differences ranged from -4.3 to 3.5 micrograms per liter, but scales were symmetrically saturated at value of ±2 micrograms per liter to prevent outliers (less than 2 percent of change values statewide) from obscuring visualization of most change values. Data summarized from Levy and Soldavini (2026).

Figure 22. Maps of California showing study sites that had significant decreases (top), significant increases (middle), and non-significant changes (bottom) for decadal comparisons of atrazine (left) and simazine (right). Change significance is indicated for initial and decadal concentration values with non-overlapping confidence intervals. Point sizes and colors are scaled to absolute and directional concentration changes, respectively. Directional differences ranged from -0.13 to 0.04 micrograms per liter for atrazine and -0.15 to 0.04 micrograms per liter for simazine. Respective measurement scales for both atrazine and simazine were symmetrically saturated at values of ±0.03 micrograms per liter to prevent outliers (less than 2 percent of change values statewide) from obscuring visualization of most change values. Data summarized from Levy and Soldavini (2026).

Tables

Conversion Factors

U.S. customary units to International System of Units

Multiply	By	To obtain
	Length	
foot (ft)	0.3048	meter (m)
mile (mi)	1.609	kilometer (km)
mile, nautical (nmi)	1.852	kilometer (km)
yard (yd)	0.9144	meter (m)

International System of Units to U.S. customary units

Multiply	By	To obtain
	Length	
centimeter (cm)	0.3937	inch (in.)
millimeter (mm)	0.03937	inch (in.)
meter (m)	3.281	foot (ft)
kilometer (km)	0.6214	mile (mi)
kilometer (km)	0.5400	mile, nautical (nmi)
meter (m)	1.094	yard (yd)
	Area	
square meter (m^2)	0.0002471	acre
hectare (ha)	2.471	acre
square hectometer (hm^2)	2.471	acre
square kilometer (km^2)	247.1	acre
square centimeter (cm^2)	0.001076	square foot (ft^2)
square meter (m^2)	10.76	square foot (ft^2)
square centimeter (cm^2)	0.1550	square inch (in^2)
square hectometer (hm^2)	0.003861	section (640 acres or 1 square mile)
hectare (ha)	0.003861	square mile (mi^2)
square kilometer (km^2)	0.3861	square mile (mi^2)
	Volume	
cubic meter (m^3)	6.290	barrel (petroleum, 1 barrel = 42 gal)
liter (L)	33.81402	ounce, fluid (fl. oz)
liter (L)	2.113	pint (pt)
liter (L)	1.057	quart (qt)
liter (L)	0.2642	gallon (gal)
cubic meter (m^3)	264.2	gallon (gal)
cubic decimeter (dm^3)	0.2642	gallon (gal)
cubic meter (m^3)	0.0002642	million gallons (Mgal)
cubic kilometer (km^3)	264.2	billion gallons (Ggal)
cubic centimeter (cm^3)	0.06102	cubic inch (in^3)
cubic decimeter (dm^3)	61.02	cubic inch (in^3)
liter (L)	61.02	cubic inch (in^3)
cubic decimeter (dm^3)	0.03531	cubic foot (ft^3)
cubic meter (m^3)	35.31	cubic foot (ft^3)
cubic meter (m^3)	1.308	cubic yard (yd^3)
cubic kilometer (km^3)	0.2399	cubic mile (mi^3)
cubic meter (m^3)	0.0008107	acre-foot (acre-ft)
cubic hectometer (hm^3)	810.7	acre-foot (acre-ft)
	Mass	

Multiply	By	To obtain
gram (g)	0.03527	ounce, avoirdupois (oz)
kilogram (kg)	2.205	pound avoirdupois (lb)
metric ton (t)	1.102	ton, short [2,000 lb]
metric ton (t)	0.9842	ton, long [2,240 lb]

Temperature in degrees Celsius (°C) may be converted to degrees Fahrenheit (°F) as follows:

°F = (1.8 × °C) + 32.

Temperature in degrees Fahrenheit (°F) may be converted to degrees Celsius (°C) as follows:

°C = (°F – 32) / 1.8.

Datums

Vertical coordinate information is referenced to the North American Vertical Datum of 1988 (NAVD 88).

Horizontal coordinate information is referenced to the North American Datum of 1983 (NAD 83).

Altitude, as used in this report, refers to distance above the vertical datum.

Supplemental Information

Results for measurements of stable isotopes of an element (with symbol E) in water, solids, and dissolved constituents commonly are expressed as the relative difference in the ratio of the number of the less abundant isotope (iE) to the number of the more abundant isotope of a sample with respect to a measurement standard.

Abbreviations

$\delta^{2}H$	Deuterium
$\delta^{13}C$	Carbon-13
$\delta^{18}O$	Oxygen-18

1,2,3-TCP	1,2,3-trichloropropane
d-excess	Deuterium excess
CI	Confidence interval
CIAT	2-Chloro-4-isopropylamino-6-amino-s-triazine
CONUS	Conterminous United States
DBCP	1,2-dibromo-3-chloropropane
DDW	Division of Drinking Water
DIC	Dissolved inorganic carbon
DO	Dissolved oxygen
DPR	California Department of Pesticide Regulation
GAMA-PBP	Groundwater Ambient Monitoring and Assessment Priority Basin Project
HBB	Health-based benchmarks\
LUFTs	Leaking underground fuel tanks
MCL	Maximum contaminant level
MDL	Method detection level
MTBE	Methyl *tert*-butyl ether
NAD 83	North American Datum of 1983
NAVD 88	North American Vertical Datum of 1988
NAWQA	National Water Quality Assessment
NWQL	National Water Quality Laboratory
PCE	Tetrachloroethene
pM	Percent modern
pmC	Percent modern carbon

PMZ	Pesticide management zone
PSW	Public supply well
RL	Reporting level
SD	Standard deviation
SDWA	Safe Drinking Water Act
SMCL	Secondary maximum contaminant level
SRL	Study reporting level
SWRCB	California State Water Resources Control Board
TCE	Trichloroethene
TDS	Total dissolved solids
USEPA	U.S. Environmental Protection Agency
USGS	U.S. Geological Survey
VOC	Volatile organic compound
VPDB	Vienna Pee Dee Belemnite
VSMOW	Vienna Standard Mean Ocean Water

Abstract

This study provides a comprehensive assessment of decadal changes in the quality of groundwater used for public drinking-water supply at 444 monitoring sites across California during 2004–2023. We assessed decadal step trends in groundwater quality for 145 water-quality constituents and geochemical indicators statewide and across geographic and land-use based network groups. We evaluated the statistical significance of directional changes (predominant

increase or decrease of constituent concentrations) and the magnitude of those changes across all network groups.

Uranium showed the most widespread directional and high-magnitude increases of all constituents with regulatory benchmarks statewide, particularly in the agriculture-dominated Central Valley as well as urban- and desert-dominated regions of Southern California. Fluoride and perchlorate showed the most widespread directional and high-magnitude decreases of all constituents with regulatory benchmarks statewide, which were also most pronounced in Southern California. Although arsenic and nitrate did not often register significant directional changes across network groups, they showed widespread, high-magnitude changes in both directions (increase and decrease) at levels often exceeding 10 percent of respective regulatory benchmarks statewide. Triazine herbicides (atrazine and simazine) and the gasoline oxygenate methyl *tert*-butyl ether (MTBE) showed significant directional decreases statewide, but not at levels considered to be of high magnitude compared to respective regulatory benchmarks.

We observed significant directional and high-magnitude increases of total dissolved solids (TDS) statewide, which were most pronounced in agricultural areas. Analysis of explanatory geochemical indicators indicated that prevalent statewide increases of alkalinity and calcium were the predominant components of the observed statewide increases in TDS by mass. Widespread increases in groundwater alkalinity and calcium across agricultural and urban areas may be related, in part, to warm-season irrigation and other anthropogenic factors that have shifted soil weathering dynamics over the long term. Increasing alkalinity concentrations were related to increasing uranium concentrations, particularly in areas with aquifer materials derived from granitic rocks. Conversely, increasing calcium concentrations were related to decreasing fluoride concentrations, particularly in areas where fluoride occurred naturally at elevated

concentrations. Decrease of perchlorate, triazine herbicides, and MTBE are likely related to decreased anthropogenic source inputs over time and natural attenuation in aquifers.

Introduction

Approximately 144 million people in the conterminous United States (CONUS) utilize groundwater resources for drinking-water supply, of which about three-quarters are served by public water systems and one-quarter are self-supplied from domestic wells (Johnson and others, 2019, 2022). Public water systems are defined under the U.S. Safe Drinking Water Act (SDWA) as providers of water for human consumption through pipes or other constructed conveyances that have 15 or more service connections or regularly serve at least 25 individuals for 60 or more days of the year (42 U.S. Code § 300f; California Health and Safety Code §116275h). As such, these systems serve diverse populations at varied scales and include: Community Water Systems (that serve, for example, municipalities and trailer parks), Non-Transient Non-Community Water Systems (that serve, for example, schools and factories), and Transient Non-Community Water Systems (that serve, for example, gas stations and campgrounds). Public water systems that utilize groundwater resources may include one or more public-supply wells (PSWs), which, by definition, serve larger populations than domestic-supply wells and tend to penetrate deeper into aquifers, have longer screened intervals, and pump continuously for greater periods (Degnan and others, 2021).

Regulatory compliance monitoring is required for public water systems under the SDWA to ensure the quality of drinking-water meets health-based Federal and State standards (42 U.S. Code § 300f). This monitoring primarily targets regulated water-quality constituents measured

from drinking-supply distribution systems before delivery to end users and is not designed to holistically characterize the quality of groundwater residing in the aquifers from which supplies are sourced. In contrast, natural resource assessments are designed to characterize the quality of groundwater residing in aquifers at broad spatial and temporal scales and can be used by stakeholders for decision support and planning purposes (Hirsch and others, 1988).

Natural resource assessments of groundwater quality can be broadly subdivided into "status" and "trends" assessments (National Research Council, 2012). Status assessments provide synoptic snapshots of groundwater-resource quality in space (Belitz and others, 2022) whereas trend assessments quantify changes of groundwater quality and associated drivers over time (Lindsey and others, 2023). Geostatistical methods can be used to assess the status of groundwater quality across different aquifer areas and depth zones (Belitz and others, 2010, 2015, 2022). Further, such status assessments may be expanded using statistical models leveraging explanatory factors such as land use, climate, and geology to understand and predict groundwater quality at broad spatial scales (Lombard and others, 2021; Ransom and others, 2021; Tokranov and others, 2024). However, groundwater-quality trends can be harder to quantify, understand, and predict because changes to aquifers usually lag those at the land surface and occur over broad and varied timescales (Broers and others, 2009; Jurgens and others, 2020). Lindsey and others (2023) identified four major obstacles to interpretation of regional-scale groundwater-quality trends data, including: (1) uncertainty in timing, mass, and location of contaminant sources; (2) variability in transit times of recharge to drinking-supply wells; (3) geochemical conditions in aquifers that affect contaminant transport; and (4) variability in hydrologic conditions.

A variety of methodological and statistical approaches have been used to detect and characterize trends in groundwater quality (Loftis, 1996; Broers and others, 2009; Visser and others, 2009). Commonly used statistical approaches to detect changes in groundwater quality are often performed at the site or network scale. Site-scale approaches have used non-parametric statistical tests (for example, the Mann-Kendall test) on time-series data, which can be used to detect monotonic trends as well as seasonal trends and trend reversals (Jurgens and others, 2020). However, these approaches necessitate repeated measurements at regular frequencies over periods of interest, which may not be feasible for regional assessments on decadal timescales. Network-scale approaches can be used to detect prevalent trends among groups of wells, which can incorporate multiple time-series (for example, the regional Kendall test; Helsel and Frans, 2006) or sets of paired samples taken decades apart from sites composing monitoring networks (herein, "step trends;" Lindsey and others, 2023). Alternatively, analysis of network-scale step trends can be used to identify prevalent regional trends without the need for detailed time-series data, but may not be able to quantify complex dynamics, such as trend reversals, or highlight groups of wells where high-magnitude water-quality changes co-occur in opposite directions (Lindsey and Rupert, 2012).

The U.S. Geological Survey (USGS) has made status and trends assessments of groundwater-resource quality on local, regional, and national scales, most notably through the approximately 30-year long (1991–2021) National Water Quality Assessment Project (NAWQA; Hirsch and others, 1988; National Research Council, 2012). Belitz and others (2022) used NAWQA results to assess the status of groundwater resources used for public supply across the CONUS and found that geogenic constituents (derived from aquifer materials; for example, arsenic and fluoride) were more prevalent at elevated concentrations compared to anthropogenic

constituents (derived from human activities; for example, nitrate and volatile organic compounds [VOCs]). Lindsey and others (2023) summarized 30 years of NAWQA trend studies to show that significant increases of sodium, chloride, sulfate, total dissolved solids (TDS), and nitrate were more commonly observed compared to other assessed constituents for regional groundwater-quality monitoring networks across the CONUS.

California is the most populous state in the U.S. with an estimated 39.5 million residents as of 2025 (California Department of Finance, 2025), about 40 percent of whom have historically depended on groundwater-sourced public systems for drinking supply (Johnson and others, 2022). During 2004–2012 the USGS, in cooperation with the California State Water Resources Control Board (SWRCB), assessed the status of groundwater resources used for public drinking-water supply statewide as part of the Groundwater Ambient Monitoring and Assessment Priority Basin Project (GAMA-PBP). This comprehensive assessment used a spatially stratified study design (Belitz and others, 2010) to target sampling of more than 2,000 PSWs distributed across 95 percent of the aquifer area used for public drinking-water supply statewide (Belitz and others, 2015). Status assessment results presented by Belitz and others (2015) were somewhat similar to the nationwide NAWQA assessment in that geogenic constituents tended to be more prevalent than anthropogenic constituents on the basis of both aquifer area and affected population. Approximately 20 percent of the initial status assessment wells have been monitored for trends since the initial sampling on about 5-year return intervals during 2004–2023.

Several studies of PSW trends have been made in California, primarily using USGS data (NAWQA, GAMA-PBP, and other studies) and regulatory monitoring data compiled by the SWRCB Division of Drinking Water (DDW) for compliance under the SDWA. Jurgens and others (2020) applied monotonic trend analysis to the combined DDW and GAMA-PBP data for

PSWs throughout the state and found recent trends (2000–2014) were most often detected for nitrate, TDS, uranium, and arsenic. Of these constituents, nitrate, TDS, and uranium had predominantly increasing trends and arsenic had predominantly decreasing trends. Harkness and Jurgens (2022) extended this analysis to show predominantly decreasing fluoride trends detected statewide were driven by increasing groundwater salinity in more arid regions of the state that receive managed recharge. Kent and Landon (2016) used an initial 3-year resampling of a portion of the GAMA-PBP's PSW trends network to show short-term increases in alkalinity and other salinity indicators across the state. Other regional trend studies have found predominantly increasing nitrate, TDS, and uranium trends as well as decreasing pesticide and arsenic trends in the San Joaquin Valley and other areas of the state where groundwater systems have been affected by decades to centuries of intensive, irrigated agriculture (Burow and others, 2008, 2013; Kent and Landon, 2013; Troiano and others, 2013; Hansen and others, 2018; Rosen and others, 2019; Haugen and others, 2021).

Although Jurgens and others (2020) assessed and aggregated site-scale trends for a large proportion of active PSWs across California, that analysis was limited to inorganic constituents for which regulatory monitoring data were available. In contrast, the GAMA-PBP's PSW trends network, though more limited with respect to the number of wells assessed, included comprehensive and consistent analyses of both inorganic and organic water-quality constituents as well as geochemical indicators of groundwater conditions, age, and recharge sources. Further, the GAMA-PBP measures many water-quality constituents, particularly anthropogenic organic compounds, at levels well below their regulatory thresholds and can therefore detect trends at low concentrations before they reach levels of concern for human health and safety (Belitz and others, 2015). Although portions of the GAMA-PBP's PSW trends monitoring results have been

reported in previous studies (Kent and Landon, 2016; Kent 2018) there has not yet been a comprehensive capstone assessment of decadal step trends encompassing the entirety of the monitoring network (more than 440 sites) across the nearly 20-year sampling program (2004–2023).

Purpose and Scope

This report provides a capstone assessment of decadal changes in the GAMA-PBP's PSW trends network (herein, "trends network") across its nearly 20-year sampling program (2004–2023). Here, the term "decadal changes" is used to broadly characterize differences between constituent concentrations for a selected "initial" sample and "trend" re-sample for wells in the trends network. Selection of sample pairs to represent decadal changes at individual study sites were prioritized so that aggregate return periods across the trends network averaged about 10 years. Both the direction and magnitude of water-quality changes at 444 PSWs statewide were assessed in this report by analysis of decadal step trends for paired samples across varied geographic or land-use based subdivisions of the trends network (herein, "network groups").

Water-quality constituents with regulatory maximum contaminant levels (MCLs; n = 48) were the primary focus of this study, but results for constituents with non-regulatory, health-based benchmarks (HBBs; n = 56) and aesthetic-based, secondary maximum contaminant levels (SMCLs; n = 6) are also presented (refer to Levy and Soldavini [2026] for further explanation of benchmark attribution for this study). Step-trend analyses for water-quality constituents without benchmarks (n = 35) were not a focus of this report but were selectively referenced as needed and included in a companion data release for informational purposes (Levy and Soldavini, 2026).

Results for select geochemical indicators and their correlations to water-quality constituents were also evaluated to assess broad drivers of changes with statewide prevalence.

The GAMA-PBP's PSW trends network represents a resampling of about 20-percent of the original status assessment wells. Therefore, study-area groupings from the initial study based on local physiographic subdivisions are sparsely represented by the trends-monitoring network and are aggregated at the scale of the ten major hydrogeologic provinces of California as defined by Johnson and Belitz (2003). These provinces were further aggregated into eight geographically distinct "province groups" for the purposes of the current study (discussed further in the "Study Region" section of this report). Such broad physiographic groupings are intended to help highlight geographies where observed trends are most pronounced and are presented to help focus future work. However, it is out of the scope of this report to understand drivers of trends in individual provinces, which likely necessitate more detailed local studies. Additionally, we assessed step trends on subdivisions of the overall network based on a simplified three-category classification of land uses surrounding study sites (agricultural, urban, natural). Although land-use classes span a large array of hydrogeologic settings statewide, they were assessed to determine whether constituents with significant statewide changes were driven by broad surficial processes affecting recharge quantity and quality. In total, trends are assessed in this study: (1) across the entire statewide trends network, (2) across eight province groups that represent geographically distinct subdivisions of the trends network, and (3) across three land-use groups that represent geographically overlapping subdivisions of the trends network.

Step trends were assessed for each constituent with greater than 300 paired samples across the statewide network because constituents represented by fewer sites had sparse and uneven spatial distribution across parts of the state originally characterized in the status

assessment presented by Belitz and others (2015). In this report, we highlight results of step trends for constituents that showed significant directional or high-magnitude changes statewide or within individual network groups. Directional changes indicate groupings of wells where a constituent shows a statistically significant increase or decrease based on median differences among paired samples. Directional changes are useful to assess water-quality trends at the scale of an entire monitoring network or network group (Lindsey and others, 2023). However, persistent directional changes of small magnitude may have lesser effects on the overall quality of the resource (Lindsey and Rupert, 2012). Therefore, we also present a novel approach for network-scale detection of "high-magnitude" changes in water quality. A monitoring network with large proportions of countervailing water-quality changes (in other words, some sites showing increasing concentrations and some sites showing decreasing concentrations) may not show a significant directional change as a whole, but results may indicate if prevalent high-magnitude increases or decreases of potential contaminants are observed. Water-quality constituents showing both directional and high-magnitude changes are most likely to have widespread effects on drinking-water resource quality at the network scale.

We used the above approach to further highlight "focal" water-quality constituents that showed either directional or high-magnitude changes statewide. Correlation analysis, dynamics of geochemical indicators, and additional discussion are provided to identify factors affecting changes in concentrations for focal water-quality constituents with regulatory benchmarks. Discussion of potential factors affecting constituents showing widespread changes across the statewide network is intended to characterize broad drivers across a wide array of hydrogeologic settings and land-use types and may vary from interpretations of local-scale studies.

Methods

This section details study methods related to: (1) the study region, (2) the constituents evaluated, (3) site and sample selection, (4) quality-control evaluation, (5) the computation of change thresholds used to determine significant difference between paired samples, (6) the evaluation of geochemical indicators, (7) the statistical evaluation of decadal water-quality changes, and (8) the correlation analysis.

Study Region

The study region for this comprehensive assessment of PSW trends across California covers a diverse array of physiographic and land-use settings. Belitz and others (2015) presented the design for the status assessment from which the current trends study is based, which covered over 95 percent of the aquifer area used for public drinking-water supply in California. The area evaluated for this trends assessment is the same as that of the initial status assessment (Belitz and others, 2015), but with a lower density of sites. A total of 444 sites had sufficient samples for step-trend analysis of at least one of the assessed water-quality constituents; however, many of the selected constituents did not have sufficient data for decadal comparison at all 444 sites (refer to "Site and Sample Selection" section for further details). The 444 sites were subsequently classified by province and land-use groups.

Hydrogeologic provinces are large regions that share similar geologic and climate characteristics. Johnson and Belitz (2003) presented delineations for major hydrogeologic provinces of California. These delineations were further adapted to summarize status assessment results by Belitz and others (2015), which included grouping some provinces with low site densities. The current study retains the province groupings of Belitz and others (2015) but further

aggregates two of the provinces—the Transverse and Selected Peninsular Ranges and the San Diego Drainages— into the Southwestern California province group (P5; fig. 1). This is due to the low density of sites in the San Diego Drainages and is consistent with the Southern California hydrogeologic zone presented by Kent and Landon (2016).

Figure 1. *A*, Map of California showing location of study sites attributed by province groups modified from the hydrogeologic provinces of California presented by Johnson and Belitz (2003); and *B*, bar plot showing number of study sites by province group. Data summarized from Levy and Soldavini (2026). CONUS, conterminous United States.

Resultant province groups were used to classify study sites and encompass a wide variety of climatic conditions, geologies, and land uses (figs. 1 and 2). California spans a large aridity gradient, with Northern California, coastal, and higher elevation mountain regions ranging from humid to wet and Southern California as well as low-lying valley and desert regions ranging from semi-arid to hyper-arid (Fram and Belitz, 2011). The assessed area includes relatively undeveloped highlands with hard-rock aquifers (for example, Klamath Mountains) to lower-lying, alluvial-filled basins that support more urban and agricultural land uses (for example, San Joaquin Valley). The assessed PSWs have broad screened or open interval lengths (median and interquartile range of 200 feet [ft] and 100–350 ft, respectively) and tended to be finished in the top 1000 ft of unconsolidated alluvial sediments or fractured hard-rock aquifers (app. 1; fig. 1.1; Levy and Soldavini, 2026).

Figure 2. *A*, Map of California showing predominant land use (urban, agricultural, or natural) from the 2011 National Land Cover Database (Jin and others, 2013) with associated classifications for study sites based on mapped land use within respective 500-meter radius buffer areas (agricultural land-use class equates to greater than 20 percent agricultural land use in buffer area, urban land-use class equates to

greater than 20 percent urban land use and less than or equal to 20 percent agricultural land use in buffer area, and natural land-use class equates to less than or equal to 20 percent of both agricultural and urban land uses in buffer area); *B*, ternary plot showing proportion of land use in 500-meter buffer areas around study sites with associated land-use classifications and median land-use proportions for sites in respective province groups; and *C*, bar plots showing proportion of study sites in province groups and statewide having respective land-use classifications. Data summarized from Levy and Soldavini (2026).

The Southwestern California province group (P5) is the most densely populated province group with the highest degree of urban land use and most sites in this study (107 sites equivalent to 24 percent of total; figs. 1 and 2). The Southern Coast Ranges (P8) extends northward along the Pacific coast from Southwestern California (P5) through the San Jose and San Francisco metropolitan areas. Taken together, province groups P5 and P8 encompass the majority of the State's population reliant on groundwater from public-supply systems (Belitz and others, 2015). California's Central Valley, a highly productive agricultural belt (Faunt, 2009), is divided into the Sacramento Valley and San Joaquin Valley province groups (P4 and P7, respectively; collectively 107 sites equivalent to 26 percent of total). These province groups are dominated by agricultural land use, with some major urban centers (figs. 1, 2). The Sacramento Valley (P4) has slightly wetter climate and finer grained sediments compared to the San Joaquin Valley (P7), which affects the mobility of some contaminants to groundwater (Faunt, 2009; Burow and others, 2013). The remaining province groups, the combined "Desert" and "Basin and Range" provinces (P1; herein referred to as "Desert, Basin and Range"), the combined "Klamath Mountains" and "Cascades and Modoc Plateau" provinces (P2; herein referred to as "Northern Mountain Regions"), and Northern Coast Ranges (P3) have comparatively lower populations and

greater proportions of natural land use (figs. 1 and 2). The P1 and P5 province groups are herein referred to collectively as the "Southern California" region.

We used a three-class categorization based on the 2011 National Land Cover Database to classify land use at each study site as either agricultural, natural, or urban (Jin and others, 2013). We used the 2011 dataset to broadly represent average land use during the period of study (2004–2023), understanding groundwater quality is often a function of historic land uses (Bastanti and Harter, 2019; Lindsey and others, 2023). Proportions of the three land-use classes were computed within a 500-meter buffer around each study site, which has been shown to adequately represent the contributing area around wells in regional groundwater-quality studies (Johnson and Belitz, 2009). A land-use class was attributed to each well based on the relative proportions of each land-use type within the buffer area (Levy and Soldavini, 2026). If more than 20 percent of land use within the buffer was agricultural, it was classified as agricultural. If a site was not classified as agricultural but had more than 20 percent urban land use within the buffer, it was classified as urban. All remaining study sites were classified as natural (fig. 2*B*). These conditional thresholds were applied to help identify and isolate sites potentially affected by proximal agriculture that would not be captured by majority land-use based classification systems (Jurgens and others, 2010), as most of the PSWs assessed in this study are in areas with at least some urban land use (for example, roads) but fewer occur in areas with any agricultural land use. This resulted in most study sites being classified as urban (47 percent) with roughly equivalent proportions classified as agricultural (26 percent) and natural (27 percent; fig. 2*C*). The classification system for individual wells reflected the areal prevalence of the different land cover types in respective provinces, with the highly developed Southwestern California province group (P5) having a high proportion of sites classified as urban (71 percent) and the heavily

farmed San Joaquin Valley (P7) having a high proportion of sites classified as agricultural (61 percent; fig. 2).

Constituents Evaluated

The GAMA-PBP samples groundwater for a comprehensive suite of inorganic constituents (major, minor, and trace elements), nutrients, organic constituents (VOCs and pesticides constituents, which include pesticides and pesticide degradates) and geochemical indicators (field measurements, stable and radioactive isotopes). The GAMA-PBP collects additional quality control samples (field replicates and field blanks) at a rate of approximately 10 percent (U.S. Geological Survey, variously dated). All constituents on the recent GAMA-PBP analyte lists (Balkan and others, 2021) were considered as potential candidates for assessment. Sampling protocols have remained relatively consistent over the 20-year project lifetime following methods described in the USGS National Field Manual (U.S. Geological Survey, variously dated) with modifications detailed by Shelton and Fram (2017) and Burow and others (2024). The GAMA-PBP's protocol targets sampling of raw, untreated groundwater. Therefore, sample-points were selected to be as close to the wellhead as possible to avoid prolonged contact of pumped groundwater with distribution systems. Analyses have mostly been made at the USGS National Water Quality Laboratory (NWQL) and other USGS facilities that specialize in isotopic analyses. Some select constituents (for example, 1,2,3-trichloropropane [1,2,3-TCP], perchlorate) were measured at contract laboratories at times during the period of study. Method and laboratory codes for all analyses presented in this report are publicly available in a data release (Levy and Soldavini, 2026).

Only analytes with at least one decadal-scale sample pair (closest resample to a 10-year time lapse from the initial sample within a 7-to-15.5-year window) at more than 300 unique

study sites were considered for trends assessment. The trace elements aluminum, copper, lead, nickel, and zinc are not considered in this report due to prevalence in field and laboratory blank data at low concentrations, perhaps due to their presence in metal fittings and other materials used in sampling and analysis (Bennett, 2020). These elements tend to be poorly soluble in groundwater aquifers (Hem, 1985) and, although typically measured in this study at levels well below benchmark concentrations, the presence of low-level detections related to sample collection and handling could potentially result in spurious trend detections. The inorganic trace element thallium is not considered in this report due to its extremely low detection frequency in GAMA-PBP samples. The VOC 1,2,4-trimethylbenzene is not considered in this report due to prevalence in field blanks during an earlier stage of the GAMA-PBP (Fram and others, 2012), which limited a robust decadal assessment of trends for this constituent.

A total of 137 water-quality constituents and 8 additional geochemical indicators were evaluated in this assessment based on the criteria detailed above (Levy and Soldavini, 2026). Of the considered water-quality constituents, 35 percent have a regulatory MCL (set by either the U.S. Environmental Protection Agency [USEPA] or the State of California), 4 percent have an SMCL, 41 percent have an HBB (for example, USEPA health advisory level, California response level, or others), and 20 percent have no benchmark (table 1). Benchmarks were selected based on a prioritization framework used in prior GAMA-PBP studies (Balkan and others, 2021) and are compiled in the data release of Levy and Soldavini (2026).

Table 1. Summary of water-quality constituents by class and benchmark type used to assess decadal trends in the quality of groundwater used for public drinking-water supply in California, 2004–2023.

Many of the organic constituents assessed by the GAMA-PBP are sparsely or not-detected in groundwater sampled by the project. Step-trend analysis was only performed on

organic constituents that were detected in greater than 10 percent of samples at either statewide or province-group scales in either the sets of initial trend samples or decadal resamples. Of the 104 organic constituents considered for assessment only 14 (13 percent) were detected at frequencies greater than the 10 percent screening threshold (table 1). Results of detection-frequency screening for organic constituents are compiled in the data release of Levy and Soldavini (2026).

Site and Sample Selection

A total of 2,007 PSW were initially sampled for the GAMA-PBP's public-supply aquifer status assessment using a spatially stratified study design, which was accomplished by subdividing component study areas into equal-area grids (Scott, 1990) with the goal of randomly sampling one PSW per grid cell (Belitz and others, 2015). The trend sampling program built off this initial status assessment network, with the original goal of resampling a random 10 percent of the status network every three years. This initial re-sampling target subsequently shifted to 20 percent of the original status network every five years after completion of the first triennial (three-year return) sampling (Kent and Landon, 2016; Kent, 2018). Trend sites were randomly selected from the pool of original status assessment wells from which permission to re-sample could be obtained. Additional site-selection protocols were designed to maintain even spatial coverage across original study areas and prioritize wells that had been sampled previously for more complete suites of water-quality constituents and geochemical indicators (Kent and Landon, 2016; Kent, 2018). During the 20-year monitoring program, attrition of PSWs in the trends network occurred for various reasons (for example, wells being decommissioned). When trend-network PSWs were not available for resampling, an effort was made to select replacement wells that were sampled during the initial status assessment to maintain similar spatial coverage

and consistent resampling rates. Because analyte lists, trend sites, and resampling frequencies also shifted over the course of the program, network wells were sometimes sampled at different times for different constituents (Kent and Landon, 2016; Kent, 2018). Therefore, sites and samples were selected for the current study on a constituent-by-constituent basis.

For each constituent, we identified the earliest sample date for that constituent at each site in the trends network. Then, we identified the date of resampling for that constituent at each respective study site closest to a 10-year return period within a 7-to-15.5-year window. The reason for this broad window was to capture replacement sites or those that had variable analyte lists in the early years of the program. Most time lapses between initial and decadal samples were between 9 and 11 years for all assessed constituents (fig. 3; Levy and Soldavini, 2026). Analytes within one of three major classes (inorganic constituents, pesticide constituents, and VOCs) were often measured synchronously if included on the same analyte schedules (in other words, groups of constituents analyzed in tandem using similar analytical methods). To illustrate this, we contrast sample and site selection for TDS (an inorganic constituent), atrazine (a pesticide constituent), and methyl *tert*-butyl ether (MTBE; a VOC). Time series representing the initial and decadal sampling for each of these constituents illustrate some variability in the number and timing of paired samples for each (fig. 3). With some minor exceptions, constituents in each of these three classes were analyzed in tandem, with most inorganic constituents having 364 sample pairs, pesticide constituents having 399 sample pairs, and VOCs having 442 sample pairs (fig. 3). However, because of the variability in resampling timeframes, well attrition and replacement, and changing analyte schedules, a number of sites in the various province groups were not sampled or re-sampled concurrently. Therefore, step-trend comparisons presented in this study represent broad, decadal-scale changes in groundwater quality occurring across the

monitoring network over 20-years and should not be considered snapshots of two distinct "before and after" periods.

Figure 3. Time-series plots showing initial and decadal sample concentrations connected by tie lines (left) and histograms showing the elapsed time between initial and decadal samples (right) for *A*, total dissolved solids (TDS); *B*, atrazine; and *C*, methyl *tert*-butyl ether (MTBE). Non-detections are plotted at the higher assigned reporting level of the two paired samples. The y-axes for panels B and C are scaled logarithmically. Data summarized from Levy and Soldavini (2026).

We compared the distribution of sites with data for the three major constituent classes to those sampled for the initial status assessment (table 2). For each constituent class, the proportion of sites sampled in each province group closely tracked the proportions of the initial assessment. For example, P7 composed 16 percent of the 2,007 sites sampled for the initial status assessment and 16 to 17 percent of sites sampled for most inorganic constituents, pesticide constituents, and VOCs sampled in the trends assessment (table 2). Further, in aggregate, the number of sites sampled for most inorganic constituents, pesticide constituents, and VOCs ranged from 18 to 22 percent of all sites sampled for the initial status assessment, indicating the general re-sampling goal of 20 percent of the network was attained across the 20-year monitoring period (table 2). Detailed compilation of all sites and dates sampled per constituent are available in the data release of Levy and Soldavini (2026).

Table 2. Summary of sites used to assess the status of drinking-water quality in aquifers used for public drinking-water supply in California during 2004–2012 compared to those used to assess decadal trends during 2004–2023.

Some prioritizations were selectively applied to account for instances when multiple laboratories reported different analyses for the same constituent with the same sample date,

which are detailed in Levy and Soldavini (2026). Of note, 1,2,3-TCP was sometimes analyzed at different laboratories with contrasting reporting levels (RLs) for the same sampling event. In those cases, the analysis with the lower RL was prioritized for each unique site and date combination. Additionally, perchlorate was analyzed using different methods on unfiltered samples at the Montgomery Watson Harza Laboratories in Monrovia, California prior to October 2007 and on filtered samples by Weck Laboratories, Inc. in City of Industry, California, as of October 2007 (Kent and Landon, 2016). For perchlorate, decadal sample pairs with exclusively filtered samples were selected to represent the single change value for a given site when multiple samples using the different methods were available. This selection protocol prioritized methodological consistency when possible, without sacrificing data for the large portion of sites where only mixed method comparisons for perchlorate data were available (46 percent).

Quality-Control Evaluation and Assignment of Reporting Levels

Reporting levels were assigned to control for false positives, ambient low-level contamination occurring during sample handling and analysis, and variability in analytical methods across the 20-year study period. Results originally reported as detections with concentrations less than the assigned reporting levels were considered non-detections for the purposes of this report. The NWQL reports detections of organic constituents with concentrations less than method detection levels (MDLs) to avoid false negatives (Foreman and others, 2021). For this study, organic constituents were assigned RLs equivalent to respective MDLs and detections of organic constituents at concentrations below MDLs were reclassified to non-detections to avoid false positives (Fram and others, 2012; Fram and Stork, 2019). This protocol minimizes potential identification of spurious trends for organic constituents that are not often detected in groundwater samples.

The GAMA-PBP implements study reporting levels (SRLs), which are developed for different periods based on detections in field blanks (Bennett, 2020). The SRLs developed by Bennett (2020) for inorganic trace elements were applied to all analyses in this study, with the most recent SRL period extended through to the end of the study period. All analyses below a given SRL are considered non-detections at some value less than the measured concentration (Kent, 2018). An SRL of 0.1 micrograms per liter (the maximum laboratory reporting level during the study period) was applied to all carbon disulfide analyses due to potential contamination from protective nitrile gloves used by field and lab personnel (Fram and others, 2012). The remaining organics selected for evaluation did not have sufficient detections in field blanks to warrant application of SRLs.

Because method-based RLs and blank-based SRLs changed over the course of the 20-year study period, the maximum effective RL of a given sample pair was assigned to both samples for each respective constituent following methods described by Kent (2018). Therefore, if an initial sample had a detection at a value less than the RL of a non-detection in the decadal sample, a change in concentrations could not be assumed and the detection was considered a non-detection at the higher of the two RLs. This method conservatively controls for concentration changes that can reasonably be inferred on paired samples considering expected variations in sample collection and analysis across the broad study period.

Determination of Change Thresholds Using Field Replicates

Variability in sample collection and analytical performance (herein, sampling error) may cause fluctuations in constituent concentrations during sampling that are unrelated to meaningful decadal changes in water quality. Sampling error tends to scale with constituent concentrations, with higher values showing greater variability between paired field replicates (in other words,

two samples collected sequentially at the same site under the same conditions; Mueller and others, 2015). Kent (2018) used a two-range model to estimate replicate variability for low- and high-concentration samples. However, the two-range model requires a subjective determination of the boundary between low- and high-concentration samples and may result in bias if many measurements occur around the boundary (Mueller and others, 2015).

Here, we implement the bias-corrected log-log regression model (herein, "log-log model") described by Mueller and others (2015) on a constituent-by-constituent basis using field replicate data collected by the GAMA-PBP during 2004–2024. The model uses linear regression to relate log-transformed means of replicate sample concentrations to their log-transformed standard deviations, effectively functioning as a lookup table to estimate variability expected from sampling error based on the measured concentration of a given sample. The terms of the model are as follows:

$$\log(SD) = B_0 + B_1 \log(C) \quad (1)$$

where

$\log(SD)$ is the logarithm (base 10) of replicate standard deviation,

B_0 is the intercept of the regression line, estimated by least squares,

B_1 is the slope of the regression line, estimated by least squares, and,

$\log(C)$ is the logarithm (base 10) of mean replicate concentration.

A bias correction factor (*bcf*) is used to back-transform predictions back to original concentration units using the Duan smearing estimate (Duan, 1983):

$$SD = bcf\{10^{[B_0 + B_1 \log(C)]}\} \quad (2)$$

where

bcf is the mean of the log-log regression model residuals.

We computed log-log regression models to assess replicate variability for each constituent evaluated for step trends in this study. We only computed replicate means for samples where water-quality constituents were detected in both samples following quality-control processing described in the prior section. Further, we only included replicate pairs where analyses yielded two unique values (identical values with standard deviations of zero were excluded from the log-log model by necessity). The latter consideration does inherently bias replicate variability upward, but identical values for replicate detections were uncommon and not expected to have a major effect on the analysis.

The log-log models were only generated for constituents having at least seven replicate pairs meeting these criteria. Linear regression models on replicate data were constructed using the lm function in the R "stats" package (R Core Team, 2024). Due to their relatively low detection frequencies in replicate data most of the 14 organic constituents evaluated for step trends had less than 60 replicate pairs, with a minimum of 9 replicate pairs for 1,1-dichloroethane and a maximum of 111 replicate pairs for chloroform. Most of the inorganic constituents had more than 200 replicate pairs, with a minimum of 9 replicate pairs for silver and a maximum of 374 replicate pairs for TDS (Levy and Soldavini, 2026). Examples of original and bias-corrected log-log models with replicate measurement data for TDS, atrazine, and MTBE are shown in fig. 4 and coefficients for all models are included in the data release of Levy and Soldavini (2026).

Figure 4. Mean versus standard deviation of replicate pairs with log-log models and bias-corrected log-log models (Mueller and others, 2015) for *A*, total dissolved solids (TDS); *B*, atrazine; and *C*, methyl *tert*-butyl ether (MTBE). Data summarized from Levy and Soldavini (2026).

We used the log-log models to generate 95 percent confidence intervals (CIs) for initial and decadal samples by substituting the *C* variable in eq. 2 with the measured sample concentration and solving for *SD*. The CIs were computed using the following equation:

$$CI = Result \pm Z_{(1-\alpha)} * SD \quad (3)$$

where

Result is the reported analytical result for the evaluated constituent, and

$Z_{(1-\alpha)}$ is the two-tailed z-score (1.96 for the 95 percent CI).

In this study, paired results for an initial and decadal sample collected at a single site were not considered to be significantly different if respective CIs overlapped.

Evaluation of Geochemical Indicators

This study utilizes additional geochemical indicators measured by the GAMA-PBP that are not routinely monitored for regulatory purposes to better understand drivers of observed water-quality changes. These indicators are grouped as: (1) indicators of geochemical conditions in aquifers (pH and dissolved oxygen [DO]), (2) indicators of groundwater source and age (oxygen-18 [$\delta^{18}O$], deuterium excess [d-excess], carbon-14, tritium), and (3) salinity indicators (TDS, calcium, alkalinity, carbon-13 [$\delta^{13}C$]). Isotopic measurements expressed in delta (δ) notation indicate a ratio of heavier to lighter isotopes in the sample with reference to a standard (app. 2). Site and sample selection to evaluate step trends for geochemical indicators was implemented as described above for water-quality constituents, with some additional

considerations for alkalinity (app. 3). Additionally, all water-quality constituents evaluated for step trends were appended with geochemical indicators measured during concurrent sampling events to evaluate correlations among change values (Levy and Soldavini, 2026; refer to "Correlation Analysis" section for further details).

The indictors pH and DO were measured in the field using a multi-parameter sonde and flow-through cell. Measurements were recorded as the well was purged by active pumping until stability criteria were reached (U.S. Geological Survey, variously dated). The pH and DO parameters represent master variables in aqueous geochemistry that can control speciation of constituents in aqueous phases and determine contaminant mobility in aquifers (Hem, 1985). Because the GAMA-PBP did not routinely collect replicate field measurements during the period of study, CIs for these constituents were computed using an estimated *SD* value of 0.1 (in standard units for pH and milligrams per liter for DO), representing the approximate precision of field measurement for both parameters (U.S. Geological Survey, variously dated).

Stable and radioactive isotopes can help identify the recharge sources and transit time in aquifers since recharge (herein, "age") of groundwater (Clark and Fritz, 1997). Stable isotopes of water ($\delta^{18}O$ and deuterium [$\delta^{2}H$]) are uniquely suited to trace sources of water as they are components of the water molecule itself. Stable isotopes of water can help to track changes in meteoric water sources and are sensitive to relative changes in the temperature and elevation of precipitation contributing to recharge (Clark and Fritz, 1997). Step-trend results are only presented for $\delta^{18}O$ (owing to its better analytical precision compared to $\delta^{2}H$) and d-excess, which is a linear transformation of $\delta^{18}O$ and $\delta^{2}H$ measurements that can indicate the extent to which source water has been affected by evaporation at the land surface or in soils prior to recharging groundwater systems (Clark and Fritz, 1997; app. 2). The log-log model is not appropriate for

isotopic constituents because they often have negative measurement scales that do not necessarily track with replicate variability. Therefore, we estimated *SD*s for $\delta^{18}O$ and d-excess as the average standard deviation of 395 replicate sample pairs (0.03 and 0.5 per mille, respectively; Levy and Soldavini, 2026).

Tritium and carbon-14 are radioactive isotopes that can be used to infer groundwater age. Both occur naturally in the atmosphere due to bombardment with naturally occurring cosmic rays and increased substantially during nuclear bomb testing in the early 1950s (Clark and Fritz, 1997). Due to its relatively short half-life (12.3 years), tritium is commonly used as a tracer of modern (post-1950s) groundwater recharge, whereas the longer-lived carbon-14 isotope (half-life of 5,730 years) can be used to date older groundwater with ages up to approximately 30,000 years (Clark and Fritz, 1997). Often, groundwater from a PSW is composed from a mixture of premodern and modern waters (Jurgens and others, 2022). Here, we do not use tritium in step-trend analysis because its short half-life and wide range of atmospheric values during nuclear testing make relative decadal changes harder to interpret in the context of assessing changes in groundwater age. Instead, we use tritium to attribute groundwater samples as premodern, mixed, or modern following the classification system of Lindsey and others (2019), which only requires site latitude, sample date, and measured tritium activity. We performed step-trend analysis on carbon-14 reported in units of percent modern carbon (pmC). Although carbon-14 is also affected by secular variations of atmospheric values that occurred during nuclear testing as well as dilution from radiocarbon-dead carbon sources in aquifers, increasing and decreasing values are often more broadly indicative of relatively younger and older groundwater sources, respectively (Zhang and others, 2024). Carbon-14 replicates showed greater variability at higher

activities and therefore a log-log model was developed to estimate sample *SD* based on 307 replicates as described in the previous section (Levy and Soldavini, 2026).

Groundwater TDS is a direct measure of the salinity of groundwater. In this study, TDS is evaluated as both a water-quality constituent with an SMCL and a geochemical indicator to determine what other water-quality constituents covary with changes in salinity. We also include calcium, one of the assessed water-quality constituents with no benchmark, as a salinity indicator as it has geochemical implications for mobility of key water-quality constituents such as fluoride and uranium. Alkalinity is operationally defined by titration as the acid neutralizing capacity of a groundwater sample and tends to be dominated in most groundwater by bicarbonate, a major component of TDS (Rounds and Wilde, 2012). We additionally included the isotope $\delta^{13}C$ in step-trend evaluations as it can provide information about the sources of dissolved inorganic carbon (DIC) in aquifers (app. 2). Similar to stable isotopes of water, we estimated sample *SD* for $\delta^{13}C$ using the average standard deviation of 279 replicate sample pairs (0.14 per mille; Levy and Soldavini, 2026).

Alkalinity is measured by titration of samples with a strong acid (Rounds and Wile, 2012). A portion of the GAMA-PBP samples have both field- and laboratory-measured alkalinities, whereas a larger proportion only have laboratory-measured alkalinities. Bennett and Fram (2014) found a small upward bias of laboratory compared to field alkalinities measured by the GAMA-PBP. Following the methods of Rosen and others (2019), we adjusted laboratory alkalinity measurements used to compute decadal changes to account for this bias using parameters derived from linear regression on 612 samples collected by the GAMA-PBP with both field- and laboratory-measured alkalinity values (app. 3; fig. 3.1; Levy and Soldavini, 2026). We developed log-log models using uncorrected values for 431 paired alkalinity

measurements made on field replicates either the field or laboratory (Levy and Soldavini, 2026). Alkalinity concentrations are expressed in units of milligrams per liter as calcium carbonate. Concentrations of bicarbonate expressed in units of milligrams per liter were estimated by dividing alkalinity concentrations by 0.8202 (Hem, 1985).

Statistical Evaluation of Decadal Changes

The following subsections detail statistical analyses used to evaluate step trends for decadal pairs of water-quality constituents and geochemical indicators compiled as described above. Evaluations of both directional and high-magnitude changes were made for each constituent statewide as well as for province and land-use based subdivisions (network groups). Results of statistical analyses are compiled in the data release of Levy and Soldavini (2026).

Directional Changes

We assessed the significance of directional changes for respective constituents in groups of paired initial and decadal samples (both statewide and for individual network groups) using the two-sided Wilcoxon signed-rank test with the Pratt modification for zeros (Pratt, 1959). We implemented this test using the wilcoxsign_test function from the R “coin” package (Hothorn and others, 2008) and evaluated test significance using an alpha value of 0.05. This test evaluates whether a group of paired samples (for example, statewide or within a given network group) shows significant directional change from the initial to the decadal sampling considering the direction (increase or decrease) and magnitude of change values. In this report, by convention, positive and negative differences indicate increasing and decreasing changes in constituent concentrations, respectively. Differences between a detection and a non-detection were numerically evaluated as the difference between the detected concentration and the RL of the

non-detection. This provides the most conservative (in other words, lowest) estimate of change magnitude (Kent, 2018). If both samples in a decadal pair were non-detections, had overlapping CIs for detections, or had a CI for a detected value that overlapped the RL of a non-detection, their respective result values were made equivalent prior to testing to indicate a statistical tie representing a difference of zero in subsequent computation steps (herein, "censored differences"). These are considered in this report to be effectively "unchanging" or "no change" values for which a difference could not be reliably detected considering sampling error derived from replicate analysis. For all significant test results (*p*-value less than 0.05), we further applied the wilcox.test function in the R "stats" package (R Core Team, 2024) to compute the Hodges-Lehmann estimator of the median difference (sometimes referred to as the pseudo-median) to infer overall change direction (Helsel and others, 2020). We took positive or negative Hodges-Lehmann estimates to indicate predominantly increasing or decreasing constituent values, respectively, when the Wilcoxon signed-rank test was significant. All non-significant test results (*p*-value greater than or equal to 0.05) represent instances where "no change" could be detected statewide or at network-group scales.

High-Magnitude Changes

We developed a novel approach to assess presence of high-magnitude changes (increases or decreases) for a given constituent across the PSW trends network statewide or within component network groups. We attributed all censored differences (concentration of decadal sample minus the concentration of the initial sample with zeros used to represent statistical ties) for respective constituents as "increase" for positive values, "decrease" for negative values, and "no change" for zeros. The term "no change" is used to signify that a change was unable to be reliably detected considering sampling error. We calculated the proportion of increasing and

decreasing constituent values for each network group. A network was considered to show high-magnitude change if it had both more than 10 percent of sites with changing values in a particular direction (increase or decrease) and if the 90th percentile of the absolute differences in that direction was greater than or equal to 10 percent of that constituent's benchmark value. For example, one may consider a hypothetical monitoring network of 100 sites with paired decadal samples for arsenic having 20 significant increases. These increases are composed of 17 increases of 0.5 microgram per liter increases and three increases of 1.1 micrograms per liter. For this example, the 90th percentile of increasing values is 1.1 micrograms per liter, which exceeds 10 percent of the MCL for arsenic (1 microgram per liter; U.S. Environmental Protection Agency, 2024). Therefore, this hypothetical network would be considered by the above approach to have had "high magnitude" increases for arsenic during the period of interest. A network may show high-magnitude changes in both directions at once. This approach effectively highlights network groups where constituent values change at levels relevant to human health and safety but can be sensitive to outliers for small network groups or those with relatively few significantly changing values.

Correlation Analysis

We used correlation analysis to identify which groups of constituents changed with each other and what geochemical factors might be driving those changes. We focused correlation analysis on water-quality constituents that showed either directional or high-magnitude changes statewide (herein, "focal constituents"). We used the non-parametric Spearman's rank correlation coefficient (herein, Spearman's rho; Helsel and others, 2020) to evaluate correlations among constituent differences (the decadal minus the initial sample values) for both water-quality constituents and geochemical indicators. Rank-based, non-parametric tests are resistant to non-

normally distributed data and outliers, which often characterize water-quality datasets (Helsel and others, 2020). We used two approaches to assess correlations of change values: (1) hierarchical agglomerative clustering of Spearman's rho values for a set of synchronously sampled inorganic constituents and geochemical indicators; and (2) correlation of non-zero, censored differences (significantly changing values) for each water-quality constituent to respective geochemical indicators.

Hierarchical agglomerative clustering is an unsupervised learning technique that can be used to explore patterns in large datasets (Hastie and others, 2009). Here, we compiled a set of uncensored concentration differences (using raw decadal change values without replacement by zeros) for inorganic constituents and geochemical indicators measured on all samples evaluated for TDS step trends (Levy and Soldavini, 2026). Uncensored differences were used for the cluster analysis to preserve the correlation structure of change values. Some constituents did not have measured change values corresponding to the selected TDS measurements at certain sites and were represented by "NA" (data not available) values in subsequent computation steps. We used the set of synchronous decadal difference values to highlight which groups of constituents more often changed with each other by clustering on Spearman's rho values. We created a correlation matrix (M) and distance matrix (1-M) from Spearman correlations among all focal constituents and geochemical indicators using the respective cor and as.dist functions from the R "stats" package (R Core Team, 2024) as described by Levy and others (2024). We then performed hierarchical agglomerative clustering on the resultant distance matrix of Spearman's rho values using the hclust function from the R "stats" package with the "ward.D2" linkage method, which produces relatively compact, globular clusters and is relatively resistant to noise (Murtagh and Legendre, 2014). We used the corrplot function in the R "corrplot" package to

visualize a heatmap of the Spearman's rho values ordered by the same hierarchical clustering method (Wei and Simko, 2024). This method allows visualization and grouping of constituents with more correlated change values.

We further computed Spearman correlations of significant change values for each focal constituent to respective changes of geochemical indicators. This approach differs from that of the cluster analysis in that not all constituents had to be measured in the same set of paired samples (Levy and Soldavini, 2026). For each water-quality constituent, we appended geochemical indicator measurements made during the same sampling events and computed a difference value for each decadal pair. We then filtered each set to only contain significant water-quality changes (in other words, non-overlapping CIs for each sample pair) for each given constituent and tested the correlation of the difference values to those of each respective geochemical indicator. We used the cor.test function in the R "stats" package to compute Spearman's rho values and evaluated the significance of correlations using an alpha value of 0.05. Only significantly changing water-quality differences were considered in this part of the analysis to better identify geochemical drivers of observed water-quality changes and prevent dilution of correlations by near-zero change values (Rosen and others, 2019).

Results

Here, we present results of step-trend analyses for water-quality constituents with benchmarks that showed at least 10 percent increasing or decreasing values or a significant directional trend statewide (table 3) and for all geochemical indicators (table 4). We highlight constituents with significant directional or high-magnitude changes statewide (focal constituents; fig. 5; tables 5–7) in presentation of results and subsequent discussion sections. We further note

which constituents had significant directional or high-magnitude changes at the scale of individual network groups (tables 5–7). Results are presented separately for inorganic and organic constituents with regulatory MCLs and non-regulatory, health- or aesthetic-based benchmarks as well as geochemical indicators without benchmarks. We also present results of correlation analyses among focal water-quality constituents and geochemical indicators.

Table 3. Summary of statewide results for water-quality constituents showing at least 10 percent increasing or decreasing values or a significant directional step trend in assessment of decadal trends in the quality of groundwater used for public drinking-water supply in California, 2004–2023.

Table 4. Summary of statewide results for geochemical indicators used to assess drivers of decadal trends in the quality of groundwater used for public drinking-water supply in California, 2004–2023.

Figure 5. Proportion of changing values statewide versus median bounded by 10th to 90th percentile of relative-concentration change (concentration change divided by constituent benchmark) for increasing (top) and decreasing (bottom) values of focal water-quality constituents showing significant directional or high-magnitude changes. Benchmarks used to calculate relative concentration changes for respective constituents can be found in Levy and Soldavini (2026). Data summarized from Levy and Soldavini (2026). MTBE, Methyl *tert*-butyl ether; TDS, total dissolved solids.

Table 5. Summary of water-quality constituents with regulatory maximum contaminant level (MCL) benchmarks showing significant directional or high-magnitude decadal changes in aquifers used for public

drinking-water supply statewide and in land-use and province-based network groups, California, 2004–2023.

Table 6. Summary of water-quality constituents with non-regulatory benchmarks showing significant directional or high-magnitude decadal changes in aquifers used for public drinking-water supply statewide and in land-use and province-based network groups, California, 2004–2023.

Table 7. Summary of geochemical indicators showing significant directional decadal changes in aquifers used for public drinking-water supply statewide and in land-use and province-based network groups, California, 2004–2023.

Inorganic Constituents with Regulatory Benchmarks

A total of eight inorganic constituents with regulatory MCLs had at least 10 percent increasing or decreasing change values statewide: arsenic, barium, chromium, fluoride, nitrate, perchlorate, selenium, and uranium (fig. 6; table 3). Of these, only uranium and perchlorate showed both significant directional and high-magnitude increases and decreases, respectively, statewide (figs. 5 and 6; table 5). Fluoride showed a significant directional decrease statewide, but changes were not of high magnitude. Nitrate and arsenic changes were detected in 67 and 48 percent of decadal pairs, respectively, with both showing high-magnitude increase and decrease statewide (fig. 6; table 5). This indicates that nitrate and arsenic changes at levels relevant to human health and safety were both prevalent and bidirectional across the dataset.

Figure 6. Decadal increases (top) and decreases (bottom) of relative concentration (concentration change divided by constituent benchmark) for inorganic water-quality constituents with regulatory benchmarks. Benchmarks used to calculate relative concentration changes for respective constituents can be found in Levy and Soldavini (2026). Data summarized from Levy and Soldavini (2026).

The directional and high-magnitude changes for uranium and perchlorate at a statewide scale were also reflected in each of the land-use network groups, indicating general prevalence of predominant trends for those constituents across the dataset irrespective of land-use type (table 5). Fluoride additionally showed significant directional and high-magnitude decreases in urban and natural land-use groups, but only directional decrease in the agricultural group (table 5). Chromium showed significant directional decrease in the natural group, but changes were not of high magnitude (table 5). Arsenic and nitrate showed both high-magnitude increases and decreases across all the land-use groups.

At the province-scale, significant directional and high-magnitude increases of uranium were detected in P1, P4, P5, and P7 (table 5), encompassing the agriculture-dominated Central Valley (P4 and P7) and Southern California (P1 and P5). Significant directional and high-magnitude decreases of fluoride and perchlorate were both detected in P1 and P5, but only fluoride showed significant and high-magnitude decreases in P6 (Sierra Nevada; table 5). Arsenic and nitrate showed both high-magnitude increases and decreases across many of the province groups, but only showed directional and high-magnitude increases for nitrate in P7 (San Joaquin Valley) and for arsenic in P2 (Northern Mountain Regions; table 5). Some individual province groups showed significant directional changes for barium and selenium, but changes were not of high magnitude (table 5).

Organic Constituents with Regulatory Benchmarks

A total of four organic constituents with regulatory MCLs had at least 10 percent increasing or decreasing change values or a significant directional step trend statewide: the pesticides atrazine and simazine, and the VOCs chloroform and MTBE (fig. 7; table 3). Some VOCs that did not show prevalent changes on the statewide scale had significant directional or

high-magnitude changes on the scale of network groups: bromodichloromethane, trichloroethene (TCE), and tetrachloroethene (PCE; table 5). Although chloroform had the most significant (non-overlapping CIs) change values for an organic constituent (sum of significantly increasing and decreasing changes of 31 percent), it did not show significant directional change statewide. In contrast, atrazine, simazine, and MTBE all showed significant directional decreases statewide, but changes were not of high magnitude (fig. 7; table 5).

Figure 7. Decadal increases (top) and decreases (bottom) of relative concentration (concentration change divided by constituent benchmark) for organic water-quality constituents with regulatory benchmarks. Benchmarks used to calculate relative concentration changes for respective constituents can be found in Levy and Soldavini (2026). Data summarized from Levy and Soldavini (2026). MTBE, methyl *tert*-butyl ether.

The herbicides atrazine and simazine both showed significant directional decreases in the urban land-use group with only atrazine showing significant directional decrease in the agricultural land-use group (table 5). The trihalomethanes chloroform and bromodichloromethane are common byproducts of disinfection by chlorination (Zogorski and others, 2006) and both showed significant directional increases in the urban land-use group (table 5). The solvent PCE showed high-magnitude decreases in the urban land-use group (table 5).

The herbicides atrazine and simazine showed significant directional decreases in the heavily urbanized Southwestern California (P5) province group (table 5). The solvents PCE and TCE also showed high-magnitude changes (bidirectional and only increasing, respectively) in P5 with high-magnitude increases in PCE also occurring in the San Joaquin Valley (P7). Chloroform also showed significant directional increases in P7 and high-magnitude decreases in the Southern Coast Ranges (P8; table 5).

Inorganic Constituents with Non-Regulatory, Aesthetic-Based Benchmarks

A total of five inorganic constituents with non-regulatory, aesthetic-based SMCLs had at least 10 percent increasing or decreasing change values statewide: chloride, iron, manganese, sulfate, and TDS (fig. 8; table 3). All of the SMCL constituents showed significant directional increases statewide, with iron, manganese, and TDS also having high-magnitude increases (fig. 8; table 6). Manganese and TDS additionally showed high-magnitude decreases statewide despite having predominantly increasing change values by proportion (fig. 8; table 6). Iron and manganese changes were of substantially greater magnitude than those of any other constituents evaluated in this study, with 10 percent of decreasing or increasing values changing at factors greater than or equal to 1–2 times respective benchmark concentrations (table 3).

Figure 8. Decadal increases (top) and decreases (bottom) of relative concentration (concentration change divided by constituent benchmark) for inorganic water-quality constituents with non-regulatory, aesthetic-based benchmarks. Benchmarks used to calculate relative concentration changes for respective constituents can be found in Levy and Soldavini (2026). Data summarized from Levy and Soldavini (2026). TDS, total dissolved solids.

Chloride, iron, and sulfate showed significant directional increases across all three land-use groups, but only iron changes were of high magnitude (table 6). Agricultural and urban groups showed significant directional increases of TDS, but changes were only of high magnitude in the agricultural group (table 6). The agricultural group also had significant directional and high-magnitude increases in manganese (table 6).

Six out of the eight province groups showed significant directional increases for either chloride or sulfate (table 6). All of the province groups showed countervailing high-magnitude increases and decreases for iron or manganese (table 6). Chloride showed significant directional

and high-magnitude increases in the Northern and Southern Coast Ranges (P3 and P8) and the Southwestern California (P5) province group, which also showed significant directional and high-magnitude increases for iron (table 6). The San Joaquin Valley (P7) showed significant directional and high magnitude increases for TDS and manganese (table 6).

Inorganic Constituents with Non-Regulatory, Health-Based Benchmarks

A total of four inorganic constituents with non-regulatory, health-based benchmarks had at least 10 percent increasing or decreasing change values statewide: boron, molybdenum, strontium, and vanadium (fig. 9; table 3). Boron, strontium, and vanadium showed significant directional increases statewide while molybdenum showed significant directional decrease (fig. 9; table 6). Although molybdenum decreases were more prevalent statewide (37 percent), the increasing changes (25 percent) were of high magnitude (fig. 9; table 3).

Figure 9. Decadal increases (top) and decreases (bottom) of relative concentration (concentration change divided by constituent benchmark) for inorganic water-quality constituents with non-regulatory, health-based benchmarks. Data summarized from Levy and Soldavini (2026).

All three land-use groups showed significant directional increases of strontium (table 6). Urban and natural land-use groups showed significant directional increases of boron (table 6). The natural land-use group showed significant directional increase of vanadium and high-magnitude increases and decreases of molybdenum (table 6). The urban land-use group showed a significant directional decrease of molybdenum (table 6).

Seven out of the eight province groups showed significant directional increases for strontium (table 6). The natural land-use dominated province groups encompassing desert and mountain regions (P1 and P2) as well as the urban land-use dominated Southwestern California

province group (P5) showed significant directional increases for boron, with Northern Coast Ranges (P3) and Sierra Nevada (P6) province groups showing high-magnitude increase and decrease, respectively (table 6). The Sacramento Valley (P4) showed significant directional increase for vanadium (table 6). Molybdenum showed significant directional decreases in the San Joaquin Valley (P7) and Southern Coast Ranges (P8) province groups (table 6). Molybdenum also showed high magnitude changes (sometimes with countervailing increases and decreases) in three of the eight province groups, but only showed significant directional and high-magnitude decreases in P8 (table 6).

Geochemical Indicators

All geochemical indicators had at least 10 percent increasing or decreasing values except for pH and d-excess, although the latter had 9 percent decreasing values (table 4). The pH measurement was the most stable, with no detectable change for 92 percent of paired samples (table 4). Alkalinity, calcium, and $\delta^{18}O$ showed significant directional increases statewide, whereas DO, d-excess, and $\delta^{13}C$ showed significant directional decreases (figs. 10–12; table 7). Calcium significantly increased across all land-use groups (table 7). Alkalinity significantly increased in agricultural and urban land use groups (table 7). Carbon-14 significantly increased in the urban land-use group (table 7). Additionally, $\delta^{13}C$ and d-excess significantly decreased in the agricultural land-use group (table 7).

Figure 10. Decadal increases (top) and decreases (bottom) for indicators of geochemical conditions. Data summarized from Levy and Soldavini (2026).

Figure 11. Decadal increases (top) and decreases (bottom) for indicators of groundwater source and age. Data summarized from Levy and Soldavini (2026). $\delta^{18}O$, oxygen-18.

Figure 12. Decadal increases (top) and decreases (bottom) for geochemical salinity indicators. Data summarized from Levy and Soldavini (2026). $\delta^{13}C$, carbon-13.

Calcium significantly increased across seven of the eight province groups, whereas alkalinity only significantly increased in the Desert, Basin and Range province group (P1) and the Central Valley (P4 and P7; table 7). Additionally, carbon-14 and d-excess significantly increased and decreased, respectively, in the San Joaquin Valley (P7; table 7). The isotope ratios $\delta^{13}C$ and $\delta^{18}O$ showed significant directional decreases and increases, respectively, in the Sacramento Valley and both Coast Ranges province groups (P3 and P8; table 7).

Categorical groundwater-age classifications (premodern, mixed, or modern; Lindsey and others, 2019) based on tritium measurements could not be evaluated for step trends as done for continuous variables. Of the 403 sites where there were sufficient data for comparison, 16 percent showed younger groundwater (either premodern changing to mixed, mixed changing to modern, or premodern changing to modern), 7 percent showed older groundwater (either modern changing to mixed or mixed changing to premodern), and the balance showed no change in groundwater age (table 8; Levy and Soldavini, 2026). Only one site switched between premodern and modern (table 8).

Table 8. Summary of groundwater age classifications based on tritium for initial compared to decadal sample pairs used to evaluate groundwater resources used for public drinking-water supply in California, 2004–2023.

Correlation Analysis

We tested Spearman correlations of uncensored difference values among 14 focal, inorganic water-quality constituents and 8 additional geochemical indicators. Out of a total of

231 unique constituent pairs, a total of 136 (59 percent) had significant Spearman correlations with p-values less than 0.05 (fig. 13*A*). We visualized Spearman's rho values as a heatmap organized by hierarchical clustering so that constituents with stronger change correlations were proximal to each other (fig. 13*A*). The strongest cross correlations (rho values 0.45–0.72, p-values less than 0.001) were among changes of chloride, sulfate, calcium, strontium, and TDS (herein, "salinity constituents"; fig. 13*A*). Iron and manganese changes also showed relatively strong positive correlation (rho = 0.51, p-value less than 0.001; fig. 13*A*). Other constituent pairs had weaker but significant statewide correlations. Cross-correlations among constituent groups and subgroups can also be visualized as a dendrogram, where branches that join at lower relative heights represent groups of constituents with more correlated changes (fig. 13*B*).

Figure 13. *A*, heatmap; and *B,* dendrogram of Spearman's correlations among decadal changes of focal water-quality constituents and geochemical indicators organized by hierarchical agglomerative clustering. Positive Spearman's rho values indicate direct correlation of decadal change values (constituents increasing or decreasing together) and negative Spearman's rho values indicate inverse correlation of change values (constituent concentrations changing in opposite directions). Black boxes in the heatmap (*A*) correspond to the two top-level cluster groups (split with maximum height value) defined in the dendrogram (*B*). Data summarized from Levy and Soldavini (2026). $\delta^{13}C$, carbon-13; $\delta^{18}O$, oxygen 18; d-excess, deuterium excess; DO, dissolved oxygen; TDS, total dissolved solids.

We also evaluated Spearman's correlations of non-zero, censored differences for all focal water-quality constituents to each geochemical indicator. All significant Spearman's rho values for each water-quality constituent are presented in fig. 14 except for $\delta^{13}C$ because it only correlated weakly with one focal water-quality constituent (uranium; rho = -0.16, p-value = 0.030; Levy and Soldavini, 2026). The strongest correlations for censored changes with rho

values greater than 0.5 were also for the salinity indicators: TDS (to strontium, chloride, and sulfate), alkalinity (to uranium), and calcium (to strontium, chloride, sulfate, and TDS; fig. 14).

Figure 14. Panels showing significant (p-values less than 0.05) Spearman's correlations for censored differences of water-quality constituents to respective geochemical indicators. Positive Spearman's rho values indicate direct correlation of decadal change values (constituents increasing or decreasing together) and negative Spearman's rho values indicate inverse correlation of change values (constituent concentrations changing in opposite directions). Data summarized from Levy and Soldavini (2026). $\delta^{18}O$, oxygen 18; d-excess, deuterium excess; TDS, total dissolved solids.

Discussion

The following discussion presents a conceptual framework for understanding geochemical drivers of groundwater-quality trends observed across the statewide monitoring network. Further focused discussion is included for the following selected constituents: TDS, uranium, fluoride, nitrate, arsenic, perchlorate, herbicides, and MTBE. Study limitations and considerations for future work are also discussed.

Conceptual Framework to Understand Geochemical Drivers of Groundwater-Quality Trends

Here, we interpret results of correlation analyses contextualized by prior research to propose a broad conceptual framework for understanding drivers of groundwater-quality trends observed on a statewide scale. We use statewide results to indicate generally what groups of water-quality constituents change more commonly with one another and associated geochemical drivers. Different considerations than those discussed below might be more pertinent to local-scale studies.

Cluster analysis broadly separated water-quality constituents into two top-level groups (fig. 13), which we interpret as having changes more influenced by "geogenic drivers" versus "anthropogenic drivers." Water-quality constituents with changes we interpret as being more associated with geogenic drivers include: vanadium, molybdenum, arsenic, boron, and fluoride. Water-quality constituents with changes we interpret as being more associated with anthropogenic drivers include nitrate, perchlorate, salinity constituents, and uranium. The groupings here differ slightly from prior classifications of geogenic and anthropogenic constituents presented by Belitz and others (2015, 2022). Specifically, we consider salinity constituents and uranium, which have geogenic sources, to be affected by anthropogenic drivers group because increasing trends of these constituents in California groundwater have been linked to land use practices, particularly agricultural development, in prior studies (Jurgens and others, 2010; Hansen and others, 2018; Rosen and others, 2019; Pauloo and others, 2021; Levy and others, 2024). We discuss additional context and considerations leading to these conceptual groupings below. The resultant conceptual framework is useful to understand broad geochemical factors influencing groundwater-quality changes statewide, but drivers of observed trends are likely to be heterogenous at the local scale.

For the purposes of this study, we characterize groundwater constituents with geogenic drivers as those originating from natural reactions with aquifer materials. Constituents with geogenic drivers tend to be observed at elevated concentrations more often in older, "geochemically evolved" groundwater with relatively long (centennial to millennial scale) transit times in the subsurface, typically indicated by elevated pH (greater than 8.0) and depleted DO (less than 0.5 milligrams per liter; Hem, 1985; Ayotte and others, 2011). Most of the constituents with geogenic drivers identified here had significant direct correlations with pH and inverse

correlations with carbon-14 and $\delta^{18}O$, indicating increases related to a shift in groundwater sources to older, more geochemically evolved groundwater that recharged under different (for example, cooler) climate conditions (figs. 13 and 14). Shifts in dominance of relatively young and old groundwater sources to PSWs can occur on short (diurnal to seasonal) and long (annual to decadal) timescales due to changes in well operations and aquifer pressure dynamics (Levy and others, 2021, 2024).

In contrast, constituents with anthropogenic drivers in groundwater may arise directly from contamination by human activities at the land surface or human-induced changes to recharge chemistry that alter natural geochemical equilibria in aquifers (Jurgens and others, 2010). Nitrate and perchlorate occur in groundwater under natural conditions at relatively low concentrations with higher concentrations generally indicative of anthropogenic sources (Dubrovsky and others, 2010; Fram and Belitz, 2011). Decadal change values for nitrate and perchlorate correlated directly with one another (fig. 13). Nitrate changes also directly correlated to those of carbon-14, DO, and $\delta^{18}O$ indicating increases associated with younger, more oxic groundwater recharged under different (for example, warmer) climate conditions (fig. 13). Younger groundwater is more likely to be affected by anthropogenic fertilizer applications, which showed increases in loading rates by factors of about 4–10 in some agricultural areas of the State during the latter part of the 20th century (Burow and others, 2008, 2013). Consequentially, nitrate changes also directly correlated with those of salinity constituents, indicating increases in salinity observed throughout the State are at least, in part, driven by anthropogenically affected source waters (fig. 13). Multiple studies have found increases in groundwater salinity and associated nitrate concentrations due to agricultural practices across

California (Burow and others, 2013; Kent and Landon, 2013; Hansen and others, 2018; Pauloo and others, 2021).

Anthropogenic-driven changes to groundwater quality need not necessarily originate from contamination at the land surface. Although uranium can be considered a geogenic constituent due to its prevalence in certain aquifer materials (Belitz and others, 2022), here we consider the potential for uranium to be anthropogenically mobilized (Jurgens and others, 2010; Burow and others, 2017). In California, increasing groundwater uranium has been attributed to anthropogenic increases in the proportion of bicarbonate contributing to total groundwater salinity (Hansen and others, 2018), which can cause naturally occurring uranium to desorb from aquifer sediments thereby increasing aqueous-phase concentrations (Jurgens and others, 2010; Rosen and others, 2019). We found uranium changes most strongly correlated with those of alkalinity, indicative of bicarbonate mediated desorption from aquifer sediments (figs. 13 and 14; Rosen and others, 2019). This correlation was proximal to salinity constituents and nitrate in the cluster analysis heatmap and dendrogram, indicating the potential influence of related anthropogenic drivers (fig. 13). Increases in bicarbonate and associated uranium concentrations have been attributed to enhanced soil mineral weathering driven by warm-season irrigation and agricultural development in areas of California (Jurgens and others, 2010; Hansen and others, 2018; Rosen and others, 2019).

Iron and manganese tend to be more mobile in anoxic (DO less than 0.5 milligrams per liter; McMahon and Chappelle, 2008) groundwater, which may be older and more geochemically evolved. Here, we found that increases in manganese correlated with decreases in DO, but also correlated with increases in salinity constituents and alkalinity (figs. 13 and 14). McMahon and others (2018) found complicated landscape factors including water-table depth and land use can

affect dissolved manganese concentrations in groundwater. Hem (1963) found that sulfate and bicarbonate may form coordination complexes with manganese that might reduce its solubility under different geochemical conditions. Because of complex geochemical and landscape-related factors, it is difficult to say if iron and manganese fit into the overall conceptual framework presented above but are clustered with the other anthropogenically affected constituents most likely due to direct associations with salinity changes in this study (fig. 13).

Factors Affecting Constituents with Prevalent Directional and High-Magnitude Changes

The following subsections provide a more in-depth discussion of factors potentially affecting observed trends for focal constituents with MCLs that showed prevalent directional or high-magnitude changes statewide (table 5). Although TDS does not have an MCL, we include it as a focal water-quality constituent in the following discussion because salinity of groundwater resources is an issue of importance to stakeholders across California (for example, salt and nutrient management planning is required by the State of California's Recycled Water Policy; California State Water Resources Control Board, 2025). Primary drivers of significantly increasing TDS concentrations are additionally discussed as they relate to potential mechanisms controlling the mobility of focal water-quality constituents, particularly uranium and fluoride.

Total Dissolved Solids (TDS)

Elevated groundwater TDS above the California SMCL of 1000 milligrams per liter (California State Water Resources Control Board, 2024) may exhibit discoloration, unpleasant odor or taste, contribute to clogging of pipes, and may not be suitable for irrigation (Hem, 1985; Pauloo and others, 2021). Saline (TDS greater than 10,000 milligrams per liter) groundwater occurs naturally in deep, confined aquifers across the State (greater than 1000 ft depths) that are

typically not used for public drinking-water supply (Kang and others, 2020). Increased salinity of public-supply aquifers has been linked to the effects of century-scale agricultural practices (Kent and Landon, 2013; Hansen and others, 2018; Pauloo and others, 2021) and focused pumping in coastal and coastal-adjacent basins (Izbicki and others, 2005; O'Leary and others, 2015).

We observed significant directional and high-magnitude increases of groundwater TDS statewide (table 6). Significant directional and high-magnitude increases of groundwater TDS also occurred in areas of agricultural land use and the San Joaquin Valley province group (P7; table 6). Other areas of the State, including coastal basins, showed countervailing high-magnitude increases and decreases co-occurring in the same province groups (table 6). The median of all significantly increasing TDS changes statewide was 64 milligrams per liter, with 10 percent of those increasing values exceeding 213 milligrams per liter (about 21 percent of the SMCL; table 3; Levy and Soldavini, 2026). Although increases of TDS were observed commonly in agricultural areas, some of the largest magnitude increases (greater than 200 milligrams per liter) occurred in the coastal and coast-adjacent areas (P3, P5, P8; fig. 15). These areas also had some of the greatest countervailing decreases (less than -100 milligrams per liter; fig. 15).

Figure 15. Maps of California showing study sites that had significant decreases (top), significant increases (middle), and non-significant changes (bottom) for decadal comparisons of total dissolved solids (TDS). Change significance is indicated for initial and decadal concentration values with non-overlapping confidence intervals. Point sizes and colors are scaled to absolute and directional concentration changes, respectively. Directional differences ranged from -729 to 1818 milligrams per liter, but scales were symmetrically saturated at value of ±274 milligrams per liter to prevent outliers (less than 2 percent of

change values statewide) from obscuring visualization of most change values. Data summarized from Levy and Soldavini (2026).

Observed TDS changes most strongly correlated (rho greater than 0.50; figs. 13 and 14) with salinity constituents, including calcium, chloride, sulfate, and strontium (fig. 13). We found these constituents showed significant directional increases broadly across most land-use and province groups (tables 6 and 7), but changes were often not of high-magnitude compared to respective benchmarks (table 6). These salinity constituents are typically the major components of groundwater TDS by mass except for strontium, which is ubiquitous in groundwater at trace levels and often co-occurs with calcium at elevated concentrations because they share similar chemical behaviors and geologic sources (Musgrove, 2021).

To better understand the nature of TDS changes across the State, we identified which major cations (calcium, magnesium, sodium, potassium) and anions (sulfate, chloride, bicarbonate) were predominant drivers of significantly changing TDS values. This was done by identifying which cation and anion showed the largest mass changes in the direction of each significant TDS change (fig. 16). Calcium was the predominant changing cation by mass for 64 percent of sites with increasing TDS values, followed by sodium at 29 percent (fig. 16*A*). Bicarbonate was the predominant changing anion by mass for 46 percent of sites with increasing TDS values, followed more closely by chloride and sulfate at 27 and 26 percent, respectively (fig. 16*B*). Calcium-bicarbonate was the most commonly changing ion pair by mass for 34 percent of sites with increasing TDS values, followed by calcium-sulfate at 19 percent (fig. 16*C*).

Figure 16. Count of sites with largest solute mass changes corresponding to significant total dissolved solids (TDS) increases and decreases for *A*, major cations; *B*, major anions; and *C*, major ion pairs. Data

summarized from Levy and Soldavini (2026). Ca, calcium; K, potassium; Mg, magnesium; Na, sodium; Cl, chloride; HCO_3, bicarbonate; SO_4, sulfate.

Observed TDS increases, dominated by calcium and bicarbonate statewide, likely have heterogenous drivers across diverse California landscapes. Increases of groundwater calcium and bicarbonate in agricultural and, to a lesser extent, urban areas of the eastern San Joaquin Valley have been attributed increased warm-season irrigation accelerating soil mineral weathering over the long term (Jurgens and others, 2010; Hansen and others, 2018). Additional drivers of TDS increases related to warm-season irrigation include evaporative enrichment of return flows, dissolution of agricultural amendments, and mobilization of naturally occurring salts from the vadose zone (Fram, 2017; Hansen and others, 2018; Pauloo and others, 2021). Imported surface waters used for irrigation and managed recharge have been shown to contribute to increased groundwater salinity and changes to the geochemical composition of recharge over the long term (Harkness and Jurgens, 2022; Harkness and others, 2023).

Stable isotopes of carbon ($\delta^{13}C$) can be used to indicate shifts in sources of groundwater DIC. Measured groundwater $\delta^{13}C$ values in this study ranged widely from -25.8 to -2.0 per mille (Levy and Soldavini, 2026), consistent with characteristic values for carbon dioxide in soil gas and carbonate minerals, respectively (Bottrell and others, 2019). Enhanced weathering of soil minerals can occur in response to irrigation-supported plant growth increasing the partial pressure of carbon dioxide in the unsaturated zone, accelerating reaction of soil minerals with isotopically depleted soil gas (Jurgens and others, 2010; Hansen and others, 2018; Seltzer and others, 2021). Significant decreases of $\delta^{13}C$ accompanied significant increases of alkalinity across both the statewide trends network and the agricultural network group (table 4), signifying broad shifts in DIC sources. Additionally, alkalinity changes showed weak but significant

inverse correlation with those of $\delta^{13}C$ statewide (rho = -0.17, p-value less than 0.010; fig. 13) and weak but significant direct correlation with carbon-14 statewide (rho = 0.14, p-value less than 0.050; fig. 13), although carbon-14 did not show significant increase statewide (table 4). Increased alkalinity accompanied by decreased $\delta^{13}C$ and increased carbon-14 is consistent with a shift to more modern DIC sources derived from open-system weathering of soil profiles beneath irrigated lands, as exemplified by prior studies in the San Joaquin Valley (Jurgens and others, 2010; Hansen and others, 2018; Seltzer and others, 2021). There is likely a great amount of variability in these relations statewide due to the complexity of carbon cycling pathways in different aquifer systems (Bottrell and others, 2019).

The geochemical indicator of d-excess also significantly decreased in areas of agricultural land use and statewide, with the strongest inverse correlation of change values to those of TDS, followed by chloride (fig. 14; table 4). More negative d-excess values generally indicate a stronger effect of evaporation on recharge, which has been linked to surface waters used for irrigation and managed recharge across the State (Levy and others, 2020; Castaldo and others, 2021; Harkness and others, 2023). This relation strengthens the hypothesis that surface-water recharge related to irrigation and managed recharge can result in increased groundwater salinity, consistent with prior work (Kent and Landon, 2013; Hansen and others, 2018; Pauloo and others, 2021; Harkness and Jurgens, 2022; Harkness and others, 2023).

Significant increases in calcium and alkalinity that occurred statewide (table 4) were most pronounced in agricultural and urban areas (table 7; Levy and Soldavini, 2026), indicating amplification of those trends by anthropogenic factors. Both Jurgens and others (2010) and Hansen and others (2018) attributed increased bicarbonate, and to a lesser degree calcium, in California's San Joaquin Valley to warm-season irrigation enhancing open-system mineral

weathering in soils over the long term. Burow and others (2017) showed decadal increases of alkalinity occurred broadly beneath irrigated lands of the western United States during 1993–2014. Klaus (2024) found decadal increases of groundwater DIC across Sweden during 1980–2020 and attributed these, in part, to enhanced soil respiration and associated mineral weathering driven by increases in temperature, primary productivity, and atmospheric carbon dioxide concentrations. Although it is out of the scope of current study to diagnose drivers of observed widespread increases of calcium and alkalinity across California, these trends may be driven, in part, by anthropogenic land uses affecting soil weathering dynamics over the long term. Additionally, calcium has many shared anthropogenic sources such as soil amendments, construction materials (such as cement and hardwall), and sewage discharges (Hansen and others, 2018; Wu and others, 2018; Harkness and others, 2023).

Some of the largest TDS increases statewide (greater than 200 milligrams per liter) occurred in coastal or coastal-adjacent basins within P3, P5, and P8 (fig. 15). These province groups also had directional and high-magnitude increases in chloride (table 6). Increased groundwater chloride in coastal and coastal-adjacent basins can occur in response to seawater intrusion or increased capture of groundwater that has reacted with aquifer materials derived from ancient marine sediments (Izbicki and others, 2005; O'Leary and others, 2015).

Uranium

Uranium is a weakly carcinogenic, radioactive element that can impair kidney function when consumed in drinking water for extended periods (years) and has an MCL of 30 micrograms per liter (Kurttio and others, 2002; U.S. Environmental Protection Agency, 2024). In California, elevated concentrations of uranium in groundwater are associated with granitic rocks and alluvium derived from granitic rocks (Belitz and others, 2015). Belitz and others (2015)

found uranium concentrations exceeding the MCL in PSWs most often occurred in the Sierra Nevada (P6), San Joaquin Valley (P7), and the Southern California (P1 and P5) province groups. In the San Joaquin Valley, irrigation-driven increases in groundwater bicarbonate have been linked to increased groundwater uranium concentrations by causing naturally occurring uranium to desorb from granitic aquifer materials (Jurgens and others, 2010; Hansen and others, 2018; Rosen and others, 2019). This uranium mobilizing desorption process can be additionally enhanced in the presence of elevated calcium through formation of ternary calcium-uranyl-carbonate complexes (Jurgens and others, 2010; Lopez and others, 2021). Rosen and others (2019) found increasing trends in groundwater uranium in the San Joaquin Valley were linked to accompanying increases in groundwater alkalinity during a 25-year monitoring period. Burow and others (2017) found decadal increases in groundwater uranium were strongly associated those of alkalinity beneath irrigated lands across the western United States.

Uranium had the most prevalent directional and high-magnitude increases of any water-quality constituent with an MCL in this study (table 5). We observed directional and high-magnitude increases of uranium statewide, across all land-use groups, and in province groups encompassing Southern California (P1 and P5) and the Central Valley (P4 and P7), which include much of the area that was noted to have already elevated levels of uranium in the prior status assessment (Belitz and others, 2015). The median of all significantly increasing uranium changes statewide was 0.5 micrograms per liter, with 10 percent of those increasing values exceeding 4.2 micrograms per liter (about 14 percent of the MCL; table 3; Levy and Soldavini, 2026). However, in the agricultural network group, the median of significantly increasing uranium changes was 0.64 micrograms per liter, with 10 percent of those increasing values exceeding 6.5 micrograms per liter (about 22 percent of the MCL; Levy and Soldavini, 2026).

Uranium changes had the strongest correlation among geochemical indicators to those of alkalinity (rho = 0.51), followed closely by calcium (rho = 0.48; fig. 14). This supports prior hypotheses that trends of increasing uranium are driven by desorption from aquifer materials due to complexation with bicarbonate and calcium ions (Jurgens and others, 2010; Rosen and others, 2019; Lopez and others, 2021). Although uranium changes showed a relatively strong correlation to those of alkalinity, large uranium increases did not always accompany those of alkalinity (fig. 17; for example, in the Coast Ranges and Northern Mountain regions). Increases of groundwater alkalinity are more likely to mobilize substantial quantities of uranium in the presence of uranium-bearing, granitic aquifer materials (Jurgens and others, 2010; Rosen and others, 2019; Lopez and others, 2021), which are less prevalent in areas of the State dominated by metamorphic, volcanic, or non-granitic plutonic rocks and sediments.

Figure 17. Maps of California showing study sites that had significant decreases (top), significant increases (middle), and non-significant changes (bottom) for decadal comparisons of uranium (left) and alkalinity (right). Change significance is indicated for initial and decadal concentration values with non-overlapping confidence intervals. Point sizes and colors are scaled to absolute and directional concentration changes, respectively. Directional differences ranged from -40 to 93 micrograms per liter for uranium and -145 to 100 milligrams per liter as calcium carbonate for alkalinity. Respective measurement scales for uranium and alkalinity were symmetrically saturated at values of ±16 micrograms per liter and ±75 milligrams per liter (as calcium carbonate) to prevent outliers (less than 2 percent of change values statewide) from obscuring visualization of most change values. Data summarized from Levy and Soldavini (2026).

Fluoride

Fluoride is a minor anion that occurs naturally in groundwater but can have carcinogenic and neurotoxic effects at elevated concentrations (Hem, 1985; Edmunds and Smedley, 2013). Fluoride has a federal MCL of 4 milligrams per liter (U.S. Environmental Protection Agency, 2024) and a California State MCL of 2 milligrams per liter (California State Water Resources Control Board, 2024), the latter of which is used as a comparative benchmark for the purposes of the current study (Levy and Soldavini, 2026). In CONUS, fluoride concentrations greater than 4 milligrams per liter are most prevalent in southwestern States in premodern groundwaters of high pH (greater than 8.0) and elevated TDS (McMahon and others, 2020). Drivers of elevated fluoride in southwestern States include water-rock interactions with aquifer materials rich in fluorine-bearing minerals, mixing with deeply circulating geothermal fluids, and evapoconcentration in discharge zones of hydrologically closed basins (McMahon and others, 2020). In California, concentrations of fluoride exceeding the MCL in PSWs typically occur in Southern California (particularly in more arid areas encompassed by the P1 province group) and the Sierra Nevada (Belitz and others, 2015; Harkness and Jurgens, 2022). Harkness and Jurgens (2022) found that about two-thirds of the areas of the State with detected PSW fluoride trends (14 percent of the assessed area) showed predominantly decreasing concentrations.

Fluoride showed the most prevalent directional decreases of any focal water-quality constituent statewide and across all land-use groups and province groups except in the Northern Mountain Regions (P2) and the Northern Coast Ranges (P3; table 5). Fluoride additionally showed both directional and high-magnitude decreases in areas of the State noted above where elevated concentrations have been observed in prior status assessments (P1, P5, and P6; table 5). The median of significantly decreasing fluoride changes statewide was -0.06 milligrams per liter,

with 10 percent of those decreasing values being less than -0.19 milligrams per liter (nearly 10 percent of the MCL; table 3; Levy and Soldavini, 2026). The Desert, Basin and Range (P1) province group had the most substantial declines, having a median of significant decreases of -0.07 milligrams per liter with 10 percent of those decreasing values being less than -0.39 milligrams per liter (nearly 20 percent of the MCL; table 3; Levy and Soldavini, 2026).

Fluoride changes had the strongest correlation among geochemical indicators to those of calcium (rho = -0.31; fig. 14), indicating increasing calcium concentrations at times accompanied decreasing fluoride concentrations. Aqueous phase fluoride concentrations are strongly controlled by the poorly soluble mineral fluorite (CaF_2; Hem, 1985; McMahon and others, 2020). The ubiquitous increases of calcium observed statewide could lower the solubility of fluoride in groundwater thereby contributing to the observed widespread decreases shown in the current study. This effect would be limited in more northern areas of the State (for example, P2 and P3) where groundwater fluoride was already naturally low (Belitz and others, 2015; Harkness and Jurgens, 2022), resulting in areas showing calcium increases unrelated to countervailing decreasing in fluoride (fig. 18). Harkness and Jurgens (2022) attributed decreasing fluoride trends in arid regions of Southern California to managed recharge with calcium-rich surface water affecting equilibrium controls on fluoride solubility in public-supply aquifers.

Figure 18. Maps of California showing study sites that had significant decreases (top), significant increases (middle), and non-significant changes (bottom) for decadal comparisons of fluoride (left) and calcium (right). Change significance is indicated for initial and decadal concentration values with non-overlapping confidence intervals. Point sizes and colors are scaled to absolute and directional concentration changes, respectively. Directional differences ranged from -1.28 to 0.42 milligrams per liter for fluoride and -71 to 252 milligrams per liter for calcium. Respective measurement scales for fluoride and

calcium were symmetrically saturated at values of ±0.44 milligrams per liter and ±48 milligrams per liter to prevent outliers (less than 2 percent of change values statewide) from obscuring visualization of most change values. Data summarized from Levy and Soldavini (2026).

Nitrate

Nitrate is a naturally occurring nutrient found in plants, soils, and natural waters but is present in elevated concentrations in human-made fertilizers and can have deleterious health effects if regularly consumed in drinking water at concentrations exceeding the MCL of 10 milligrams (of nitrate as nitrogen) per liter (Dubrovsky and others, 2010; U.S. Environmental Protection Agency, 2024). In California, concentrations of nitrate exceeding the MCL in PSWs typically occur in agriculture-dominated areas (P7 and P8) and urban-dominated areas of Southern California (P5; Belitz and others, 2015). Increasing trends of nitrate in PSWs have been observed in the agriculturally dominated areas of the San Joaquin Valley (P7; Burow and others, 2008, 2013) as well as now comparatively urbanized areas of legacy agricultural land use in San Bernadino County (within P5; Kent and Landon, 2013). Jurgens and others (2020) found that of the areas of the State where a recent (2000–2014) nitrate trend could be detected, about two-thirds showed predominantly increasing concentrations with the remainder decreasing.

Nitrate showed both high-magnitude increases and decreases statewide and across many of the network groups (table 3). The only network group that showed both directional and high-magnitude nitrate change was that of the San Joaquin Valley (P7), where concentrations increased. Medians for significantly increasing and decreasing nitrate changes statewide were 0.5 and -0.2 milligrams per liter, respectively, with 10 percent of those increasing values exceeding 2.7 milligrams per liter (27 percent of the MCL) and 10 percent of those decreasing values being less than -1.8 milligrams per liter (18 percent of the MCL; table 3; Levy and Soldavini, 2026). In

the San Joaquin Valley, the median of significantly increasing nitrate changes was 1.0 milligrams per liter, with 10 percent of those increasing values exceeding 2.8 milligrams per liter (28 percent of the MCL; Levy and Soldavini, 2026).

Nitrate changes had the strongest direct correlations among geochemical indicators to those of calcium and TDS (rho values of 0.38 and 0.31, respectively) followed by less strong but significant correlations to carbon-14 (rho = 0.29) and DO (rho = 0.26; fig. 14). This supports a broad conceptual model that increasing nitrate concentrations are associated with wells tapping larger proportions of younger, more oxic groundwater bearing anthropogenic salinity over time as has been shown by several studies of agricultural areas of the State (Burow and others, 2008, 2013; Kent and Landon, 2013; Hanson and others, 2018; Levy and others, 2021, 2024). However, the bidirectional changes observed statewide indicate that some areas are showing improved water quality as well. Decreases in groundwater nitrate may be linked to past land uses including variable rates of nitrate loading over time (Burow and others, 2008, 2013) and adoption of best management practices in source areas contributing to PSWs (Bastanti and Harter, 2019), both of which may lag current groundwater quality conditions by decades (Lindsey and others, 2023). The most substantial increases occurred in areas where already high concentrations have been noted in prior work (P5, P7, P8; fig. 19), whereas the most substantial decreases occurred across the agriculture-dominated Central Valley (P4 and P7) and now urbanized areas of Southwestern California (P5; fig. 19), portions of which have been noted in prior studies to have supported legacy agricultural land use (for example, the Upper Santa Ana drainage basin; Kent and Belitz, 2012; Kent and Landon, 2013; Jurgens and others, 2020).

Figure 19. Maps of California showing study sites that had significant decreases (top), significant increases (middle), and non-significant changes (bottom) for decadal comparisons of nitrate. Change

significance is indicated for initial and decadal concentration values with non-overlapping confidence intervals. Point sizes and colors are scaled to absolute and directional concentration changes, respectively. Directional differences ranged from -5.2 to 28.5 milligrams per liter as nitrogen, but scales were symmetrically saturated at value of ±7 milligrams per liter as nitrogen to prevent outliers (less than 2 percent of change values statewide) from obscuring visualization of most change values. Data summarized from Levy and Soldavini (2026).

Arsenic

Arsenic is a trace metalloid that is ubiquitous in most aquifer types and can have carcinogenic and other deleterious health effects if consumed over the long-term at concentrations exceeding the MCL of 10 micrograms per liter (Lombard and others, 2021; U.S. Environmental Protection Agency, 2024). Arsenic is often present in aquifers in reduced mineral phases (such as pyrite) or sorbed to clay surfaces and amorphous iron and manganese oxyhydroxide coatings on mineral grains (Smedley and Kinniburgh, 2002). Arsenic tends to be most mobile in the aqueous phase in groundwater that is anoxic, which promotes reductive dissolution of iron and manganese coatings, or has pH greater than 8.5, which promotes release from sorption sites (Smedley and Kinniburgh, 2002). In California, arsenic concentrations exceeding the MCL most often occur in the Desert, Basin and Range (P1), the Sierra Nevada (P6), and the Central Valley (P4 and P7; Belitz and others, 2015), particularly in historic groundwater discharge zones with fine-grained sediments along the valley's axial trough (Ayotte and others, 2016). Jurgens and others (2020) found that of the areas of the State where a recent (2000–2014) arsenic trend could be detected, about two-thirds showed predominantly decreasing concentrations with the remainder increasing. Haugen and others (2021) found predominantly decreasing groundwater arsenic trends in the San Joaquin Valley and attributed this to the long-

term migration of oxic, agriculturally affected groundwater into more reducing portions of drinking-supply aquifers over the past several decades.

Arsenic showed both high-magnitude increases and decreases statewide and across many of the network groups (table 3). The only network group that showed both directional and high-magnitude arsenic change was that of the Northern Mountain Regions (P2), where concentrations increased. Median of significantly increasing and decreasing arsenic changes statewide were 0.8 and -0.5 micrograms per liter, respectively, with 10 percent of those increasing values exceeding 5.3 micrograms per liter (53 percent of the MCL) and 10 percent of those decreasing values being less than -3.7 micrograms per liter (37 percent of the MCL; table 3; Levy and Soldavini, 2026). In the Northern Mountain Regions, the median of significantly increasing arsenic changes was 0.8 micrograms per liter, with 10 percent of those increasing values exceeding 5.3 micrograms per liter (53 percent of the MCL), but this province group was small (number of decadal arsenic pairs equal to 24) and therefore more sensitive to outlier values (Levy and Soldavini, 2026).

Arsenic changes had the strongest correlations among geochemical indicators with those of carbon-14 (inverse; rho = -0.40) and pH (direct; rho = 0.33), followed by less strong but significant correlations to calcium (inverse; rho = -0.27), $\delta^{18}O$ (inverse; rho = -0.26), and DO (inverse; rho = -0.24; fig. 14). The primary correlations to carbon-14 and pH are consistent with a conceptual model that increased arsenic is associated with older (lower carbon-14), more geochemically evolved (higher pH) groundwater (Ayotte and others, 2011; Levy and others, 2024). Secondary inverse relations to calcium, $\delta^{18}O$, and DO are consistent with decreased arsenic concentrations related to a shift toward more oxic, modern groundwater bearing anthropogenic salinity, consistent with prior studies in areas dominated by agriculturally affected

recharge (Haugen and others, 2021). The most substantial arsenic decreases occurred in the San Joaquin Valley (P7) and Southern Coast Ranges (P8), whereas the substantial increases appeared more dispersed statewide with some clustering in Southern California (fig. 20). The presence of countervailing, high-magnitude changes in arsenic concentrations across the State could be due to changes in water sources to PSWs. Levy and others (2024) observed relatively rapid seasonal and drought-induced changes in PSW arsenic concentrations occurred in response to pumping dynamics shifting the proportion of older, more geochemically evolved groundwater captured by PSWs.

Figure 20. Maps of California showing study sites that had significant decreases (top), significant increases (middle), and non-significant changes (bottom) for decadal comparisons of arsenic. Change significance is indicated for initial and decadal concentration values with non-overlapping confidence intervals. Point sizes and colors are scaled to absolute and directional concentration changes, respectively. Directional differences ranged from -23 to 29 micrograms per liter, but scales were symmetrically saturated at value of ±14 micrograms per liter to prevent outliers (less than 2 percent of change values statewide) from obscuring visualization of most change values. Data summarized from Levy and Soldavini (2026).

Perchlorate

Perchlorate (ClO_4^-) is a trace inorganic compound that can disrupt formation of thyroid hormones by interfering with iodide uptake and has a California State MCL of 6 micrograms per liter (California State Water Resources Control Board, 2024). Perchlorate forms naturally in the atmosphere and is therefore present at low levels in precipitation (Dasgupta and others, 2005). Perchlorate concentrations may become elevated in groundwater by mobilization from the vadose zone by natural recharge or irrigation return flows (Rajagopalan and others, 2006). Anthropogenic contamination sources include legacy use of fertilizers sourced from Chile's

Atacama Desert (herein, “Atacama fertilizers”); manufacture, use, and disposal of rocket fuel; military munitions; fireworks; and other explosive devices (Eriksen, 1981; Trumpolt and others, 2005). Perchlorate is generally persistent in natural waters, although it may degrade under anoxic conditions in some settings (Urbansky, 2005; Nozawa-Inoue and others, 2005). In California, perchlorate most often occurs at elevated concentrations greater than 2 micrograms per liter at PSWs located in areas of the Central Valley (P4 and P7), Southern Coast Ranges (P8), and of Southern California (P1 and P5; Fram and Belitz, 2011). Colorado River water imported to Southern California is an additional source of exogenous perchlorate originating from groundwater and surface water contaminated by perchlorate manufacturing facilities near Henderson, Nevada, with peak river-water concentrations occurring in the late 1990s and subsequently leveling off after 2009 (U.S. Environmental Protection Agency, 2020).

Perchlorate showed directional and high-magnitude decreases statewide and across all land use groups (table 5). These trends are likely in large part due to observed directional and high-magnitude decreases within the Southern California province groups (P1 and P5; table 5). Perchlorate additionally showed limited high-magnitude increases in areas of the State where elevated concentrations have been noted in prior assessments (P5 and P8; table 5). The median of significantly decreasing perchlorate changes statewide was -0.3 micrograms per liter, with 10 percent of those decreasing values being less than -1.2 micrograms per liter (20 percent of the MCL; table 3; Levy and Soldavini, 2026). The urban-dominated Southwestern California province group (P5) had the most substantial declines, having a median of significantly decreasing perchlorate changes of -0.8 micrograms per liter with 10 percent of those decreasing values being less than -1.8 micrograms per liter (30 percent of the MCL; table 3; Levy and Soldavini, 2026).

Perchlorate changes were most strongly correlated to changes in the geochemical indicator TDS (rho = 0.23; fig. 14) and the water-quality constituent nitrate (rho = 0.30; fig. 13). This indicates relations of perchlorate dynamics to those of legacy agricultural contamination sources, which may show accompanying attenuation due to changes in land-use practices over time. The most substantial perchlorate changes occurred in Southern California, particularly in the highly urbanized Southwestern California province group (P5; fig. 21). The areas where decreases of perchlorate were most pronounced had some of the highest concentrations in the initial status assessment (Fram and Belitz, 2011). Historic applications of Atacama fertilizers and recharge of imported Colorado River water are both reasonable sources of initially elevated ambient groundwater perchlorate in the Southwestern California province group (P5) observed in the early 2000s, which would be decreased in more recent recharge. Additionally, legacy industrial discharges, particularly from the aerospace industry, have caused groundwater contamination by perchlorate in this region (Wright and others, 2021). The substantial declines of perchlorate in Southwestern California groundwater may represent lessening of anthropogenic source inputs over time and natural attenuation in aquifers.

Figure 21. Maps of California showing study sites that had significant decreases (top), significant increases (middle), and non-significant changes (bottom) for decadal comparisons of perchlorate. Change significance is indicated for initial and decadal concentration values with non-overlapping confidence intervals. Point sizes and colors are scaled to absolute and relative concentration changes, respectively. Directional differences ranged from -4.3 to 3.5 micrograms per liter, but scales were symmetrically saturated at value of ±2 micrograms per liter to prevent outliers (less than 2 percent of change values statewide) from obscuring visualization of most change values. Data summarized from Levy and Soldavini (2026).

Herbicides

Atrazine and simazine are pre-emergent triazine herbicides with California State and federal MCLs of 1 and 4 micrograms per liter (U.S. Environmental Protection Agency, 2024; California State Water Resources Control Board, 2024), respectively, that can have carcinogenic and endocrine-disrupting effects when consumed in drinking water over the long term (California State Office of Health and Hazard Assessment, 2014). Atrazine and simazine are among the top 21 most frequently detected pesticides in groundwater nationwide (Bexfield and others, 2020). Triazine herbicides were widely applied to agricultural crops (for example, vineyards and citrus orchards) and roadside vegetation control in California, with regulations limiting use beginning in the early 1990s (Troiano and others, 2013). Triazine herbicides are more frequently detected in aquifers underlying coarse soils with high leaching capacity and legacy agricultural land uses, such as those found in the San Joaquin Valley (P7; Troiano and others, 2001, 2013) and the Upper Santa Ana River drainage basin (within the Southwestern California province group [P5]; Troiano and others, 2001; Kent and Belitz, 2012). Troiano and others (2013) attributed trends of decreasing atrazine and simazine observed in domestic wells in the San Joaquin Valley during 2000–2012 to regulatory controls on applications in California beginning in the 1990s, representing a reversal from increasing regional trends observed in prior decades (Burow and others, 2008).

Both atrazine and simazine showed significant directional decreases statewide, with simazine decreasing in areas of urban land use and atrazine decreasing in areas of both urban and agricultural land use (table 5). Both herbicides significantly decreased in the Southwestern California province group (P5; table 5). The medians of significantly decreasing atrazine and simazine changes statewide were -0.003 and -0.004 micrograms per liter, respectively, with 10

percent of those decreasing values being less than -0.028 and -0.020 micrograms per liter (2.8 and 0.5 percent of respective MCLs; table 3; Levy and Soldavini, 2026). In the Southwestern California province group (P5), the medians of significantly decreasing atrazine and simazine changes were -0.010 and -0.008 micrograms per liter, respectively, with 10 percent of those decreasing values less than -0.033 and -0.048 micrograms per liter (3 and 1 percent of respective MCLs; table 3; Levy and Soldavini, 2026).

Among geochemical indicators, simazine changes only showed significant correlation to those of alkalinity (rho = 0.40; fig. 14). Although not much is known regarding the effects of groundwater alkalinity on degradation of simazine, this correlation could also indicate a shift in groundwater sources to PSWs (higher alkalinity groundwater with simazine to lower alkalinity water without simazine) or be a spurious correlation due to the relatively low proportion of computed change values for simazine (15 percent; table 3). Atrazine changes did not show any significant correlation to the considered geochemical indicators.

We further assessed correlations of herbicide changes to those of known herbicide degradation byproducts. Of note, uncensored differences in atrazine and simazine were significantly correlated with each other (rho = 0.22) in addition to those of the herbicide degradates 3,4-dichloroaniline (rho values of 0.25 and 0.20, respectively) and 2-Chloro-4-isopropylamino-6-amino-s-triazine (CIAT; rho values of 0.20 and 0.21, respectively; Levy and Soldavini, 2026). The compound 3,4-dichloroaniline is a known degradate of the herbicide diuron and CIAT is a known degradate of atrazine (Kent and others, 2005). Although diuron has been sampled by the GAMA-PBP over the lifetime of the project, insufficient data was available for decadal trends analysis. Of the two correlated herbicide degrades, 3,4-dichloroaniline showed significant directional decreases statewide, in the urban land-use group, and in the Southwestern

California province group (P5), but CIAT did not show any significant directional changes (Levy and Soldavini, 2026).

The most substantial herbicide decreases occurred in the highly urbanized Southwestern California province (P5; fig. 22), which has a history of legacy agricultural land use, particularly in the Upper Santa Ana River drainage basin where triazine herbicides and diuron are known to have been widely applied (Kent and others, 2005; Kent and Belitz, 2012). Concomitant decreases in triazine herbicides and herbicide degradation byproducts indicate attenuation of historic herbicide applications has occurred in groundwater, particularly in the Southwestern California province group (P5) and parts of the San Joaquin Valley (P7; fig. 22). Troiano and others (2013) showed decadal attenuation of triazine herbicides and diuron occurred in groundwater within the San Joaquin Valley following establishment of compound-specific pesticide management zones (PMZs) by the California Department of Pesticide Regulation (DPR) in the 1990s. Regulatory controls implemented by the DPR in PMZs include limiting the application of pesticides if they or their degradates are detected in groundwater and establishment of agricultural best management practices to curb transport of pesticides to groundwater aquifers (Troiano and others, 2013).

Figure 22. Maps of California showing study sites that had significant decreases (top), significant increases (middle), and non-significant changes (bottom) for decadal comparisons of atrazine (left) and simazine (right). Change significance is indicated for initial and decadal concentration values with non-overlapping confidence intervals. Point sizes and colors are scaled to absolute and directional concentration changes, respectively. Directional differences ranged from -0.13 to 0.04 micrograms per liter for atrazine and -0.15 to 0.04 micrograms per liter for simazine. Respective measurement scales for both atrazine and simazine were symmetrically saturated at values of ±0.03 micrograms per liter to prevent

outliers (less than 2 percent of change values statewide) from obscuring visualization of most change values. Data summarized from Levy and Soldavini (2026).

Methyl *tert*-butyl ether (MTBE)

Methyl *tert*-butyl ether (MTBE) is a gasoline oxygenate that is carcinogenic when consumed over the long term and has a California State MCL of 13 micrograms per liter (California State Water Resources Control Board, 2017, 2024). The MTBE compound increases the combustion efficiency of gasoline and was widely used as a fuel additive in California from 1992 through 2003, when it was phased out due to concerns of groundwater contamination from leaking underground fuel tanks (LUFTs; California Air Resources Board, 2003). Landon and others (2013) found MTBE was most frequently detected in densely populated urban areas proximal to LUFTs (particularly in the Southwestern California province group [P5]), but was also detected in areas of agricultural and natural land use. Fram and Belitz (2014) attributed MTBE detections in areas of natural land use in the Sierra Nevada to non-point source pollution from atmospheric emissions of MTBE during the period of high use from 1992–2003. Schade and others (2002) found that diffusion of atmospheric sources of MTBE into surface waters could account for concentrations up to 2 micrograms per liter at a rural mountain site in the Sierra Nevada. McHugh and others (2014) found that detections of MTBE at PSWs in California peaked in 2000 and declined in the decade following its removal from gasoline formulations in the State. This is consistent with the findings of Lindsey and others (2017), which showed a decrease in detections of MTBE in groundwater that was recharged after its widespread discontinuation as a gasoline additive across the northeastern United States by 2007.

Concentrations of MTBE showed significant directional decreases statewide and in the urban land use group (table 5). The median of significantly decreasing MTBE changes statewide was -0.06 micrograms per liter, with 10 percent of those decreasing values being less than -0.36 micrograms per liter (3 percent of the MCL; table 3; Levy and Soldavini, 2026). The median of significantly decreasing MTBE changes for the urban land-use group was -0.06 micrograms per liter with 10 percent of those decreasing values being less than -0.26 micrograms per liter (2 percent of the MCL; table 3; Levy and Soldavini, 2026).

Changes in MTBE did not show significant correlations among any of the considered geochemical indicators (fig. 14). This is likely due to the relatively low proportion of changing values in the dataset (7 percent; table 3). Decreasing values were somewhat concentrated in the urbanized Southwestern California province group (P5) but occurred throughout the state including natural land use dominated areas of the Sierra Nevada (P6) and Northern Mountain Regions (P3; fig. 23). For the most part, measured concentrations were less than 10 percent of the MCL, except at four sites, three of which had urban land use. Some relatively large MTBE concentration changes (up to about -3 micrograms per liter) were classified as “no change” based on the log-log concentration model (figs. 4 and 23). This is because the relatively large changes that were classified as “no change” occurred at sites with substantially elevated concentrations (from 1.3 to 28 micrograms per liter; Levy and Soldavini, 2026). Of the respective initial and decadal sample sets, 65 and 76 percent of detected MTBE concentrations were below 0.2 micrograms per liter (Levy and Soldavini, 2026). This indicates a prevalence of low-level MTBE detections that could potentially have originated from historic non-point sources. Concentrations of MTBE at PSWs originating from both non-point and point sources are likely declining due to regulations prohibiting its use as a widespread gasoline additive in California beginning in 2004

(McHugh and others, 2014). A small number of sites (2 percent) showed increasing concentrations from initial samples collected during 2004–2011 to decadal samples collected during 2014–2022 (fig. 23), which notably occurred after MTBE use as a gasoline additive declined in California. Lindsey and others (2017) found increases of MTBE could occur in drinking-supply wells following phasing out of MTBE as a gasoline additive depending on the age distribution of groundwater captured by a given well.

Figure 23. Maps of California showing study sites that had significant decreases (top), significant increases (middle), and non-significant changes (bottom) for decadal comparisons of methyl *tert*-butyl ether (MTBE). Change significance is indicated for initial and decadal concentration values with non-overlapping confidence intervals. Point sizes and colors are scaled to absolute and directional concentration changes, respectively. Directional differences ranged from -3.2 to 2.3 micrograms per liter, but scales were symmetrically saturated at value of ±0.29 micrograms per liter to prevent outliers (less than 2 percent of change values statewide) from obscuring visualization of most change values. Data summarized from Levy and Soldavini (2026).

Study Limitations and Considerations for Future Work

The current study presents a network-scale analysis of trends in the quality of groundwater used for public drinking supply across California. Network-scale analyses of step trends can be used to determine prevalent changes to a resource in specific geographic or land-use settings (Lindsey and Rupert, 2012). A latent assumption in this analysis is that similar drivers of change are occurring within a given network group, which may be complicated by various factors discussed by Lindsey and others (2023), including uncertainty in contaminant sources and heterogenous transit times of recharge to well intakes. The current study leveraged about 20 percent of the original statewide network used to statistically characterize public-supply

aquifers across California (Belitz and others, 2015). Therefore, to improve statistical power, original geographic groupings were aggregated into large province groups where groundwater quality is likely affected by diverse factors. Detection of significant groundwater-quality trends at the network-group scale is therefore a first order indicator of change within various geographies or land-use settings, and further work could help to identify sub-populations of monitoring sites that may be contributing most to positive test results.

Further, detection of a network-scale trend is inherently biased towards constituents that have regionally prevalent sources, such as those from ubiquitous geologic materials or anthropogenic, non-point sources. The current study therefore is biased against detection of trends for contaminants that tend to have point sources, such as solvent plumes from industrial discharges. Relatedly, many organic constituents with anthropogenic sources had relatively low detection frequencies in this study and could not easily be evaluated for network-scale regional trends. For example, 1,2,3-TCP, a fumigant constituent, had a 13 percent detection frequency at decadal trends sites in the San Joaquin Valley (P7; either in initial or decadal samples after censoring to the higher of the two RLs; Levy and Soldavini, 2026), where historical agricultural applications were widespread (Burow and others, 2019). Although no trend in 1,2,3-TCP was detected in the San Joaquin Valley, it was only detected at 9 study sites, which limits quantification of regional dynamics when aggregated with a majority of unchanging values from study sites where it was not detected. A similarly non-significant trend result was shown for the nematocide 1,2-dibromo-3-chloropropane (DBCP), despite some studies that have shown localized trends in different portions of regional aquifer systems in the San Joaquin Valley where it was widely applied prior to the late-1970s (Burow and others, 2008). Therefore, understanding trends for organic constituents with relatively low network-scale detection frequencies may also

benefit from targeted, local-scale trend studies to understand drivers and dynamics in areas where those constituents are known to occur in groundwater (Troiano and others, 2013).

In this study, we present a novel approach for identification of high-magnitude water-quality changes at the monitoring-network scale. This system helped to identify constituents that did not often have significant directional changes but showed large and sometimes countervailing shifts in groundwater quality (for example, nitrate and arsenic; table 5). This method effectively highlights constituents that show large (greater than 10 percent of the benchmark) decadal changes in groundwater quality but is sensitive to the presence of outliers in small network groups or for constituents where very few decadal pairs had quantifiable changes. For example, the Northern Mountain Regions province group (P2) was the smallest network group and only had 24 decadal pairs for arsenic, of which 33 percent (n = 8) showed increasing values. For such a small dataset, relatively few increases exceeding 1 microgram per liter (10 percent of the MCL) would be enough to trigger the high-magnitude change designation. In this specific case, four of the increases were greater than 1 microgram per liter including an outlier increase of 13 micrograms per liter (Levy and Soldavini, 2026). Therefore, although high-magnitude change designations may warrant more in-depth investigation they can still serve as a first-order indicator that water-quality changes at levels relevant to human health and safety are potentially occurring in a network group.

Conclusions

This study made a comprehensive assessment of decadal changes in the quality of groundwater used for public drinking-water supply across California at 444 public-supply well network monitoring sites during 2004-2023. We assessed decadal step trends in groundwater quality for 145 water-quality constituents and geochemical indicators statewide and across hydrogeologic province and land-use based network groups. We evaluated the statistical significance of directional changes (increase or decrease of constituent concentrations) and the magnitude of those changes across all network groups.

Of the inorganic constituents with regulatory, health-based benchmarks, uranium showed the most widespread directional and high-magnitude increases statewide, particularly in the agriculture-dominated Central Valley and urban- and desert-dominated regions of Southern California. Fluoride and perchlorate showed the most widespread directional and high-magnitude decreases statewide, which were also most pronounced in Southern California. Nitrate and arsenic tended to show high-magnitude changes in water quality, with many changes being greater than 10 percent of respective regulatory benchmarks, but were often bidirectional at the network scale and did not show persistent directional changes except for in the San Joaquin Valley and Northern Mountain Regions, where they respectively increased.

Of the organic constituents with regulatory, health-based benchmarks triazine herbicides (atrazine and simazine) significantly decreased statewide, particularly in agricultural areas and urbanized areas of Southern California with historic agricultural land use. The gasoline oxygenate methyl *tert*-butyl ether (MTBE) also decreased statewide and in areas of

predominantly urban land use. However, changes for these constituents were not considered to be of high magnitude compared to respective regulatory benchmarks.

Constituents with non-regulatory health-based or aesthetic benchmarks that showed significant directional or high-magnitude changes included boron, molybdenum, strontium, vanadium, chloride, iron, manganese, sulfate, and total dissolved solids (TDS). Of these, TDS, iron, and manganese showed directional and high-magnitude increases statewide and in agricultural areas, with iron and manganese showing both high-magnitude increases and decreases across most of the network groups. The salinity constituents chloride, strontium, and sulfate showed prevalent and directional increases statewide and across many of the network groups, but increasing values were not of high magnitude compared to respective benchmarks.

Analysis of geochemical indicators showed prevalent directional increases of alkalinity and calcium statewide and across many of the network groups, which are predominant components of increasing groundwater TDS. Widespread increases in groundwater alkalinity and calcium across agricultural and urban areas may be related, in part, to warm-season irrigation and other anthropogenic factors that have shifted soil weathering dynamics over the long term. Increasing alkalinity concentrations were related to increasing uranium concentrations, particularly in areas with aquifer materials derived from granitic rocks. Conversely, increasing calcium concentrations were related to decreasing fluoride concentrations, particularly in areas where fluoride occurred naturally at elevated concentrations.

Perchlorate, triazine herbicides, and MTBE all showed prevalent decreases that may be related to lessening of anthropogenic source inputs over time and natural attenuation in aquifers. Decreases in perchlorate concentrations were most pronounced in groundwater systems in Southern California, which could be due to multiple factors including land-use changes, lessened

use of Atacama fertilizers, and mitigation of contamination in the Colorado River by 2010. Triazine herbicides and MTBE both had increased regulatory controls in California beginning in the 1990s and early 2000s, respectively, that limited their inputs to groundwater. Additionally, decreases in herbicides were often associated with accompanying decreases in herbicide degradates, providing additional evidence of their decay and attenuation within regional aquifer systems. These results indicate that controls over inputs of anthropogenic contaminants coupled with natural attenuation in aquifers over time have resulted in decreasing trends for these constituents in aquifers used for public drinking-water supply.

References Cited

Ayotte, J.D., Szabo, Z., Focazio, M.J., and Eberts, S.M., 2011, Effects of human-induced alteration of groundwater flow on concentrations of naturally-occurring trace elements at water-supply wells: Applied Geochemistry, v. 26, no. 5, p. 747–762, accessed March 5, 2025, at https://doi.org/10.1016/j.apgeochem.2011.01.033.

Ayotte, J.D., Nolan, B.T., and Gronberg, J.A.M., 2016, Predicting arsenic in drinking water wells of the Central Valley, California: Environmental Science & Technology, v. 50, no. 4, p. 7555–7563, accessed March 5, 2025, at https://doi.org/10.1021/acs.est.6b01914.

Balkan, M., Levy, Z.F., Dupuy, D.I., Shelton, J.L., Johnson, T.D., and Watson, E., 2021, Groundwater-quality data in the Modesto-Turlock-Merced Domestic-Supply Aquifer Study Unit, 2020-2021: Results from the California GAMA Priority Basin Project: U.S. Geological Survey data release, https://doi.org/10.5066/P96R55KQ.

Bastani, M., and Harter, T., 2019, Source area management practices as remediation tool to address groundwater nitrate pollution in drinking supply wells: Journal of Contaminant

Hydrology, v. 103521, p. 1–17, accessed March 5, 2025, at https://doi.org/10.1016/j.jconhyd.2019.103521.

Bexfield, L.M., Belitz, K., Lindsey, B.D., Toccalino, P.L., and Nowell, L.H., 2020, Pesticides and pesticide degradates in groundwater used for public supply across the United States: Occurrence and human-health context: Environmental Science & Technology, v. 55, no. 1, p. 362–372, accessed March 5, 2025, at https://doi.org/10.1021/acs.est.0c05793.

Bottrell, S., Hipkins, E.V., Lane, J.M., Zegos, R.A., Banks, D., and Frengstad, B.S., 2019, Carbon-13 in groundwater from English and Norwegian crystalline rock aquifers: A tool for deducing the origin of alkalinity?: Sustainable Water Resources Management, v. 5, p. 267–287, accessed March 5, 2025, at https://doi.org/10.1007/s40899-017-0203-7.

Burow, K.R., Belitz, K., Dubrovsky, N.M., and Jurgens, B.C., 2017, Large decadal-scale changes in uranium and bicarbonate in groundwater of the irrigated western U.S: Science of the Total Environment, v. 586, p. 87–95, accessed March 5, 2025, at https://doi.org/10.1016/j.scitotenv.2017.01.220.

Burow, K.R., Floyd, W.D., and Landon, M.K., 2019, Factors affecting 1,2,3-trichloropropane contamination in groundwater in California: Science of the Total Environment, v. 672, p. 324–334, accessed March 5, 2025, at https://doi.org/10.1016/j.scitotenv.2019.03.420.

Burow, K.R., Jurgens, B.C., Belitz, K., and Dubrovsky, N.M., 2013, Assessment of regional change in nitrate concentrations in groundwater in the Central Valley, California, USA, 1950s–2000s: Environmental Earth Sciences, v. 69, no. 8, 2609–2621, accessed March 5, 2025, at https://doi.org/10.1007/s12665-012-2082-4.

Burow, K.R., Shelton, J.L., and Dubrovsky, N.M., 2008, Regional nitrate and pesticide trends in ground water in the eastern San Joaquin Valley, California: Journal of Environmental Quality, v. 37, no. S5, p. S249–S263, accessed March 5, 2025, at https://doi.org/10.2134/jeq2007.0061.

Burow, K.R., Shelton, J.L., and Fram, M.S., 2024, Status of water quality in groundwater resources used for drinking-water supply in the southeastern San Joaquin Valley, 2013–15—California GAMA Priority Basin Project: U.S. Geological Survey Scientific Investigations Report 2024–5009, 135 p., accessed March 5, 2025, at https://doi.org/10.3133/sir20245009.

Belitz, K., Fram, M.S., and Johnson, T.D., 2015, Metrics for assessing the quality of groundwater used for public supply, CA, USA—Equivalent-population and area: Environmental Science & Technology, v. 49, no. 14, p. 8330–8338, accessed March 5, 2025, at https://doi.org/10.1021/acs.est.5b00265.

Belitz, K., Fram, M.S., Lindsey, B.D., Stackelberg, P.E., Bexfield, L.M., Johnson, T.D., Jurgens, B.C., Kingsbury, J.A., McMahon, P.B., Dubrovsky, N.M., 2022, Quality of groundwater used for public supply in the continental United States: A comprehensive assessment: ACS EST Water, v. 2, p. 2645−2656, accessed March 5, 2025, at https://doi.org/10.1021/acsestwater.2c00390.

Belitz, K., Jurgens, B.C., Landon, M.K., Fram, M.S., and Johnson, T., 2010, Estimation of aquifer scale proportion using equal area grids—Assessment of regional scale groundwater quality: Water Resources Research, v. 46, no. 11, p. 1–14, accessed March 5, 2025, at https://doi.org/10.1029/2010WR009321.

Bennett, G.L., V, 2020, Updated study reporting levels (SRLs) for trace-element data collected for the California Groundwater Ambient Monitoring and Assessment (GAMA) Program Priority Basin Project, October 2009–October 2018: U.S. Geological Survey Scientific

Investigations Report 2020–5034, 24 p., accessed March 5, 2025, at https://doi.org/10.3133/sir20205034.

Bennett, G.L., V, and Fram, M.S., 2014, Groundwater-quality data in the North San Francisco Bay Shallow Aquifer study unit, 2012—Results from the California GAMA Program: U.S. Geological Survey Data Series 865, 94 p., accessed March 5, 2025, at http://dx.doi.org/10.3133/ds865.

Broers, H.P, Visser, A., Chilton, J.P., Stuart, M.E., 2009, Assessing and Aggregating Trends in Groundwater Quality, *in* Quevauviller, P., Fouillac, A.M., Grath, J., Ward, R., eds., Groundwater Monitoring: Wiley, 15 p., accessed March 5, 2025, at https://doi.org/10.1002/9780470749685.ch12.

California Air Resources Board, 2003, California Code of Regulations, Title 13, Division 3 Air Resources Board, Chapter 5, Standards for motor vehicle fuels, Article 1, Standards for gasoline, §2262.6 Prohibition of MTBE and oxygenates other than ethanol in California gasoline starting December 31, 2003.

California Department of Finance, 2025, Estimates – E1: Population and Housing Estimates for Cities, Counties, and the State — January 1, 2024 and 2025, accessed November 19, 2025, at https://dof.ca.gov/forecasting/demographics/estimates-e1/.

California State Office of Health and Hazard Assessment, 2014, Notice of Intent to List: Atrazine, Propazine, Simazine and their Chlorometabolites DACT, DEA and DIA, accessed March 5, 2025, at https://oehha.ca.gov/proposition-65/crnr/notice-intent-list-atrazine-propazine-simazine-and-their-chlorometabolites-dact-dea-and-dia

California State Water Resources Control Board, 2017, Groundwater Fact Sheet Methyl tertiary-butyl ether (MTBE), 6 p., accessed March 5, 2025, at https://www.waterboards.ca.gov/gama/docs/coc_mtbe.pdf.

California State Water Resources Control Board, 2024, California Drinking Water-Related Statutes and Regulations, accessed March 5, 2025, at https://www.waterboards.ca.gov/drinking_water/certlic/drinkingwater/Lawbook.html.

California State Water Resources Control Board, 2025, Salt and Nutrient Management Planning (SNMP), accessed November 19, 2025, at https://www.waterboards.ca.gov/water_issues/programs/recycled_water/snmp.html.

Castaldo, G., Visser, A., Fogg, G.E., and Harter, T., 2021, Effect of groundwater age and recharge source on nitrate concentrations in domestic wells in the San Joaquin Valley: Environmental Science & Technology, v. 55, no. 4, p. 2265–2275, accessed March 5, 2025, at https://doi.org/10.1021/acs.est.0c03071.

Clark, I.D., and Fritz, P., 1997, Environmental isotopes in hydrogeology: New York, CRC Press, 328 p.

Dasgupta, P.K., Martinelango, P.K., Jackson, W.A., Anderson, T.A., Tain, K., Tock, R.W., and Rajagopalan, S., 2005, The origin of naturally occurring perchlorate: the role of atmospheric processes: Environmental Science & Technology, v. 39, no. 6, p. 1569–1575, accessed November 19, 2025, at https://doi.org/10.1021/es048612x.

Degnan, J.R., Kauffman, L.J., Erickson, M.L., Belitz, K., and Stackelberg, P.E., 2021, Depth of groundwater used for drinking-water supplies in the United States: U.S. Geological Survey Scientific Investigations Report 2021–5069, 69 p., accessed March 5, 2025, at https://doi.org/10.3133/sir20215069.

Duan, N., 1983, Smearing estimate—A nonparametric retransformation method: Journal of the American Statistics Association, v. 78, p. 605–610, accessed March 5, 2025, at https://doi.org/10.2307/2288126.

Dubrovsky, N.M., Burow, K.R., Clark, G.M., Gronberg, J.M., Hamilton P.A., Hitt, K.J., Mueller, D.K., Munn, M.D., Nolan, B.T., Puckett, L.J., Rupert, M.G., Short, T.M., Spahr, N.E., Sprague, L.A., and Wilber, W.G., 2010, The quality of our Nation's waters—Nutrients in the Nation's streams and groundwater, 1992–2004: U.S. Geological Survey Circular 1350, 174 p., accessed November 19, 2025, at http://water.usgs.gov/nawqa/nutrients/pubs/circ1350.

Edmunds, W.M., and Smedley, P.L., 2013. Fluoride in natural waters, *in* Selinus, O., ed., Essentials of Medical Geology: Springer, Dordrecht, p. 311–336, accessed March 5, 2025, at https://doi.org/10.1007/978-94-007-4375-5_13.

Ericksen, G.E., 1981, Geology and Origin of the Chilean Nitrate Deposits: U.S. Geological Survey Professional Paper 1188, 37 p., accessed November 19, 2025, at https://pubs.usgs.gov/pp/1188/report.pdf.

Faunt, C.C., ed., 2009, Groundwater availability of the Central Valley Aquifer, California: U.S. Geological Survey Professional Paper 1766, 225 p., accessed March 5, 2025, at https://pubs.usgs.gov/pp/1766/.

Foreman, W.T., Williams, T.L., Furlong, E.T., Hemmerle, D.M., Stetson, S.J., Jha, V.K., Noriega, M.C., Decess, J.A., Reed-Parker, C., Sandstrom, M.W., 2021, Comparison of detection limits estimated using single- and multi-concentration spike-based and blank-based procedures: Talenta, v. 228, 122139, accessed November 19, 2025, at https://doi.org/10.1016/j.talanta.2021.122139.

Fram, M.S., 2017, Groundwater quality in the Western San Joaquin Valley study unit, 2010: California GAMA Priority Basin Project: U.S. Geological Survey Scientific Investigations Report 2017–5032, 130 p., accessed December 16, 2025, at https://doi.org/10.3133/sir20175032.

Fram, M.S., and Belitz, K., 2011, Probability of detecting perchlorate under natural conditions in deep groundwater in California and the southwestern United States: Environmental Science & Technology, v. 45, no. 4, p. 1271–1277, accessed March 5, 2025, at https://doi.org/10.1021/es103103p.

Fram, M.S., and Belitz, K., 2014, Status and understanding of groundwater quality in the Sierra Nevada Regional study unit, 2008—California GAMA Priority Basin Project: U.S. Geological Survey Scientific Investigations Report 2014–5174, 118 p., accessed March 5, 2025, at https://doi.org/10.3133/sir20145174.

Fram, M.S., Olsen, L.D., and Belitz, K., 2012, Evaluation of volatile organic compound (VOC) blank data and application of study reporting levels to groundwater data collected for the California GAMA Priority Basin Project, May 2004 through September 2010: U.S. Geological Survey Scientific Investigations Report 2012–5139, 94 p., accessed March 5, 2025, at https://pubs.usgs.gov/sir/2012/5139/pdf/sir20125139.pdf.

Fram, M.S., and Stork, S.V., 2019, Determination of study reporting limits for pesticide constituent data for the California Groundwater Ambient Monitoring and Assessment Program Priority Basin Project, 2004–2018—Part 1: National Water Quality Schedules 2003, 2032, or 2033, and 2060: U.S. Geological Survey Scientific Investigations Report 2019–5107, 129 p., accessed March 5, 2025, at https://doi.org/10.3133/sir20195107.

Hansen, J.A., Jurgens, B.C., and Fram, M.S., 2018, Quantifying anthropogenic contributions to century-scale groundwater salinity changes, San Joaquin Valley, California, USA: Science of the Total Environment, v. 642, p. 125–136, accessed March 5, 2025, at https://doi.org/10.1016/j.scitotenv.2018.05.333.

Harkness, J.S., and Jurgens, B.C., 2022, Effects of imported recharge on fluoride trends in groundwater used for public supply in California: Science of the Total Environment, v. 830, no. 15, 154782, accessed March 5, 2025, at https://doi.org/10.1016/j.scitotenv.2022.154782.

Harkness, J.S., McCarthy, P.M., Jurgens, B.C., and Levy, Z.F., 2023, Salinity trends in a groundwater system supplemented by 50 years of imported Colorado River water: Environmental Science & Technology, v. 3, no. 10, p. 3253–3264, accessed December 12, 2025, at https://doi.org/10.1021/acsestwater.3c00239.

Hastie, T., Tibshirani, R., and Friedman, J.H., 2009, The elements of statistical learning: Data mining, inference, and prediction: Springer, 745 p.

Haugen, E.A., Jurgens, B.C., Arroyo-Lopez, J.A., and Bennett, G.L., V, 2021, Groundwater development leads to decreasing arsenic concentrations in the San Joaquin Valley, California: Science of the Total Environment, v. 771, 145223, accessed March 5, 2025, at https://doi.org/10.1016/j.scitotenv.2021.145223.

Helsel, D.R., and Frans, L.M., 2006, Regional Kendall test for trend: Environmental Science & Technology, v. 40, no. 13, p. 4066–4073, accessed March 5, 2025, at https://doi.org/10.1021/es051650b.

Helsel, D.R., Hirsch, R.M., Ryberg, K.R., Archfield, S.A., and Gilroy, E.J., 2020, Statistical methods in water resources: U.S. Geological Survey Techniques and Methods, book 4, chap. A3, 458 p., accessed March 5, 2025, at https://doi.org/10.3133/tm4a3.

Hem, J.D., 1967, Chemical equilibria and rates of manganese oxidation: U.S. Geological Survey Water-Supply Paper 1667-A, 71 p., accessed March 5, 2025, at https://pubs.usgs.gov/publication/wsp1667A.

Hem, J.D., 1985, Study and interpretation of the chemical characteristics of natural water (3rd ed.): U.S. Geological Survey Water Supply Paper 2254, 263 p., accessed March 5, 2025, at https://doi.org/10.3133/wsp2254.

Hirsch, R.M., Alley, W.M., and Wilber, W.G., 1988, Concepts for a National Water-Quality Assessment Program: U.S. Geological Survey Circular 1021, 54 p., accessed March 5, 2025, at https://pubs.usgs.gov/circ/1988/1021/report.pdf.

Hothorn, T., Hornik, K., van de Wiel, M.A., and Zeileis, A., 2008, Implementing a class of permutation tests: The coin package: Journal of Statistical Software, v. 28, no. 8, p. 1–23, accessed March 5, 2025, at https://doi.org/10.18637/jss.v028.i08.

Izbicki, J.A., Christensen, A.H., Newhouse, M.W., Smith, G.A., and Hansen, R.T., 2005, Temporal changes in the vertical distribution of flow and chloride in deep wells: Groundwater, v. 4, no. 4, p. 531–544, accessed March 5, 2025, at https://doi.org/10.1111/j.1745-6584.2005.0032.x.

Jin, S., Yang, L., Danielson, P., Homer, C., Fry, J., and George, X., 2013, A comprehensive change detection method for updating the National Land Cover Database to circa 2011: Remote Sensing of Environment, v. 132, p. 159–175, accessed March 5, 2025, at https://doi.org/10.1016/j.rse.2013.01.012.

Johnson, T. and Belitz, K., 2003, Hydrogeologic Provinces for California based upon established groundwater basins and watershed polygons: U.S. Geological Survey data release, accessed March 5, 2025, at https://doi.org/10.5066/P9UTSDXK.

Johnson, T.D., and Belitz, K., 2009, Assigning land use to supply wells for the statistical characterization of regional groundwater quality: Correlating urban land use and VOC occurrence: Journal of Hydrology, v. 370, p. 100–108, accessed March 5, 2025, at https://doi.org/10.1016/j.jhydrol.2009.02.056.

Johnson, T.D., Belitz, K., and Lombard, M.A., 2019, Estimating domestic well locations and populations served in the contiguous U.S. for years 2000 and 2010: Science of the Total Environment, v. 687, p. 1261–1273, accessed March 5, 2025, at https://doi.org/10.1016/j.scitotenv.2019.06.036.

Johnson, T.D., Belitz, Kenneth, Kauffman, L.J., Watson, Elise, and Wilson, J.T., 2022, Populations using public-supply groundwater in the conterminous U.S. 2010; Identifying the wells, hydrogeologic regions, and hydrogeologic mapping units: Science of the Total Environment, v. 806, Part 2, 150618, p. 1–15, accessed March 5, 2025, at https://doi.org/10.1016/j.scitotenv.2021.150618.

Jurgens, B.C., Faulkner, K.E., McMahon, P. B., Hunt, A.G., Casile, G., Young, M.B., and Belitz, K., 2022, Over a third of groundwater in USA public-supply aquifers is Anthropocene-age and susceptible to surface contamination: Communications Earth & Environment, v. 3, no. 153, p. 1–9, accessed March 5, 2025, at https://doi.org/10.1038/s43247-022-00473-y.

Jurgens, B.C., Fram, M.S., Belitz, K., Burow, K.R., and Landon, M.K., 2010, Effects of groundwater development on uranium: Central Valley, California, USA: Groundwater, v. 48, no. 6, p. 913–928, accessed March 5, 2025, at https://doi.org/10.1111/j.1745-6584.2009.00635.x.

Jurgens, B.C., Fram, M.S., Rutledge, J., and Bennett, G.L., V, 2020, Identifying areas of degrading and improving groundwater-quality conditions in the State of California, USA,

1974-2014: Environmental Monitoring and Assessment, v. 192, no. 250, p. 1–23, accessed March 5, 2025, at https://doi.org/10.1007/s10661-020-8180-y.

Kang, M., Perrone, D., Wang, Z., Jasechko, S., and Rohde, M.M., 2020, Base of fresh water, groundwater salinity, and well distribution across California: Proceedings of the National Academy of Sciences, v. 117, no. 51, p. 32302–32307, accessed March 5, 2025, at https://doi.org/10.1073/pnas.2015784117.

Kent, R., 2018, Variations on a method for evaluating decadal-scale changes in the groundwater quality of two GAMA coastal study units 2004–14, California GAMA Priority Basin Project: U.S. Geological Survey Scientific Investigations Report 2018–5088, 75 p., accessed March 5, 2025, at https://doi.org/10.3133/sir20185088.

Kent, R., and Belitz, K., 2012, Status of groundwater quality in the Upper Santa Ana Watershed, November 2006–March 2007—California GAMA Priority Basin Project: U.S. Geological Survey Scientific Investigations Report 2012–5052, 88 p., accessed March 5, 2025, at https://pubs.usgs.gov/sir/2012/5052/.

Kent, R., Belitz, K., Altmann, A.J., Wright, M.T., and Mendez, G.O., 2005, Occurrence and distribution of pesticide compounds in surface water of the Santa Ana Basin, California, 1998–2001: U.S. Geological Survey Scientific Investigations Report 2005-5203, 143 p., accessed March 5, 2025, at https://pubs.usgs.gov/sir/2005/5203/sir2005-5203.pdf.

Kent, R., and Landon, M.K., 2013, Trends in concentrations of nitrate and total dissolved solids in public supply wells of the Bunker Hill, Lytle, Rialto, and Colton groundwater subbasins, San Bernardino County, California: Influence of legacy land use: Science of the Total Environment, v. 452–453, no. 1, p. 125–136, accessed March 5, 2025, at https://doi.org/10.1016/j.scitotenv.2013.02.042.

Kent, R., and Landon, M.K., 2016, Triennial changes in groundwater quality in aquifers used for public supply in California: utility as indicators of temporal trends: Environmental Monitoring and Assessment, v. 188, no. 610, p. 1–17, accessed March 5, 2025, at https://doi.org/10.1007/s10661-016-5618-3.

Klaus, M., 2024, Decadal increase in groundwater inorganic carbon concentrations across Sweden: Communications Earth & Environment, v. 4, no. 221, accessed March 5, 2025, at https://doi.org/10.1038/s43247-023-00885-4.

Kurttio, P., Auvinen, A., Salonen, L., Saha, H., Pekkanen, J., Mäkeläinen, I., Väisänen, S.B., Penttilä, I.M., Komulainen, H., 2002. Renal effects of uranium in drinking water: Environmental Health Perspectives, v. 110, no. 4, p. 337–342, accessed March 5, 2025, at https://doi.org/10.1289/ehp.0211033.

Levy, Z.F., Jurgens, B.C., Burow, K.R., Voss, S.A., Faulkner, K.E., Arroyo-Lopez, J.A., and Fram, M.S., 2021, Critical aquifer overdraft accelerates degradation of groundwater quality in California's Central Valley during drought: Geophysical Research Letters, v. 48, e2021GL094398, accessed March 5, 2025, at https://doi.org/10.1029/2021GL094398.

Levy, Z.F., Jurgens, B.C., Faulkner, K.E., Harkness, J.S., and Fram, M.S., 2024, Basin-scale responses of groundwater-resource quality to drought and recovery, San Joaquin Valley, California: Hydrological Processes, v. 38, no. 4, e15131, accessed March 5, 2025, at https://doi.org/10.1002/hyp.15131.

Levy, Z.F., and Soldavini, A.L., 2026, Data for Analysis of Decadal Trends in the Quality of Groundwater Used for Public Drinking-Water Supply in California, 2004-2023, California GAMA Priority Basin Project: U.S. Geological Survey data release, https://doi.org/10.5066/P137ZTJE.

Lindsey, B.D., Jurgens, B.C., and Belitz, K., 2019, Tritium as an indicator of modern, mixed, and premodern groundwater age: U.S. Geological Survey Scientific Investigations Report 2019–5090, 18 p., accessed March 5, 2025, at https://doi.org/10.3133/sir20195090.

Lindsey, B.D. Fleming, B.J., Goodling, P.J., and Dondero, A.M., 2023, Thirty years of regional groundwater-quality trend studies in the United States: Major findings and lessons learned: Journal of Hydrology, v. 627, Part A, 130427, p. 1–22, accessed March 5, 2025, at https://doi.org/10.1016/j.jhydrol.2023.130427.

Lindsey, B.D., Ayotte, J.D., Jurgens, B.C., and Desimone, L.A., 2017, Using groundwater age distributions to understand changes in methyl *tert*-butyl ether (MtBE) concentration in ambient groundwater, northeastern United States: Science of the Total Environment, v. 579, no. 1, p. 579–587, accessed September 22, 2025, at https://doi.org/10.1016/j.scitotenv.2016.11.058.

Lindsey, B.D., and Rupert, M.G., 2012, Methods for evaluating temporal groundwater quality data and results of decadal-scale changes in chloride, dissolved solids, and nitrate concentrations in groundwater in the United States, 1988–2010: U.S. Geological Survey Scientific Investigations Report 2012–5049, 46 p., accessed March 5, 2025, at https://pubs.usgs.gov/sir/2012/5049/support/sir2012-5049.pdf.

Lopez, A.M., Wells, A., and Fendorf, S., 2021, Soil and aquifer properties combine as predictors of groundwater uranium concentrations within the Central Valley, California: Environmental Science & Technology, v. 55, p. 352–361, accessed March 5, 2025, at https://dx.doi.org/10.1021/acs.est.0c05591.

Loftis, J.C., 1996, Trends in groundwater quality: Hydrological Processes, v. 10, no. 2, p. 335–355, accessed March 5, 2025, at https://doi.org/10.1002/(SICI)1099-1085(199602)10:2%3C335::AID-HYP359%3E3.0.CO;2-T.

Lombard, M.A., Bryan, M.S., Jones, D.K., Bulka, C., Bradley, P.M., Backer, L.C., Focazio, M.J., Silverman, D.T., Toccalino, P., Argos, M., Gribble, M.O., and Ayotte, J.D., 2021, Machine learning models of arsenic in private wells throughout the conterminous United States as a tool for exposure assessment in human health studies: Environmental Science & Technology, v. 55, no. 8, p. 5012–5023, accessed March 5, 2025, at https://doi.org/10.1021/acs.est.0c05239.

McHugh, T.E., Rauch, S.R., Paquette, S.M., Connor, J.A., and Daus, A.D., 2015, Life cycle of methyl tert-butyl ether in California public water supply wells: Environmental Science & Technology Letters, v. 2, no. 1, p. 7–11, accessed March 5, 2025, at https://doi.org/10.1021/ez500377t.

McMahon, P.B., Belitz, K., Reddy, J.E., and Johnson, T.D., 2018, Elevated Manganese Concentrations in United States Groundwater, Role of Land Surface–Soil–Aquifer Connections: Environmental Science & Technology, v. 53, no. 1, p. 29–38, accessed March 5, 2025, at https://doi.org/10.1021/acs.est.8b04055.

McMahon, P.B., Brown, C.J., Johnson, T.D., Belitz, K., and Lindsey, B.D., 2020, Fluoride occurrence in United States groundwater: Science of the Total Environment, v. 732, 139217, p. 1–15, accessed March 5, 2025, at https://doi.org/10.1016/j.scitotenv.2020.139217.

McMahon, P., Chapelle, F.H., 2008, Redox processes and water quality of selected principal aquifer systems: Ground Water, v. 46, no. 2, p. 259-271, accessed February 23, 2026, at https://doi.org/10.1111/j.1745-6584.2007.00385.x.

Murtagh, F., and Legendre, P., 2014, Ward's hierarchical agglomerative clustering method: Which algorithms implement Ward's criterion?: Journal of Classification, v. 31, p. 274–295, accessed March 5, 2025, at https://doi.org/10.1007/s00357-014-9161-z.

Mueller, D.K., Schertz, T.L., Martin, J.D., and Sandstrom, M.W., 2015, Design, analysis, and interpretation of field quality-control data for water-sampling projects: U.S. Geological Survey Techniques and Methods, book 4, chap. C4, 54 p., accessed March 5, 2025, at http://dx.doi.org/10.3133/tm4C4.

Musgrove, M., 2021, The occurrence and distribution of strontium in U.S. groundwater: Applied Geochemistry, v. 126, no. 104867, p. 1–18, accessed September 22, 2025, at https://doi.org/10.1016/j.apgeochem.2020.104867.

National Research Council, 2012, Preparing for the Third Decade of the National Water-Quality Assessment Program: The National Academies Press, Washington, DC, 200 p., accessed March 5, 2025, at https://doi.org/10.17226/13464.

Nozawa-Inoue, M., Scow, K.M., and Rolston, D.E., 2005, Reduction of perchlorate and nitrate by microbial communities in vadose soil: Applied and Environmental Microbiology, v. 71, no. 7, p. 3928–3934, accessed November 19, 2025, at https://doi.org/10.1128/AEM.71.7.3928-3934.2005.

O'Leary, D., Izbicki, J.A., and Metzger, L.F., 2015, Sources of high-chloride water and managed aquifer recharge in an alluvial aquifer in California, USA: Hydrogeology Journal, v. 23, p. 1515–1533, accessed March 5, 2025, at https://doi.org/10.1007/s10040-015-1277-7.

Pauloo, R.A., Fogg, G.E., Guo, Z., and Harter, T., 2021, Anthropogenic basin closure and groundwater salinization (ABCSAL): Journal of Hydrology, v. 593, 125787, p. 1–13, accessed March 5, 2025, at https://doi.org/10.1016/j.jhydrol.2020.125787.

Pratt, J.W., 1959, Remarks on zeros and ties in the Wilcoxon signed rank procedures: Journal of the American Statistical Association, v. 54, p. 655–667, accessed March 5, 2025, at https://doi.org/10.1080/01621459.1959.10501526.

R Core Team, 2024, R: A language and environment for statistical computing: R Foundation for Statistical Computing, accessed March 5, 2025, at https://www.R-project.org/.

Ransom, K.M., Nolan, B.T., Traum, J.A., Faunt, C.C., Bell, A.M., Gronberg, J.A., Wheeler, D.C., Rosecrans, C.Z., Jurgens, B.C., Schwarz, G.E., and Belitz, K., 2017, A hybrid machine learning model to predict and visualize nitrate concentration throughout the Central Valley aquifer, California, USA: Science of the Total Environment, v. 601–602, p. 1160–1172, accessed March 5, 2025, at https://doi.org/10.1016/j.scitotenv.2017.05.192.

Rajagopalan, S., Anderson, T.A., Fahlquist, L., Rainwater, K.A., Ridley, M., and Jackson, W.A., 2006, Widespread presence of naturally occurring perchlorate in high plains of Texas and New Mexico: Environmental Science & Technology, v. 40, no. 10, p. 3156–3162, accessed November 19, 2025, at https://doi.org/10.1021/es052155i.

Rosen, M.R., Burow, K.R., and Fram, M.S., 2019, Anthropogenic and geologic causes of anomalously high uranium concentrations in groundwater used for drinking water supply in the southeastern San Joaquin Valley, CA: Journal of Hydrology, v. 577, 124009, p. 1–15, accessed March 5, 2025, at https://doi.org/10.1016/j.jhydrol.2019.124009.

Rounds, S.A., Wilde, F.D., 2012, Chapter A6. Section 6.6. Alkalinity and acid neutralizing capacity (Version 3, Revised Jul 2006): U.S. Geological Survey Techniques of Water-Resources Investigations 09-A6.6, 53 p., accessed February 23, 2026, at https://doi.org/10.3133/twri09A6.6.

Schade, G.W., Dreyfus, G.B., and Goldstein, A.H., 2002, Atmospheric methyl tertiary butyl ether (MTBE) at a rural mountain site in California: Journal of Environmental Quality, v. 31, no. 4, p. 1088–1094, accessed March 5, 2025, at https://doi.org/10.2134/jeq2002.1088.

Scott, J.C., 1990, Computerized stratified random site-selection approaches for design of a ground-water quality sampling network: U.S. Geological Survey Water-Resources Investigations Report 90-4101, 109 p., accessed September 22, 2025, at https://pubs.usgs.gov/wri/1990/4101/report.pdf.

Seltzer, A.M., Bekaert, D.V., Barry, P.H., Durkin, D.V., Mace, E.K., Aalseth, C.E., Zappala, J.C., Mueller, P., Jurgens, B.C., and Kulongoski, J.T., 2021, Groundwater residence time estimates obscured by anthropogenic carbonate: Science Advances, v. 7, no. 17, eabf3503, p. –9, accessed December 15, 2025, at https://doi.org/10.1126/sciadv.abf3503/

Shelton, J.L., and Fram, M.S., 2017, Groundwater-quality data for the Madera/Chowchilla–Kings shallow aquifer study unit, 2013–14: Results from the California GAMA Program: U.S. Geological Survey Data Series 1019, 115 p., accessed March 5, 2025, at https://doi.org/10.3133/ds1019.

Smedley, P.L., and Kinniburgh, D.G., 2002, A review of the source, behaviour and distribution of arsenic in natural waters: Applied Geochemistry, v. 17, p. 517–568, accessed March 5, 2025, at https://doi.org/10.1016/S0883-2927(02)00018-5.

Tokranov, A.K., Ransom, K.M, Bexfield, L.M., Lindsey, B.D., Watson, E., Dupuy, D.I., Stackelberg, P.E., Fram, M.S., Voss, S.A., Kingsbury, J.A., Jurgens, B.C., Smalling, K.L., and Bradley, P.M., 2024, Predictions of PFAS Occurrence in groundwater at drinking-water supply depths in the United States: Science, v. 386, no. 6723, p. 748-755, accessed March 5, 2025, at https://doi.org/10.1126/science.ado6638.

Troiano, J., Weaver, D., Marade, J., Spurlock, F., Pepple, M., Nordmark, C., and Bartkowiak, D., 2001, Summary of well water sampling in California to detect pesticide residues resulting from

nonpoint-source applications: Journal of Environmental Quality, v. 30, no. 2, p. 448–459, accessed March 5, 2025, at https://doi.org/10.2134/jeq2001.302448x.

Troiano, J., Garretson, C., Dasilva, A., Marade, J., Barry, T., 2013, Pesticide and nitrate trends in domestic wells where pesticide use is regulated in Fresno and Tulare Counties, California: Journal of Environmental Quality, v. 42, no. 6, p. 1711–1723, accessed March 5, 2025, at https://doi.org/10.2134/jeq2013.06.0219.

Trumpolt, C.W., Crain, M., Cullison, G.D., Flanagan, S.J.P., Siegel, L., and Lathrop, S., 2005, Perchlorate: Sources, uses, and occurrences in the environment: Remediation, v. 16, no. 1, p. 65–89, accessed November 19, 2025, at https://doi.org/10.1002/rem.20071.

United States Environmental Protection Agency, 2020, Reductions of Perchlorate in Drinking Water: Office of Ground Water and Drinking Water, EPA-815-F-20-002, 13 p., accessed March 5, 2025, at https://www.epa.gov/sites/default/files/2020-05/documents/perchlorate_reductions_5.14.20.pdf.

United States Environmental Protection Agency, 2024, National Primary Drinking Water Regulations, accessed March 5, 2025, at https://www.epa.gov/ground-water-and-drinking-water/national-primary-drinking-water-regulations.

Urbansky, E.T., 2002, Perchlorate as an environmental contaminant: Environmental Science and Pollution Research, v. 9, p. 187–192, accessed November 19, 2025, at https://doi.org/10.1007/BF02987487.

U.S. Geological Survey, 2006, National Elevation Dataset: U.S. Geological Survey database.

U.S. Geological Survey, variously dated, National field manual for the collection of water quality data: U.S. Geological Survey Techniques of Water-Resources Investigations, book 9, chap. A1-A9, accessed March 5, 2025, at http://water.usgs.gov/owq/FieldManual/.

Visser, A., Dubus, I., Broers, H.P., Brouyère, S., Korcz, M., Orban, P., Goderniaux, P., Batlle-Aguilar, J., Surdyk, N., Amraoui, N., Job, H., Pinault, J.L., Bierkens, M., 2009. Comparison of methods for the detection and extrapolation of trends in groundwater quality: Journal of Environmental Monitoring, v. 11, p. 2030–2043, accessed March 5, 2025, at https://doi.org/10.1039/B905926A.

Wei, T., and Simko, V., 2024, R package 'corrplot': Visualization of a Correlation Matrix (Version 0.95).

Wright, M.T., Izbicki, J.A., and Jurgens, B.C., 2021, A multi-tracer and well-bore flow profile approach to determine occurrence, movement, and sources of perchlorate in groundwater: Applied Geochemistry, v. 129, 104959, p. 1–18, accessed March 5, 2025, at https://doi.org/10.1016/j.apgeochem.2021.104959.

Wu, P., Yin, A., Fan, M., Wu, J., Yang, X., Zhang, H., and Gao, C., 2018, Phosphorus dynamics influenced by anthropogenic calcium in an urban stream flowing along an increasing urbanization gradient: Landscape and Urban Planning, v. 177, p. 1–9, accessed March 5, 2025, at https://doi.org/10.1016/j.landurbplan.2018.04.005.

Zhang, Y., Jiang, X., Zhang, X., Zhang, Z., Wang, X., Cao, G., Wei, W., and Wan, L., 2024, Pumping-induced groundwater aging and rejuvenation in aquifer-aquitard systems: A perspective from regional groundwater flow: Journal of Hydrology, v. 632, 130718, accessed March 5, 2025, at https://doi.org/10.1016/j.jhydrol.2024.130718.

Zogorski, J.S., Carter, J.M., Ivahnenko, T., Lapham, W.W., Moran, M.J., Rowe, B.L., Squillace, P.J., and Toccalino, P.L., 2006, Volatile organic compounds in the nation's ground water and drinking-water supply wells: U.S. Geological Survey Circular 1292, 101 p., accessed March 5, 2025, at https://doi.org/10.3133/cir1292.

Appendix 1. Well Construction Characteristics

We compiled well construction information for the 444 sites used in this study (Levy and Soldavini, 2026). Most of the sites are public-supply wells (PSWs) finished in either unconsolidated, alluvial sediments ("alluvial;" 79 percent of sites) with a smaller proportion being finished in fractured, hard-rock aquifers ("hard-rock;" 21 percent of sites; Levy and Soldavini, 2026). Seventeen (4 percent) of the sites that were considered were hard-rock springs developed for public drinking-water supply (refer to Stork and Fram, 2021 for attribution information), but are referred to as PSWs when the aggregate dataset is discussed in this report for ease of representation. We compiled depth to top of perforated or open intervals for wells and composite well depth (prioritizing "depth to bottom of open or perforated interval" over "well depth" over "borehole depth" depending on availability of information derived from well completion reports; Levy and Borkovich, 2022) in the data release of Levy and Soldavini (2026). Wells in this study were mostly finished within the top 1000 feet (ft) of regional aquifers (fig. 1.1).

Figure 1.1. Boxplots showing depth to top of the open or perforated interval and composite well depth for public-supply well sites used to analyze decadal trends in this study by province group. Data summarized from Levy and Soldavini (2026).

References Cited

Levy, Z.F., and Borkovich, J.G., 2022, Compilation of Public-Supply Well Construction Depths in California: U.S. Geological Survey data release, https://doi.org/10.5066/P90OHVIC.

Levy, Z.F., and Soldavini, A.L., 2026, Data for Analysis of Decadal Trends in the Quality of Groundwater Used for Public Drinking-Water Supply in California, 2004-2023, California GAMA Priority Basin Project: U.S. Geological Survey data release, https://doi.org/10.5066/P137ZTJE.

Stork, S.V., and Fram, M.S., 2021, Water use information for sites sampled by the California Groundwater Ambient Monitoring and Assessment Program Priority Basin Project (GAMA-PBP), 2004-2021 (ver. 3.0, October 2023): U.S. Geological Survey data release, https://doi.org/10.5066/P9EHLFZM.

Appendix 2. Isotope Units and Nomenclature

Stable isotopes of water (oxygen and hydrogen) and carbon are expressed in this report in delta (δ) notation, where the ratio of the more abundant to less abundant isotope in the sample (R_{sample}) are related to the ratio of isotopes in a standard ($R_{standard}$) by the following equation (Clark and Fritz, 1997):

$$\delta = \left[\frac{R_{sample}}{R_{standard}} - 1\right] \text{ x } 1{,}000 \qquad (1.1)$$

where

δ is delta notation, in per mille ($\delta^{18}O$ signifies ratio of oxygen-18 to oxygen-16 to that of a standard, $\delta^{2}H$ signifies ratio of hydrogen-2 to hydrogen-1 to that of a standard, and $\delta^{13}C$ signifies ratio of carbon-13 to carbon-12 to that of a standard),

R_{sample} is the ratio of the more abundant to less abundant isotope in the sample and,

$R_{standard}$ is the ratio of the more abundant to less abundant isotope in a standard (for stable isotopes of water this refers to Vienna Standard Mean Ocean Water [VSMOW] and for stable isotopes of carbon this refers to Vienna Pee Dee Belemnite [VPDB]).

Stable isotopes of water can be further related to each other by the d-excess parameter, which is expressed in the following equation (Clark and Fritz, 1997):

$$\text{d-excess} = \delta^{2}H - 8\,\delta^{18}O \quad (1.2)$$

Where

$\delta^{18}O$ is delta notation for the ratio of oxygen-18 to oxygen-16 to that of a standard (VSMOW) and,

$\delta^{2}H$ is delta notation for the ratio of hydrogen-2 to hydrogen-1 to that of a standard (VSMOW).

The d-excess parameter is generally used to indicate deviations of stable isotopes of water from ratios expected in precipitation following the global meteoric water line. Values of d-excess less than 10 per mille indicate enrichment of isotopes from what would be expected in mean global precipitation and can be indicative of the effects of kinetic isotope fractionation of meteoric waters by evaporation following precipitation (Clark and Fritz, 1997).

Radiogenic carbon-14 measurements are typically reported either as percent modern (pM) or percent modern carbon (pmC). The carbon-14 measurements reported by laboratory convention as pM were normalized for carbon isotope fractionation based on a standard reference $\delta^{13}C$ value of -25 per mille. Here, we report non-normalized carbon-14 values in units of pmC. Percent modern carbon refers to the percent carbon activity of the sample compared to

that of the atmosphere in 1950. Values of carbon-14 reported as pmC in excess of 100 percent are possible because nuclear bomb testing in the 1950s raised the carbon-14 activity in the atmosphere above natural background levels. Data were converted from pM to pmC using the following equation adapted from Plummer and others (2004):

$$pmC = \frac{pM(1+\frac{\delta^{13}C}{1000})^2}{0.975^2} \quad (1.3)$$

Where

pmC is the measured carbon-14 value in units of percent modern carbon,

pM is the normalized carbon-14 value in units of percent modern and,

$\delta^{13}C$ is the measured ratio of carbon-13 to carbon-12 to that of a standard (VPDB).

References Cited

Clark, I.D., and Fritz, P., 1997, Environmental isotopes in hydrogeology: New York, CRC Press, 328 p.

Plummer, L.N., Bexfield, L.M., Anderholm, S.K., Sanford, W.E., and Busenberg, E., 2004, Geochemical characterization of ground-water flow in the Santa Fe Group aquifer system, Middle Rio Grande Basin, New Mexico: U.S. Geological Survey Water-Resources Investigations Report 03–4131, 395 p., accessed March 5, 2025, at https://doi.org/10.3133/wri034131.

Appendix 3. Alkalinity Measurements

Alkalinity is operationally defined as the capacity for solutes in a sample to react with and neutralize acid and is typically measured by titration of a strong acid into a sample until a

predetermined pH value is reached (Hem, 1985). The Groundwater Ambient Monitoring and Assessment Priority Basin Project (GAMA-PBP) has measured alkalinity both in the field for select samples and in the laboratory for almost all samples. Generally, field alkalinity is considered more reliable than lab alkalinity as groundwater samples may experience degassing of carbon dioxide during handling and transport, which may affect carbonate equilibria in the sample (Hem, 1985). Bennett and Fram (2014) found a slight upward bias in laboratory compared to field-measured alkalinity values for samples collected by the GAMA-PBP and attributed this to the laboratory values being measured by the fixed-endpoint method compared to field measurements that are typically done by gran titration. Here, we adopted the following prioritization order to select alkalinity measurements associated with a single sampling event: (1) incremental titration in the field (U.S. Geological Survey parameter code of "39086"), (2) Gran titration in the field (U.S. Geological Survey parameter code of "29802"), and (3) fixed-endpoint titration in the laboratory (U.S. Geological Survey parameter code of "29801"; Rounds and Wilde, 2012; Dupré and others, 2013). Additionally, laboratory-measured alkalinity values made during the calendar year 2022 were not considered in this analysis due to frequent hold-time violations during this period.

Because of the slight upwards bias of the laboratory fixed-endpoint titration method, a correction was applied to all laboratory alkalinity measurements as described by Rosen and others (2019). We compiled 612 paired field and laboratory alkalinity measurements taken by the GAMA-PBP for the same sampling event and regressed laboratory on field values using the lm function from the R "stats" package (fig. 3.1; R Core Team, 2024). This resulted in a linear regression equation of the following form:

$$FIELD = 0.9697LAB - 1.5257 \quad (3.1)$$

Where

FIELD is the field-measured alkalinity value, in units of milligrams per liter as calcium carbonate, and

LAB is the laboratory-measured alkalinity value, in units of milligrams per liter as calcium carbonate.

All laboratory alkalinity measurements used to compute decadal-change values in this study were bias corrected to be consistent with field measurements using Eq. 3.1.

Figure 3.1. Comparison of laboratory to field measured alkalinity values analyzed by the Groundwater Ambient Monitoring and Assessment Program Priority Basin Project (GAMA-PBP) during 2005–2023 with regression line and equation. Data summarized from Levy and Soldavini (2026).

References Cited

Bennett, G.L., V, and Fram, M.S., 2014, Groundwater-quality data in the North San Francisco Bay Shallow Aquifer study unit, 2012—Results from the California GAMA Program: U.S. Geological Survey Data Series 865, 94 p., accessed March 5, 2025, at http://dx.doi.org/10.3133/ds865.

Dupré, D.H, Scott, J.C., Clark, M.L., Canova, M.G, and Stoker, Y.E., 2013, User's manual for the National Water Information System of the U.S. Geological Survey: Water-Quality System, Version 5.0: U.S. Geological Survey Open-File Report 2013–1054, 730 p., accessed March 5, 2025, at http://pubs.usgs.gov/of/2013/1054/pdf/OFR2013-1054_NWIS_ver5.pdf

Hem, J.D., 1985, Study and interpretation of the chemical characteristics of natural water (3rd ed.): U.S. Geological Survey Water Supply Paper 2254, 263 p., accessed March 5, 2025, at https://doi.org/10.3133/wsp2254.

Levy, Z.F., and Soldavini, A.L., 2026, Data for Analysis of Decadal Trends in the Quality of Groundwater Used for Public Drinking-Water Supply in California, 2004-2023, California GAMA Priority Basin Project: U.S. Geological Survey data release, https://doi.org/10.5066/P137ZTJE.

R Core Team, 2024, R: A language and environment for statistical computing: R Foundation for Statistical Computing, accessed March 5, 2025, at https://www.R-project.org/.

Rosen, M.R., Burow, K.R., and Fram, M.S., 2019, Anthropogenic and geologic causes of anomalously high uranium concentrations in groundwater used for drinking water supply in the southeastern San Joaquin Valley, CA: Journal of Hydrology, v. 577, 124009, p. 1–15, accessed March 5, 2025, at https://doi.org/10.1016/j.jhydrol.2019.124009.

Rounds, S.A., Wilde, F.D., 2012, Chapter A6. Section 6.6. Alkalinity and acid neutralizing capacity (Version 3, Revised Jul 2006): U.S. Geological Survey Techniques of Water-Resources Investigations 09-A6.6, 53 p., accessed February 23, 2026, at https://doi.org/10.3133/twri09A6.6.

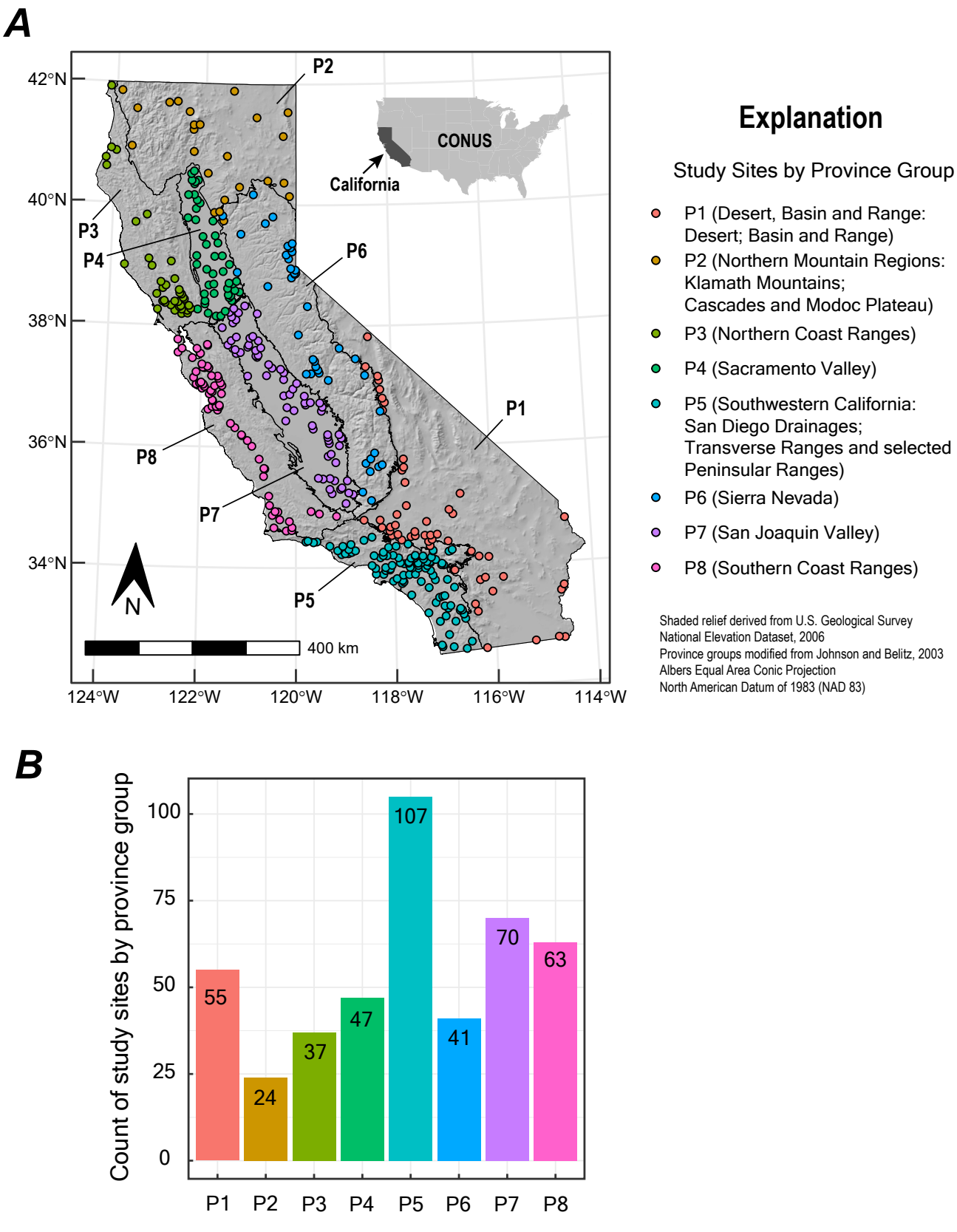

Figure 1. A, Map of California showing location of study sites attributed by province groups modified from the hydrogeologic provinces of California presented by Johnson and Belitz (2003); and B, bar plot showing number of study sites by province group. Data summarized from Levy and Soldavini (2026). CONUS, conterminous United States.

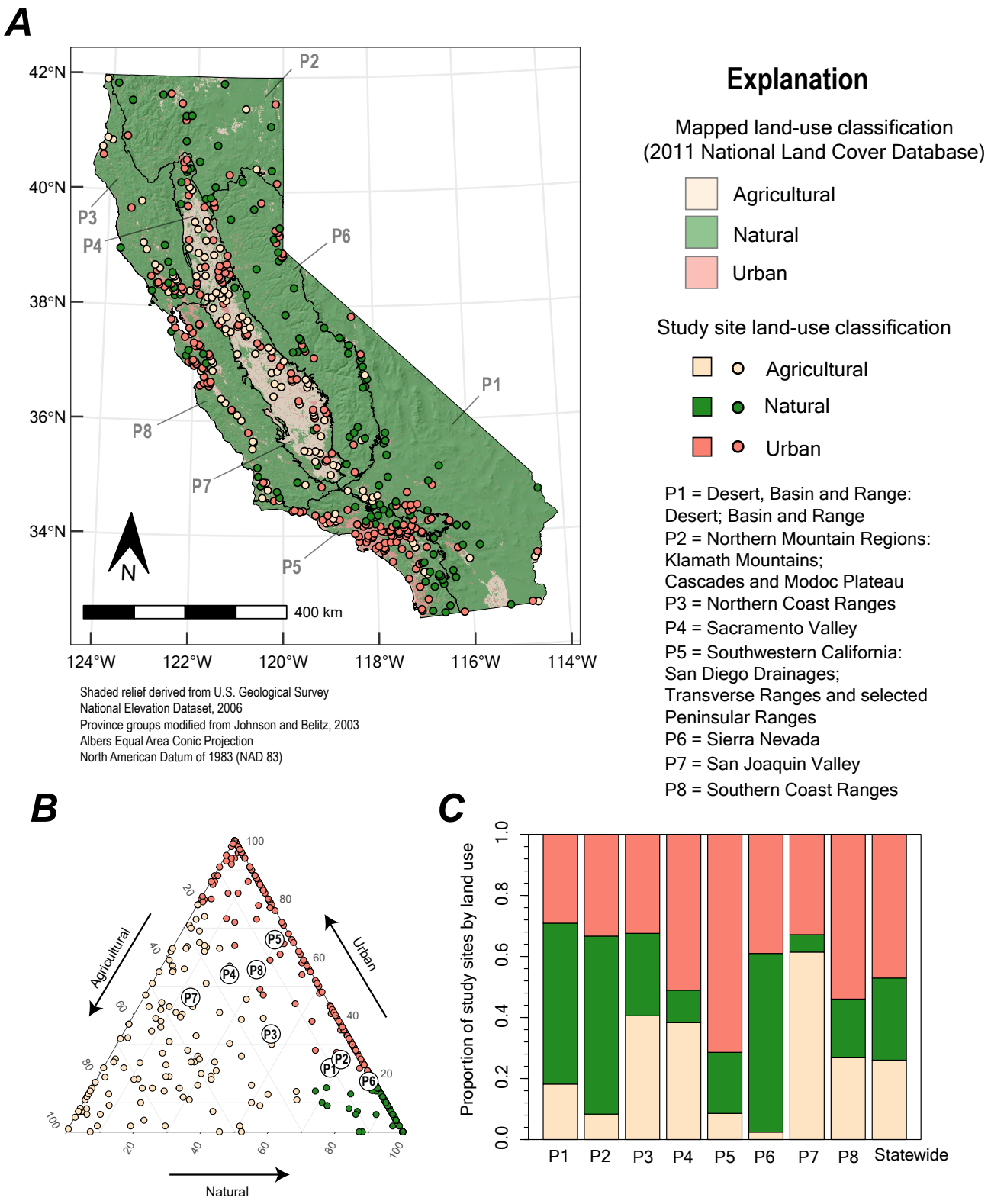

Figure 2. A, Map of California showing predominant land use (urban, agricultural, or natural) from the 2011 National Land Cover Database (Jin and others, 2013) with associated classifications for study sites based on mapped land use within respective 500-meter radius buffer areas (agricultural land-use class equates to greater than 20 percent agricultural land use in buffer area, urban land-use class equates to greater than 20 percent urban land use and less than or equal to 20 percent agricultural land use in buffer area, and natural land-use class equates to less than or equal to 20 percent of both agricultural and urban land uses in buffer area); B, ternary plot showing proportion of land use in 500-meter buffer areas around study sites with associated land-use classifications and median land-use proportions for sites in respective province groups; and C, bar plots showing proportion of study sites in province groups and statewide having respective land-use classifications. Data summarized from Levy and Soldavini (2026).

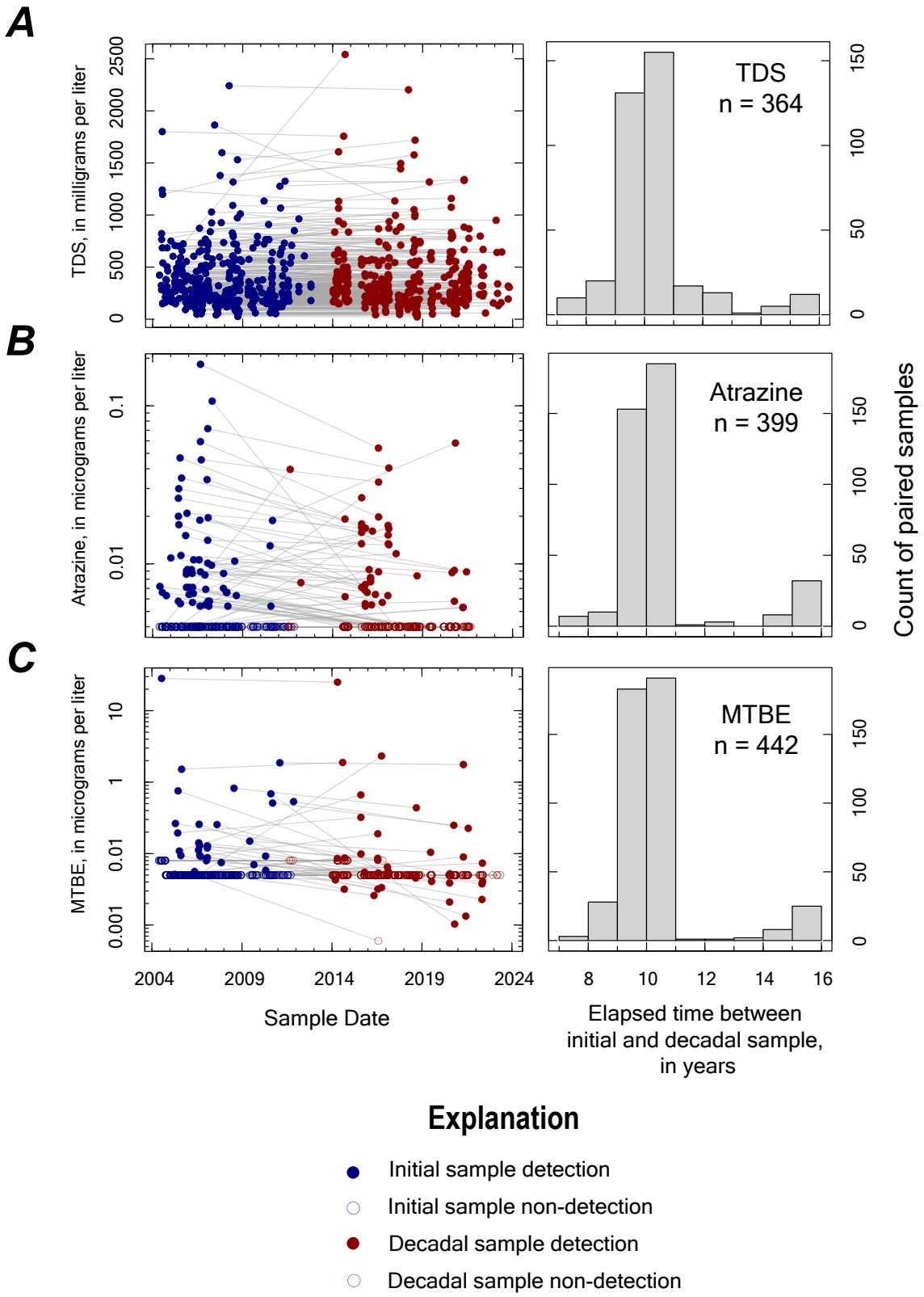

Figure 3. Time-series plots showing initial and decadal sample concentrations connected by tie lines (left) and histograms showing the elapsed time between initial and decadal samples (right) for A, total dissolved solids (TDS); B, atrazine; and C, methyl tert-butyl ether (MTBE). Non-detections are plotted at the higher assigned reporting level of the two paired samples. The y-axes for panels B and C are scaled logarithmically. Data summarized from Levy and Soldavini (2026).

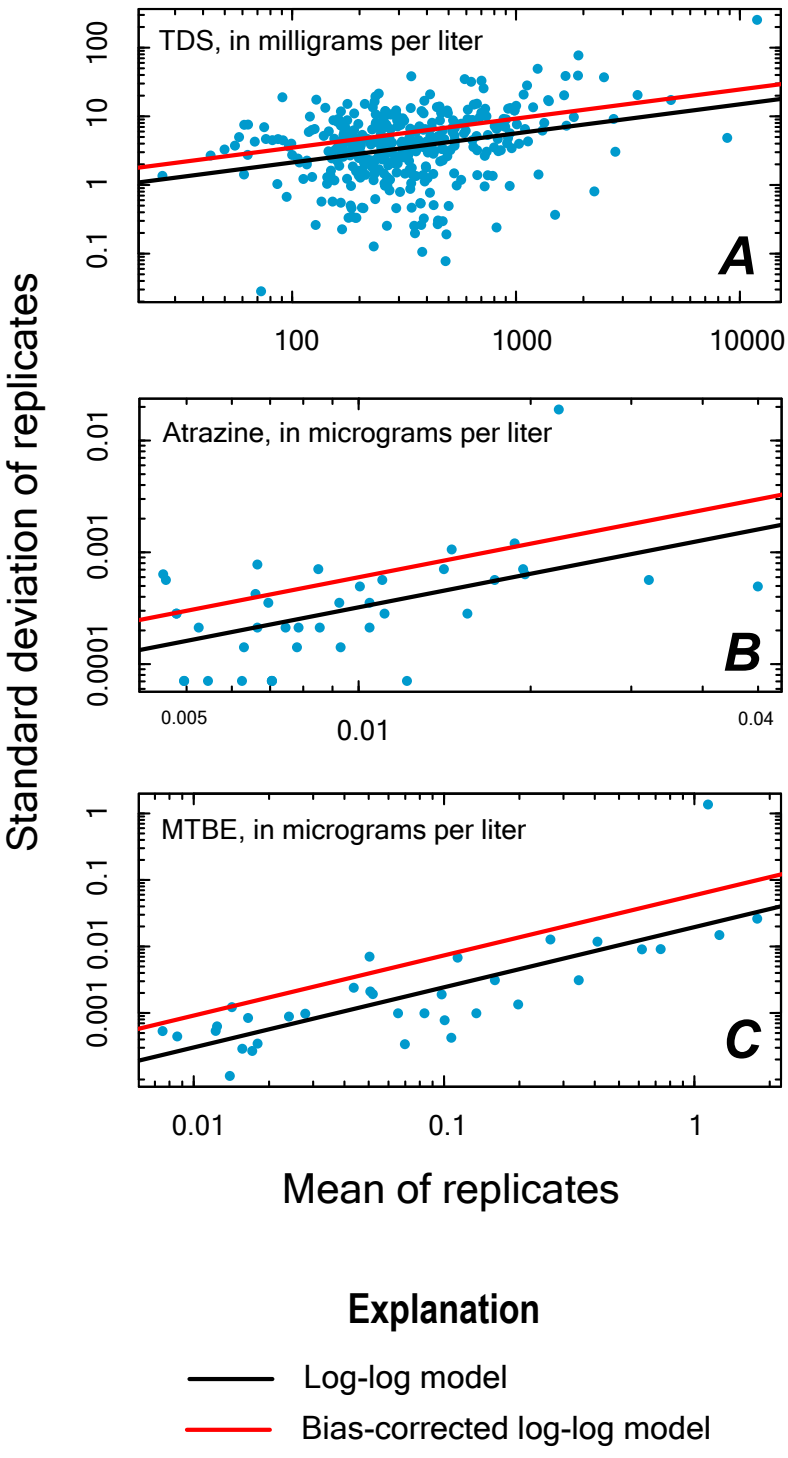

Figure 4. Mean versus standard deviation of replicate pairs with log-log models and bias-corrected log-log models (Mueller and others, 2015) for A, total dissolved solids (TDS); B, atrazine; and C, methyl tert-butyl ether (MTBE). Data summarized from Levy and Soldavini (2026).

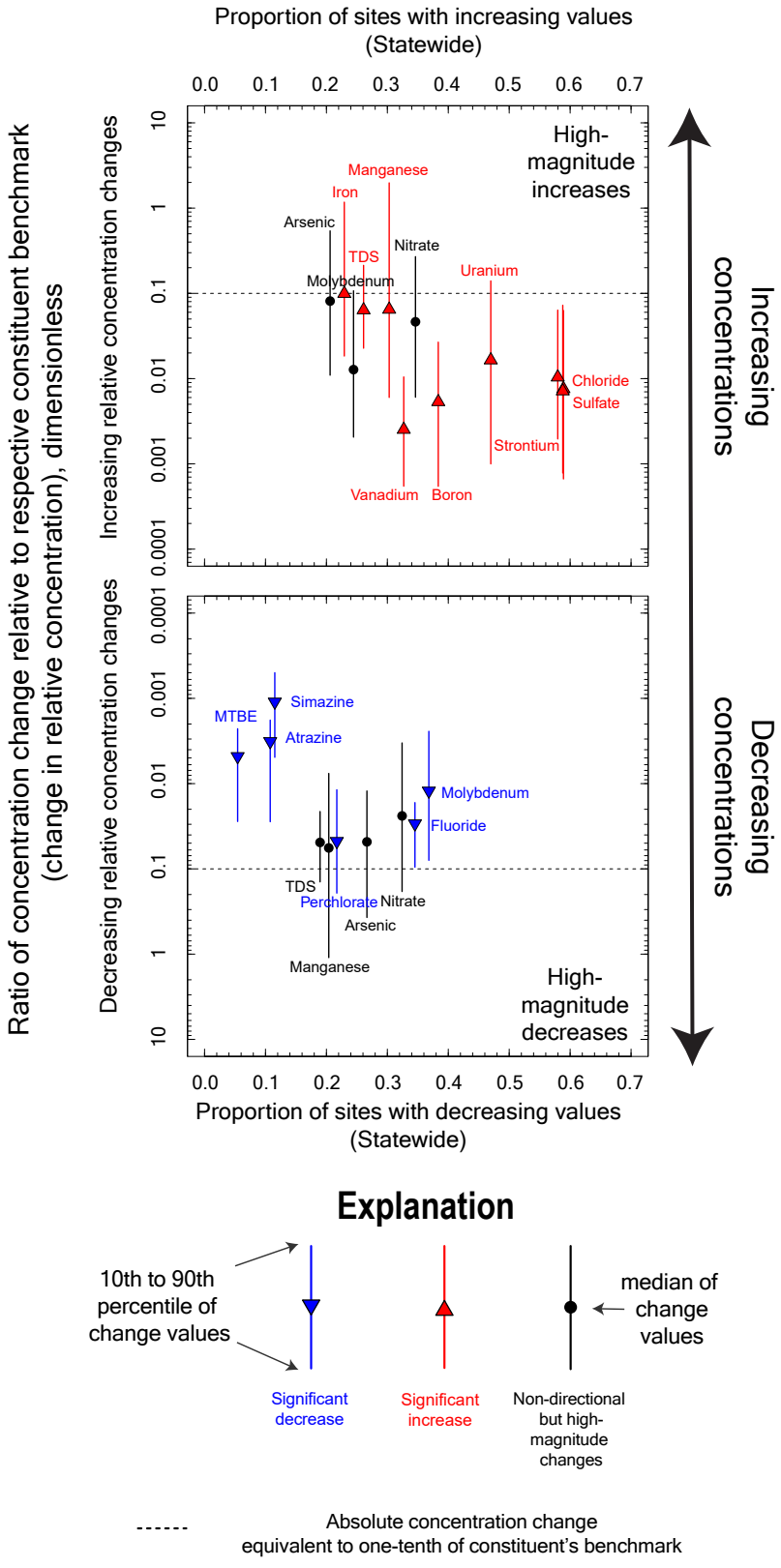

Figure 5. Proportion of changing values statewide versus median bounded by 10th to 90th percentile of relative-concentration change (concentration change divided by constituent benchmark) for increasing (top) and decreasing (bottom) values of focal water-quality constituents showing significant directional or high-magnitude changes. Benchmarks used to calculate relative concentration changes for respective constituents can be found in Levy and Soldavini (2026). Data summarized from Levy and Soldavini (2026). MTBE, Methyl *tert*-butyl ether; TDS, total dissolved solids.

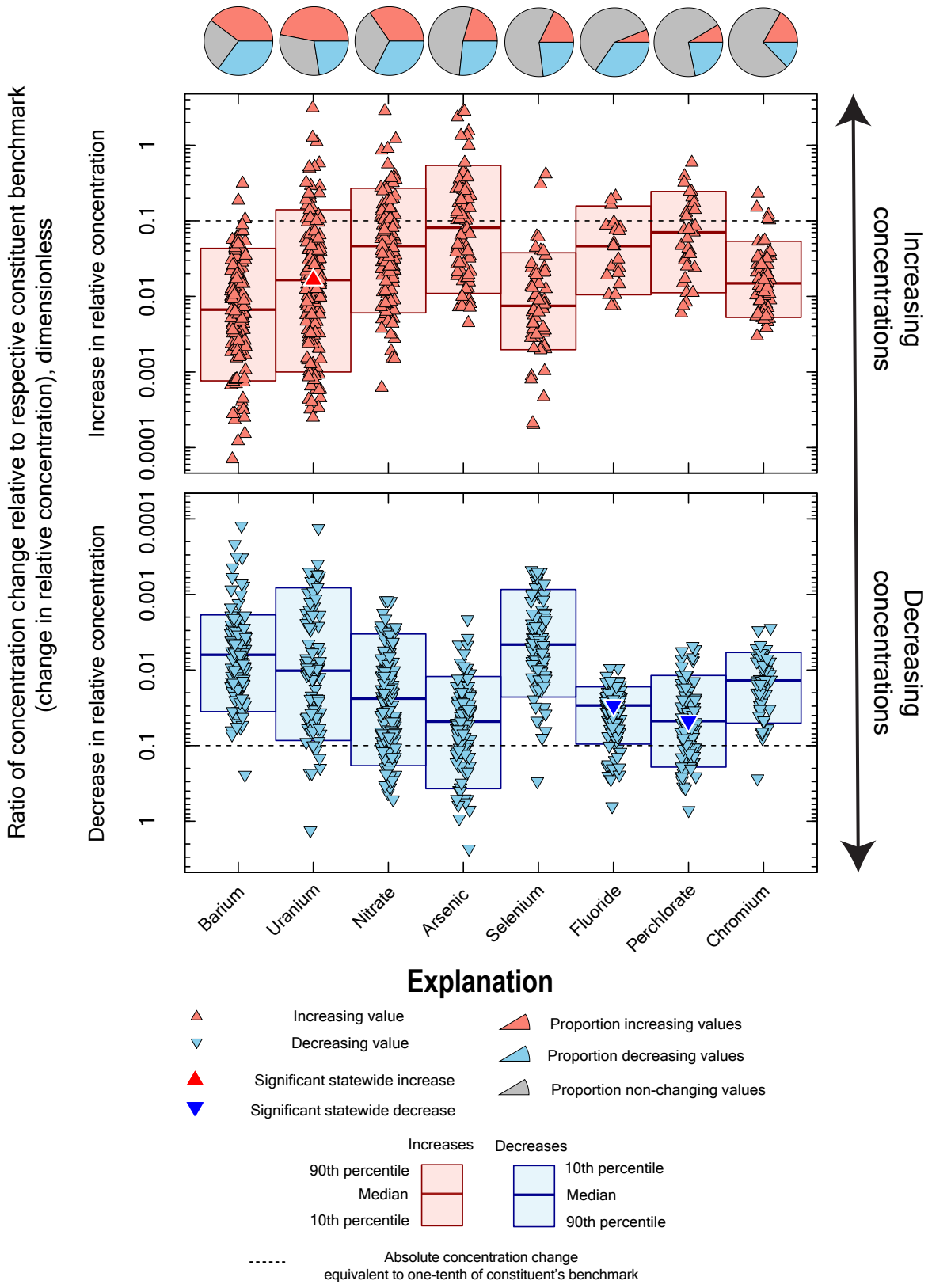

Figure 6. Decadal increases (top) and decreases (bottom) of relative concentration (concentration change divided by constituent benchmark) for inorganic water-quality constituents with regulatory benchmarks. Benchmarks used to calculate relative concentration changes for respective constituents can be found in Levy and Soldavini (2026). Data summarized from Levy and Soldavini (2026).

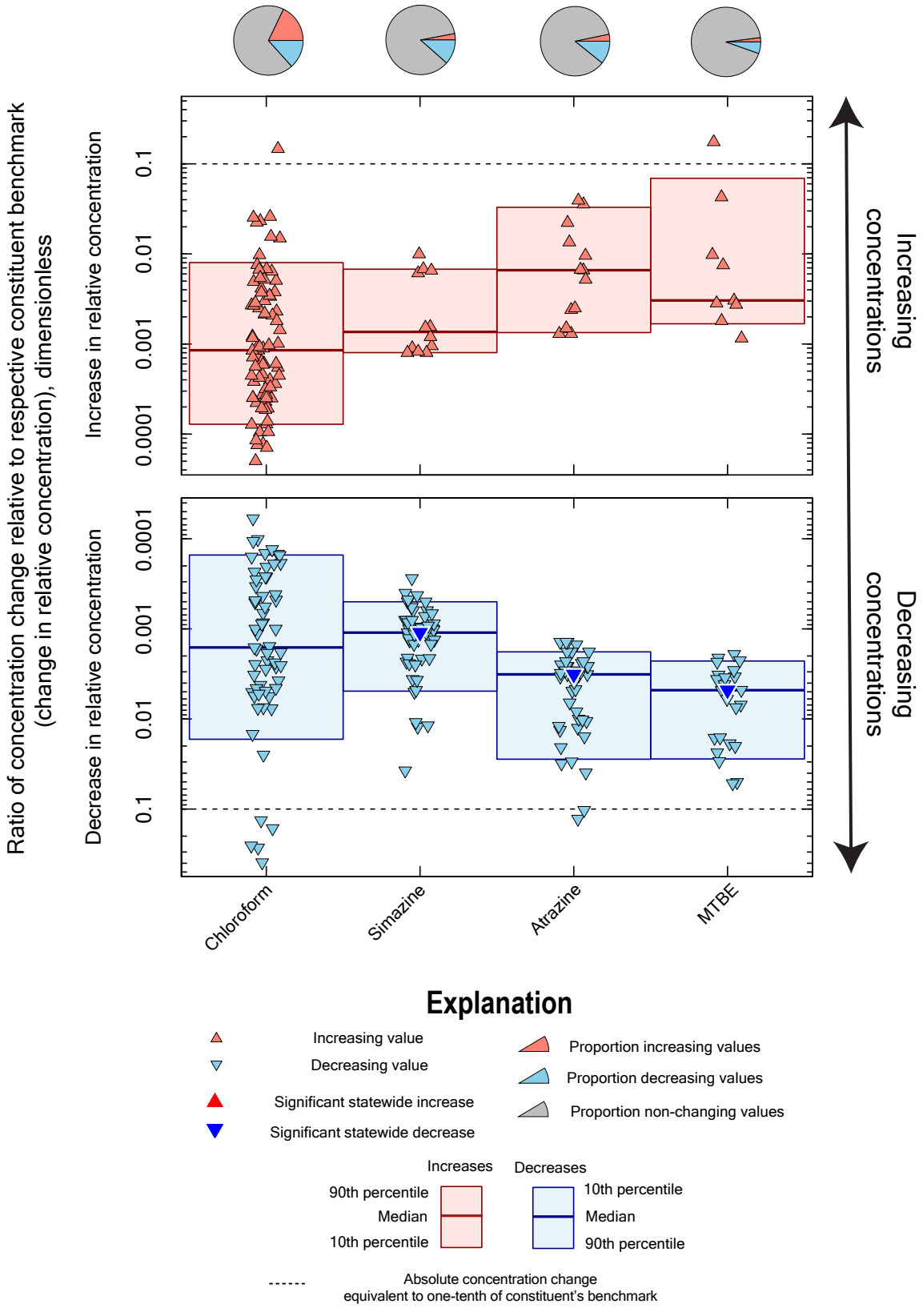

Figure 7. Decadal increases (top) and decreases (bottom) of relative concentration (concentration change divided by constituent benchmark) for organic water-quality constituents with regulatory benchmarks. Benchmarks used to calculate relative concentration changes for respective constituents can be found in Levy and Soldavini (2026). Data summarized from Levy and Soldavini (2026). MTBE, methyl *tert*-butyl ether.

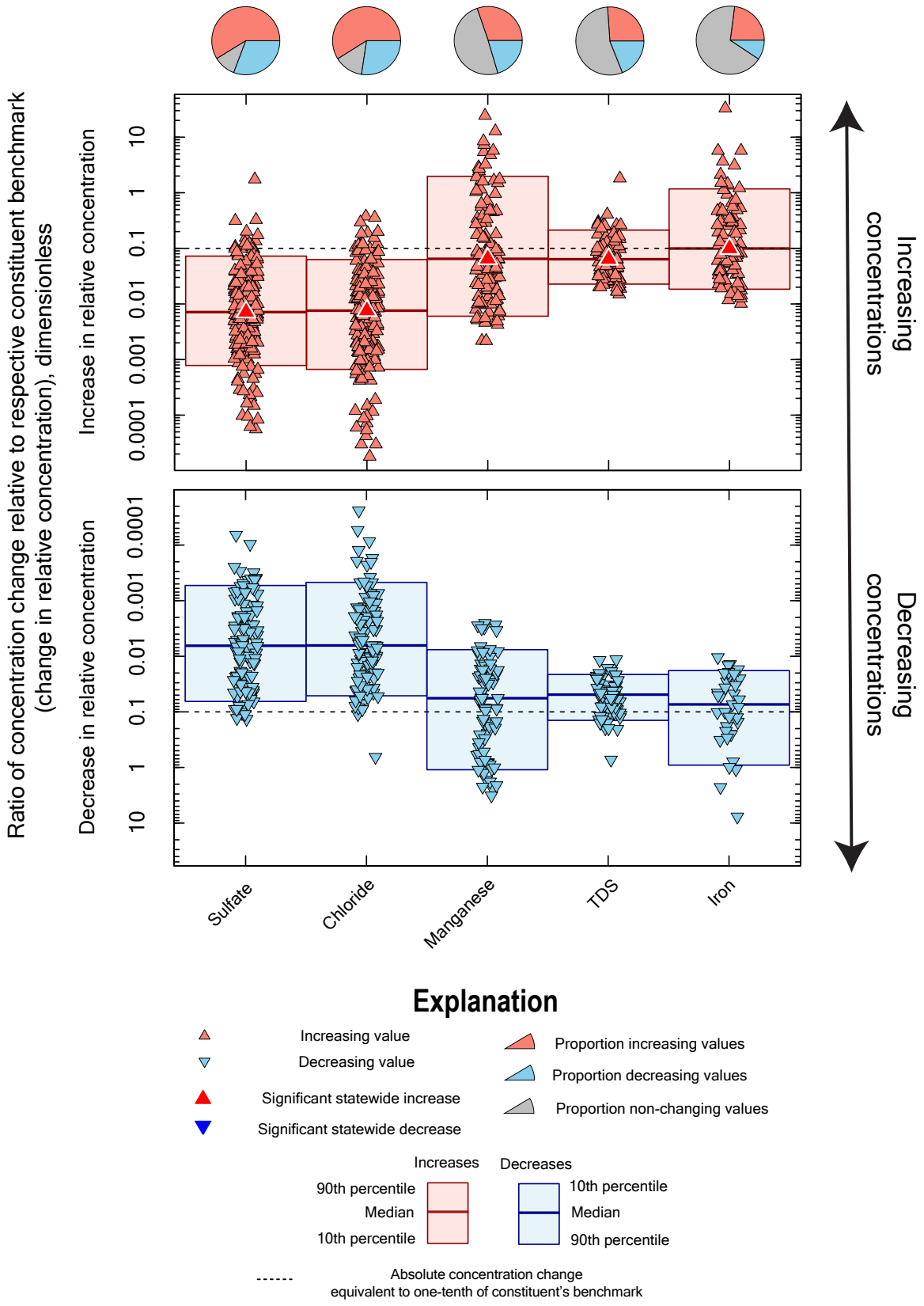

Figure 8. Decadal increases (top) and decreases (bottom) of relative concentration (concentration change divided by constituent benchmark) for inorganic water-quality constituents with non-regulatory, aesthetic-based benchmarks. Benchmarks used to calculate relative concentration changes for respective constituents can be found in Levy and Soldavini (2026). Data summarized from Levy and Soldavini (2026). TDS, total dissolved solids.

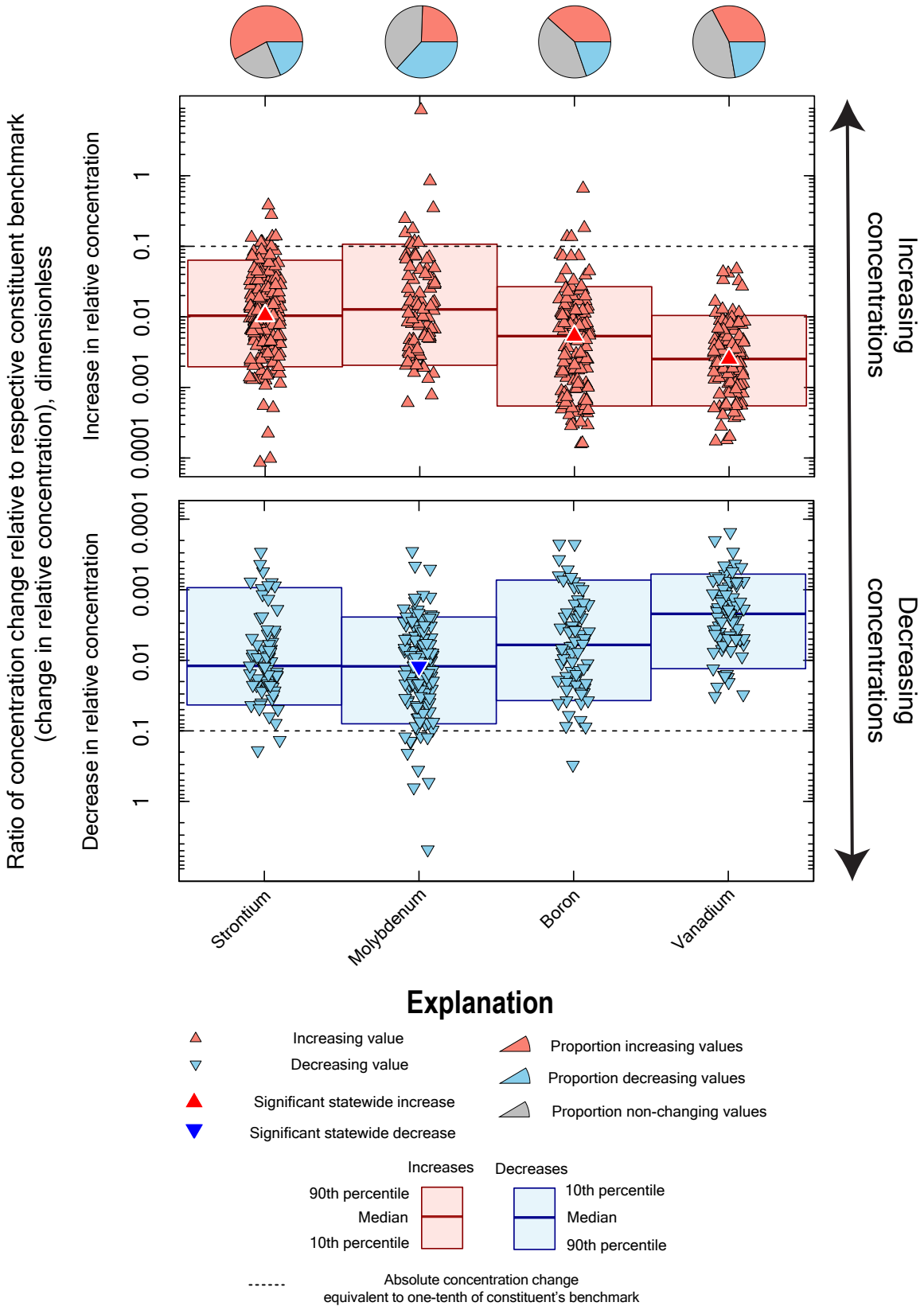

Figure 9. Decadal increases (top) and decreases (bottom) of relative concentration (concentration change divided by constituent benchmark) for inorganic water-quality constituents with non-regulatory, health-based benchmarks. Data summarized from Levy and Soldavini (2026).

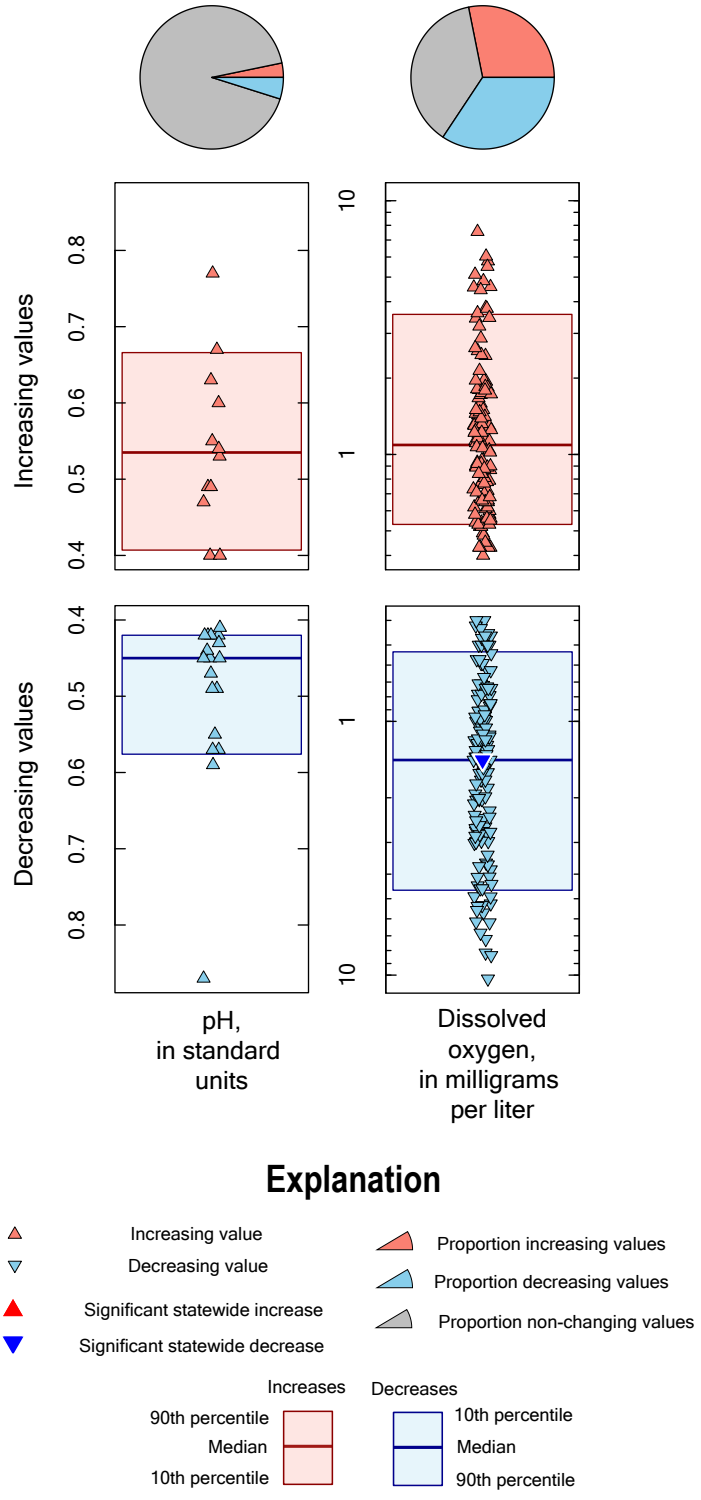

Figure 10. Decadal increases (top) and decreases (bottom) for indicators of geochemical conditions. Data summarized from Levy and Soldavini (2026).

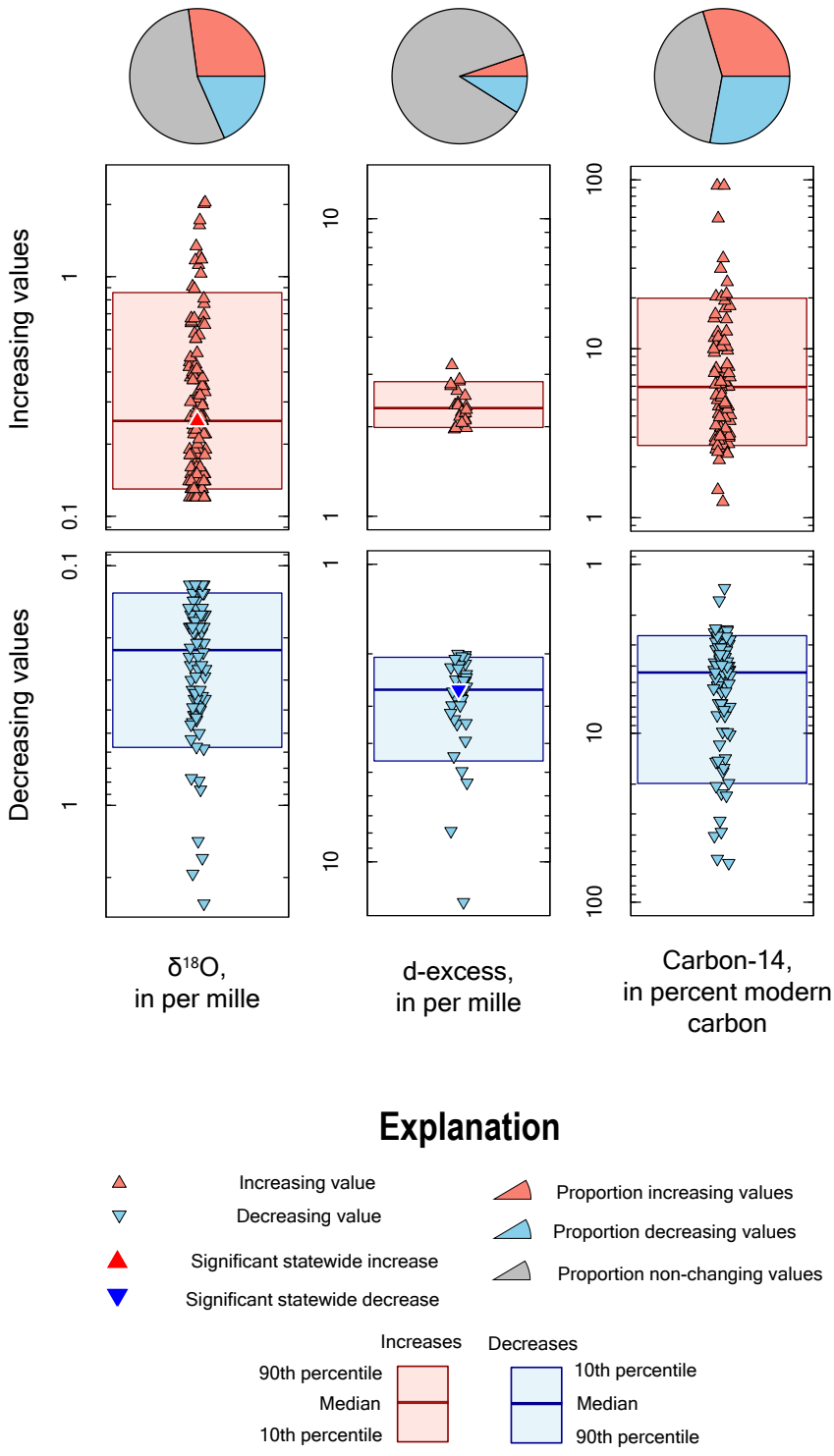

Figure 11. Decadal increases (top) and decreases (bottom) for indicators of groundwater source and age. Data summarized from Levy and Soldavini (2026). $\delta^{18}O$, oxygen-18.

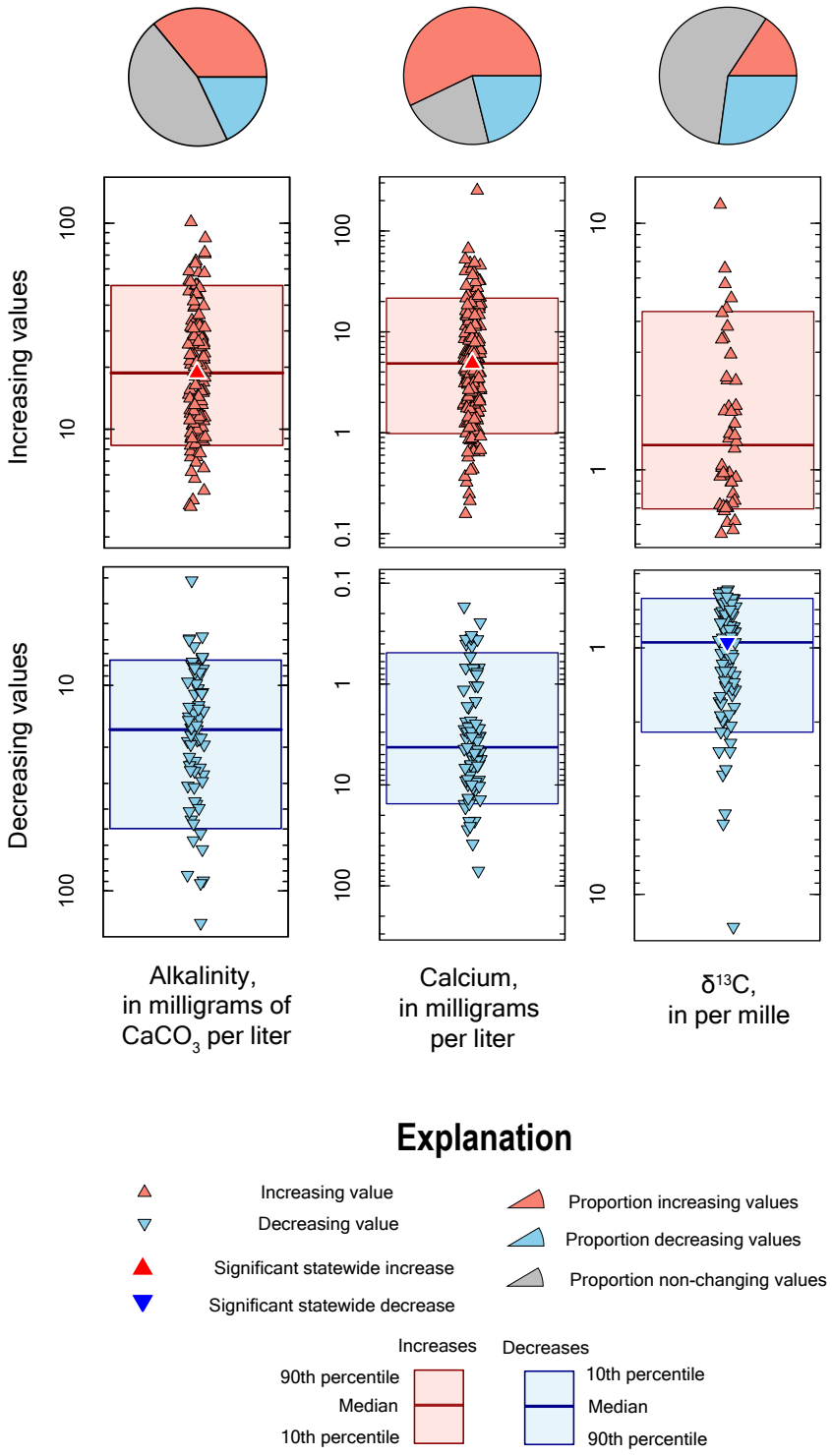

Figure 12. Decadal increases (top) and decreases (bottom) for geochemical salinity indicators. Data summarized from Levy and Soldavini (2026). $\delta^{13}C$, carbon-13.

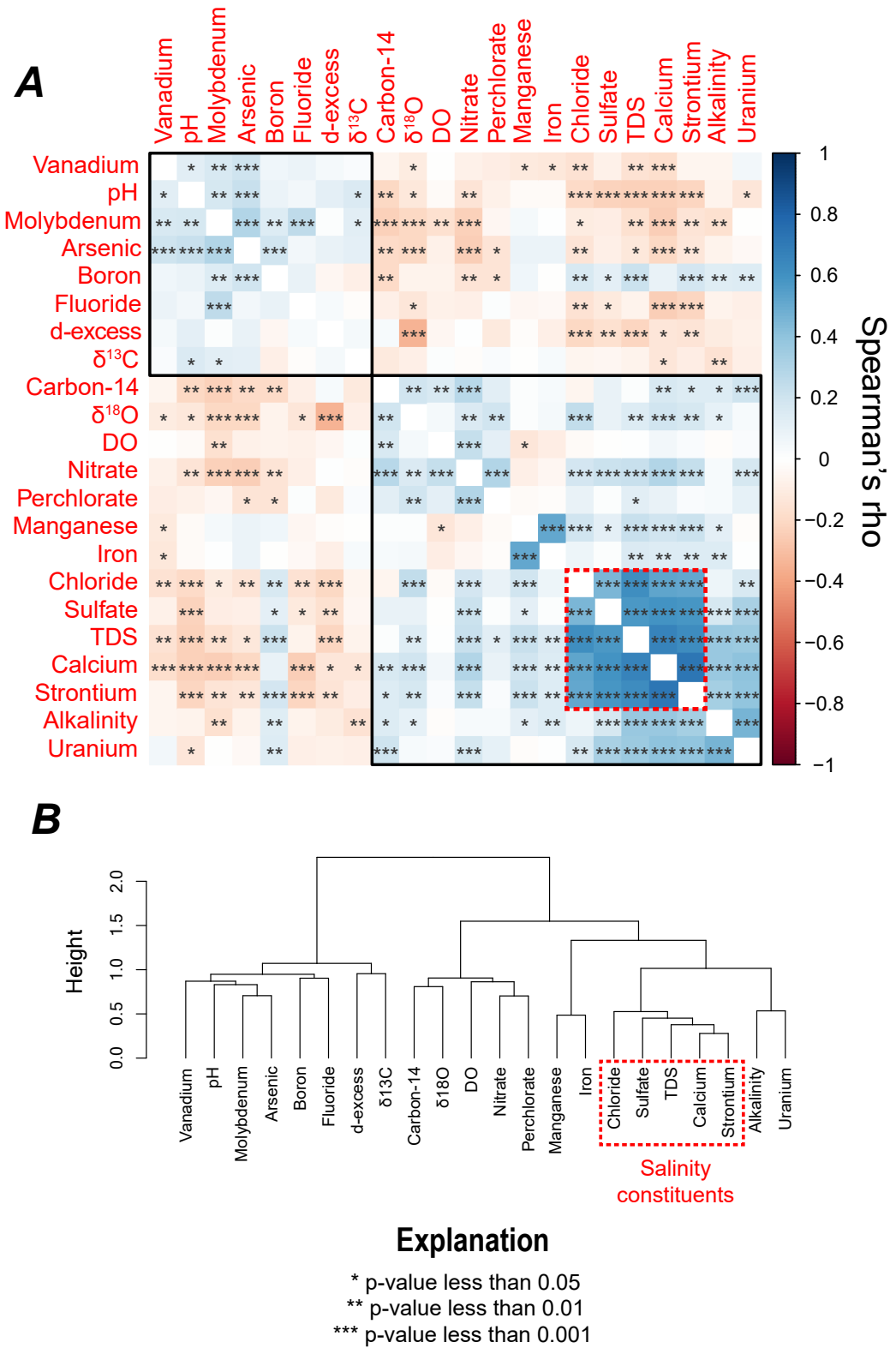

Figure 13. A, heatmap; and B, dendrogram of Spearman's correlations among decadal changes of focal water-quality constituents and geochemical indicators organized by hierarchical agglomerative clustering. Positive Spearman's rho values indicate direct correlation of decadal change values (constituents increasing or decreasing together) and negative Spearman's rho values indicate inverse correlation of change values (constituent concentrations changing in opposite directions). Black boxes in the heatmap (A) correspond to the two top-level cluster groups (split with maximum height value) defined in the dendrogram (B). Data summarized from Levy and Soldavini (2026). $\delta^{13}C$, carbon-13; $\delta^{18}O$, oxygen 18; d-excess, deuterium excess; DO, dissolved oxygen; TDS, total dissolved solids.

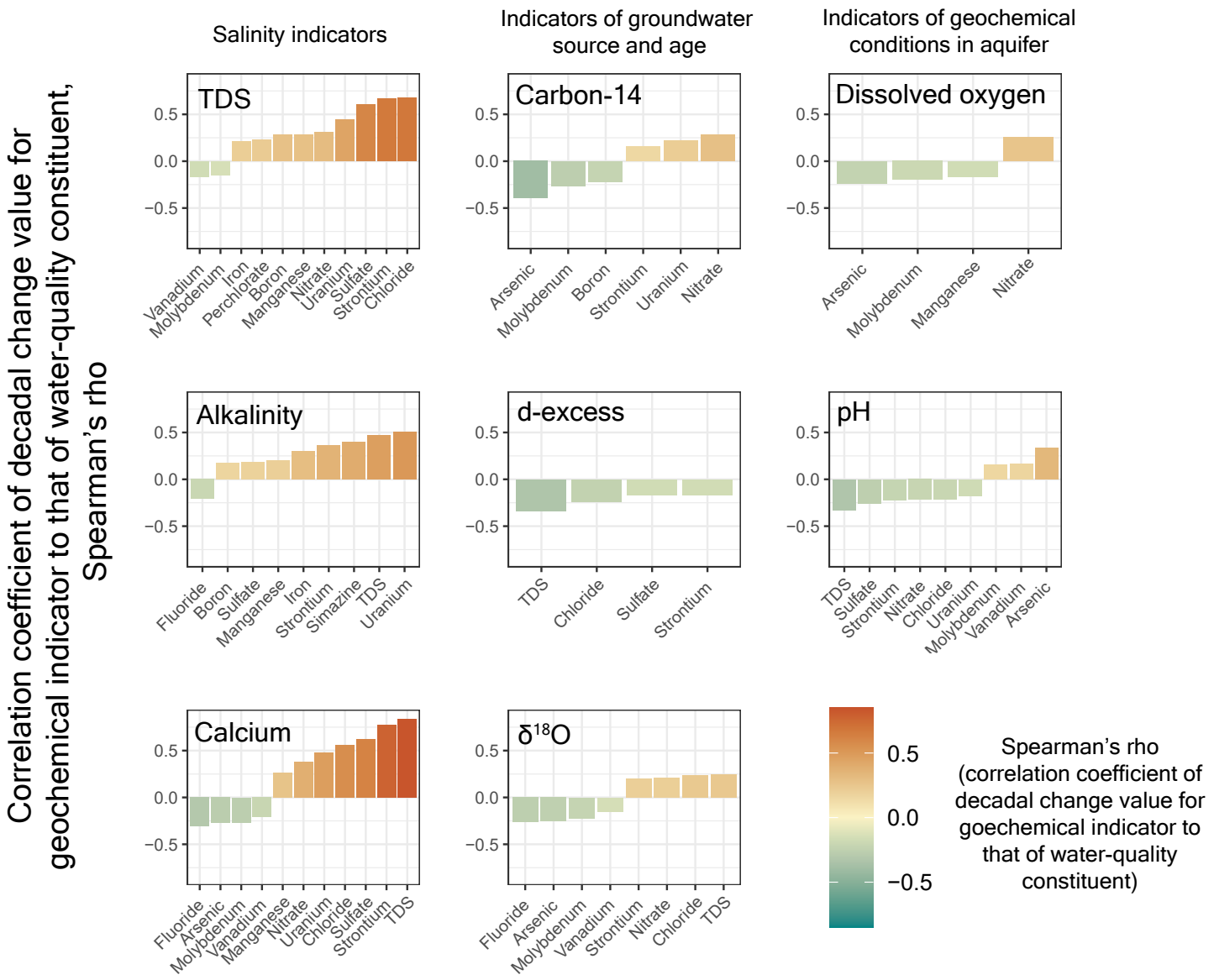

Figure 14. Panels showing significant (p-values less than 0.05) Spearman's correlations for censored differences of water-quality constituents to respective geochemical indicators. Positive Spearman's rho values indicate direct correlation of decadal change values (constituents increasing or decreasing together) and negative Spearman's rho values indicate inverse correlation of change values (constituent concentrations changing in opposite directions). Data summarized from Levy and Soldavini (2026). $\delta^{18}O$, oxygen 18; d-excess, deuterium excess; TDS, total dissolved solids.

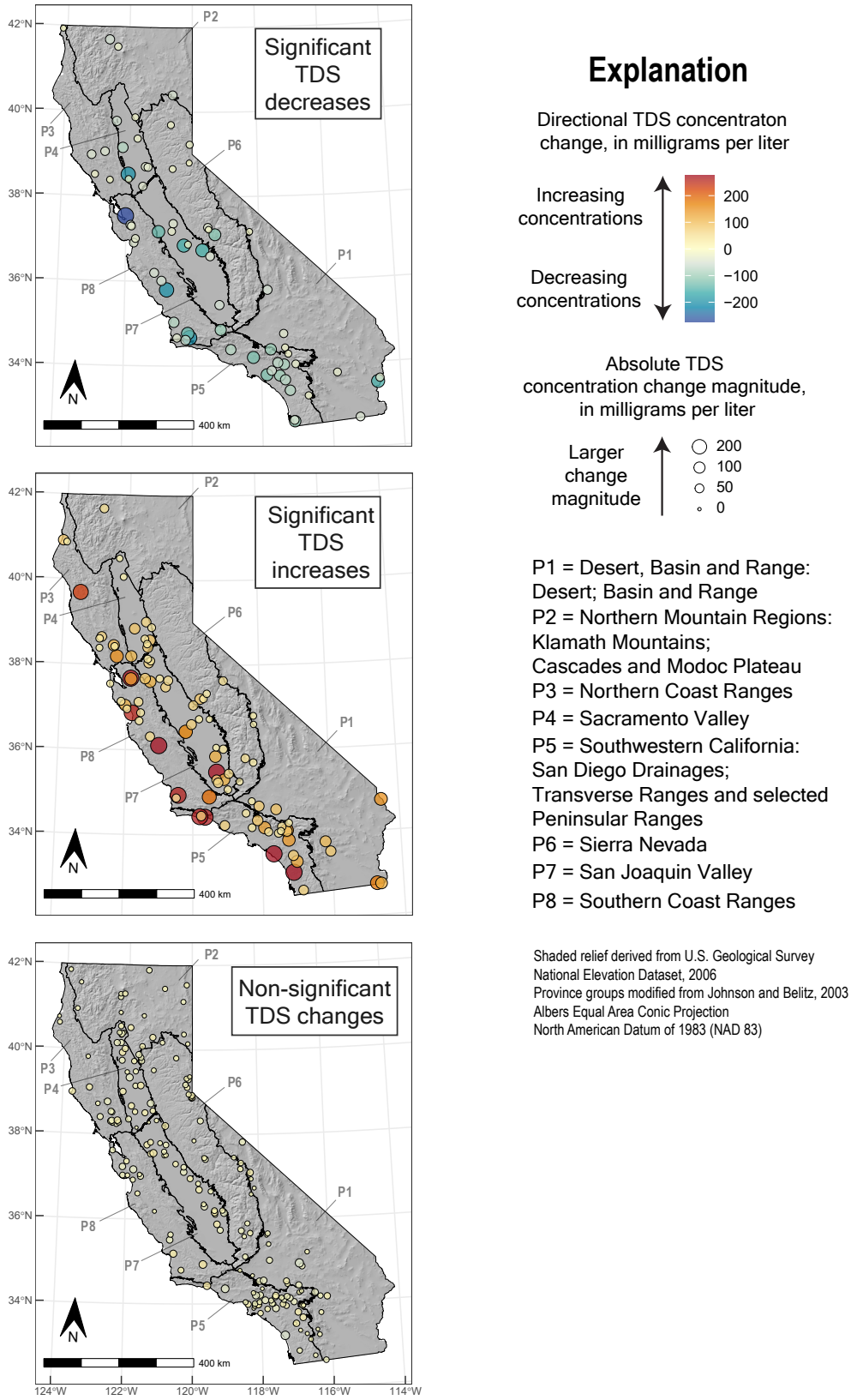

Figure 15. Maps of California showing study sites that had significant decreases (top), significant increases (middle), and non-significant changes (bottom) for decadal comparisons of total dissolved solids (TDS). Change significance is indicated for initial and decadal concentration values with non-overlapping confidence intervals. Point sizes and colors are scaled to absolute and directional concentration changes, respectively. Directional differences ranged from -729 to 1818 milligrams per liter, but scales were symmetrically saturated at value of ±274 milligrams per liter to prevent outliers (less than 2 percent of change values statewide) from obscuring visualization of most change values. Data summarized from Levy and Soldavini (2026).

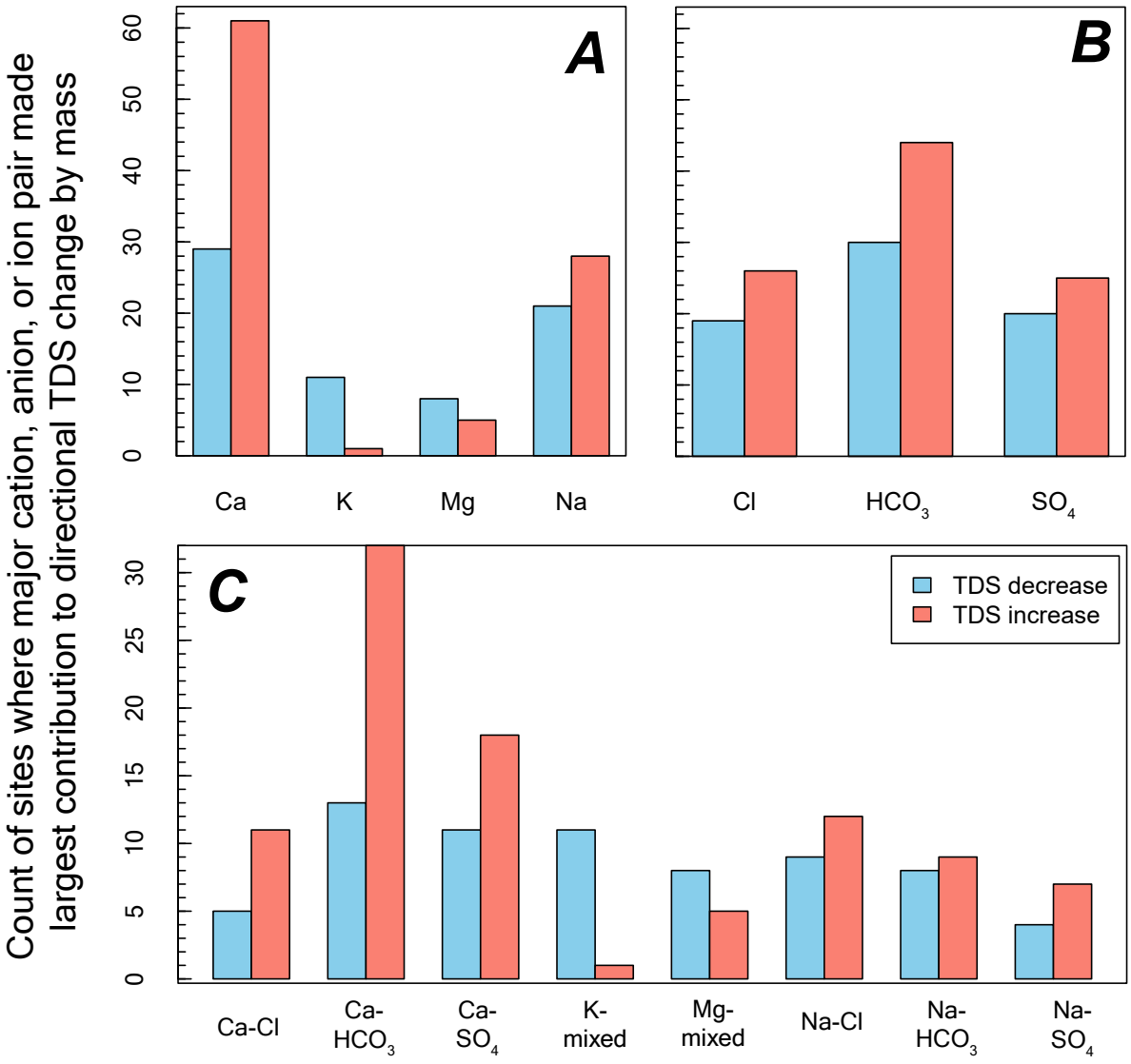

Figure 16. Count of sites with largest solute mass changes corresponding to significant total dissolved solids (TDS) increases and decreases for A, major cations; B, major anions; and C, major ion pairs. Data summarized from Levy and Soldavini (2026). Ca, calcium; K, potassium; Mg, magnesium; Na, sodium; Cl, chloride; HCO_3, bicarbonate; SO_4, sulfate.

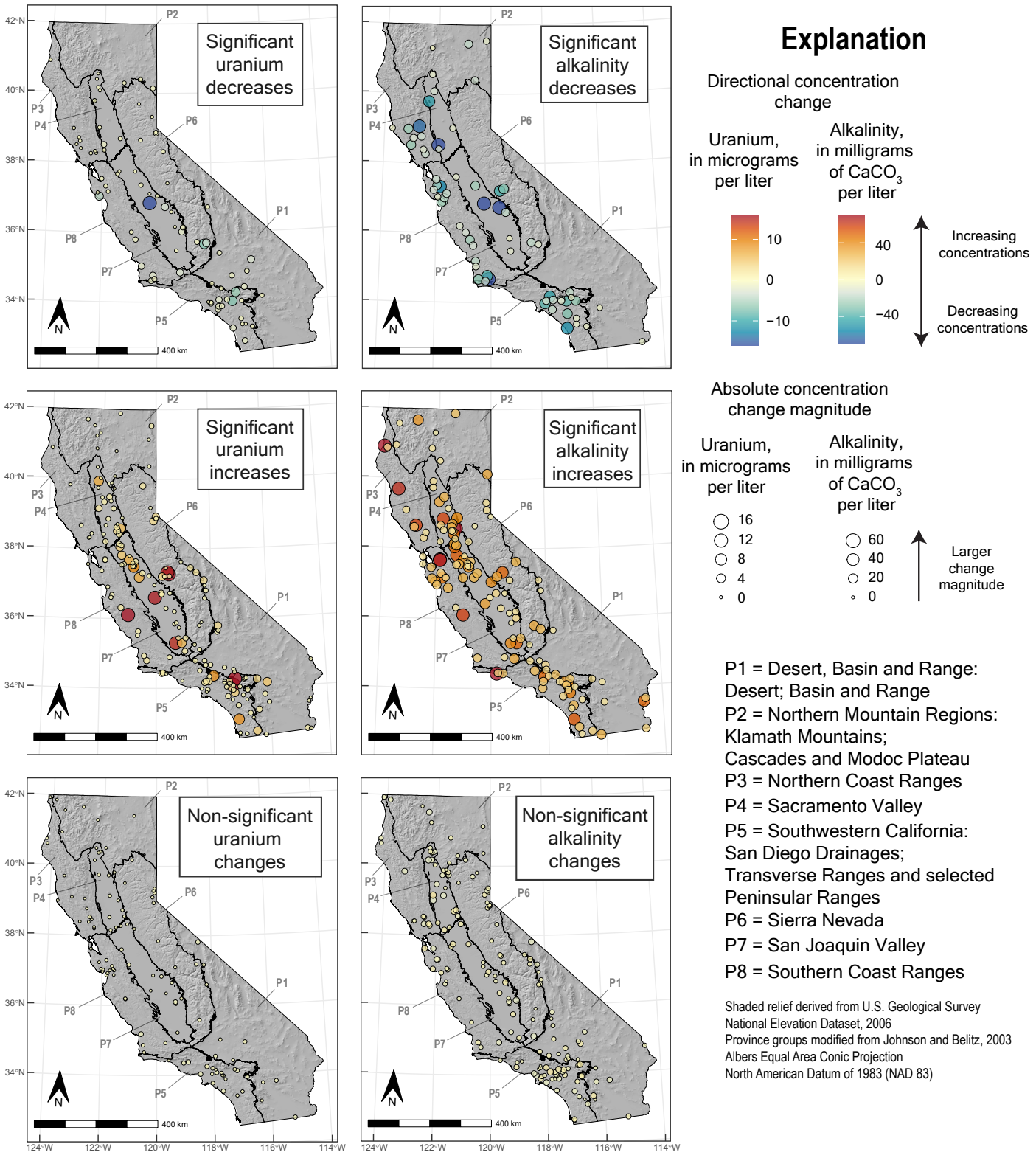

Figure 17. Maps of California showing study sites that had significant decreases (top), significant increases (middle), and non-significant changes (bottom) for decadal comparisons of uranium (left) and alkalinity (right). Change significance is indicated for initial and decadal concentration values with non-overlapping confidence intervals. Point sizes and colors are scaled to absolute and directional concentration changes, respectively. Directional differences ranged from -40 to 93 micrograms per liter for uranium and -145 to 100 milligrams per liter as calcium carbonate for alkalinity. Respective measurement scales for uranium and alkalinity were symmetrically saturated at values of ±16 micrograms per liter and ±75 milligrams per liter (as calcium carbonate) to prevent outliers (less than 2 percent of change values statewide) from obscuring visualization of most change values. Data summarized from Levy and Soldavini (2026).

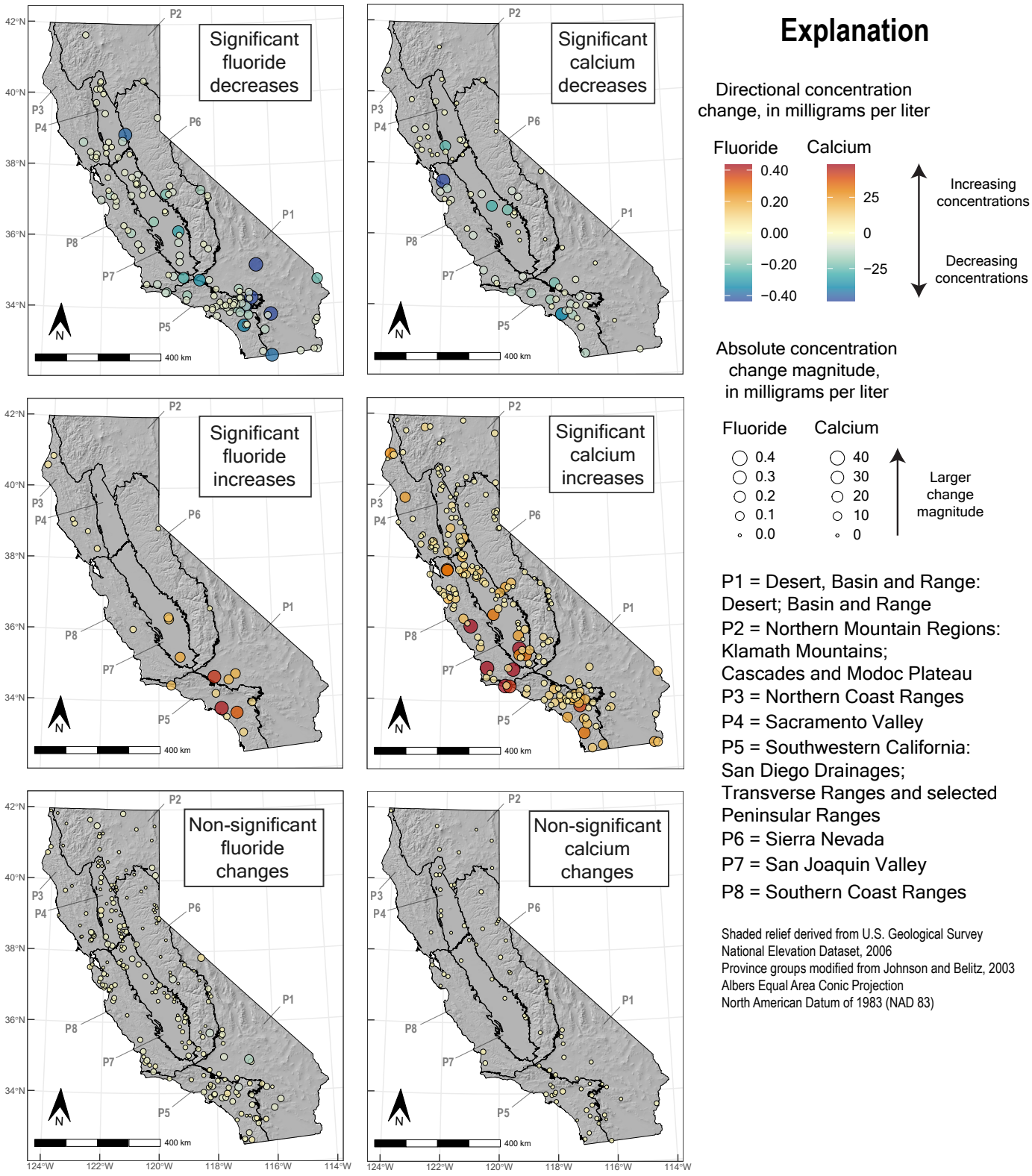

Figure 18. Maps of California showing study sites that had significant decreases (top), significant increases (middle), and non-significant changes (bottom) for decadal comparisons of fluoride (left) and calcium (right). Change significance is indicated for initial and decadal concentration values with non-overlapping confidence intervals. Point sizes and colors are scaled to absolute and directional concentration changes, respectively. Directional differences ranged from -1.28 to 0.42 milligrams per liter for fluoride and -71 to 252 milligrams per liter for calcium. Respective measurement scales for fluoride and calcium were symmetrically saturated at values of ±0.44 milligrams per liter and ±48 milligrams per liter to prevent outliers (less than 2 percent of change values statewide) from obscuring visualization of most change values. Data summarized from Levy and Soldavini (2026).

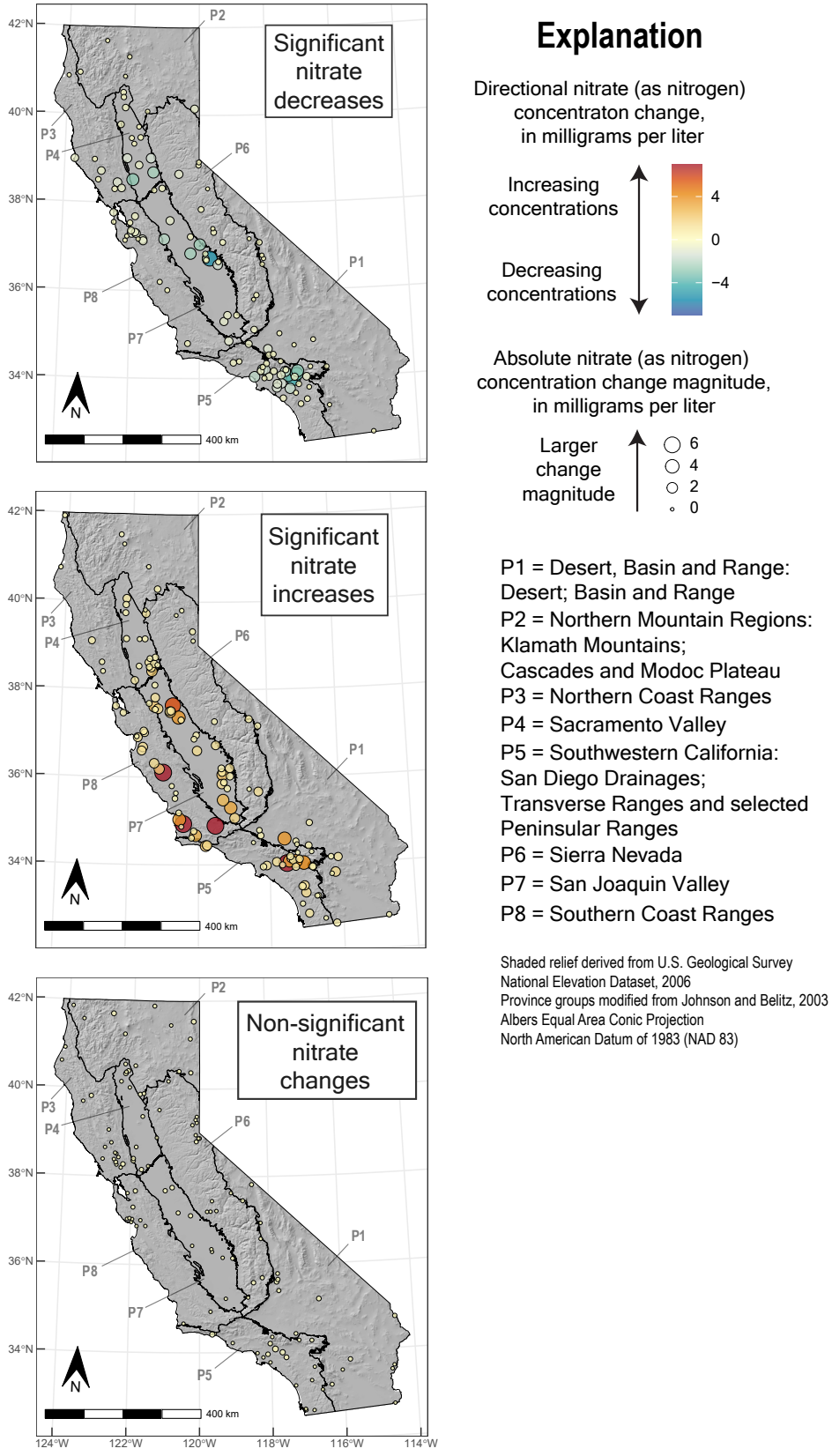

Figure 19. Maps of California showing study sites that had significant decreases (top), significant increases (middle), and non-significant changes (bottom) for decadal comparisons of nitrate. Change significance is indicated for initial and decadal concentration values with non-overlapping confidence intervals. Point sizes and colors are scaled to absolute and directional concentration changes, respectively. Directional differences ranged from -5.2 to 28.5 milligrams per liter as nitrogen, but scales were symmetrically saturated at value of ±7 milligrams per liter as nitrogen to prevent outliers (less than 2 percent of change values statewide) from obscuring visualization of most change values. Data summarized from Levy and Soldavini (2026).

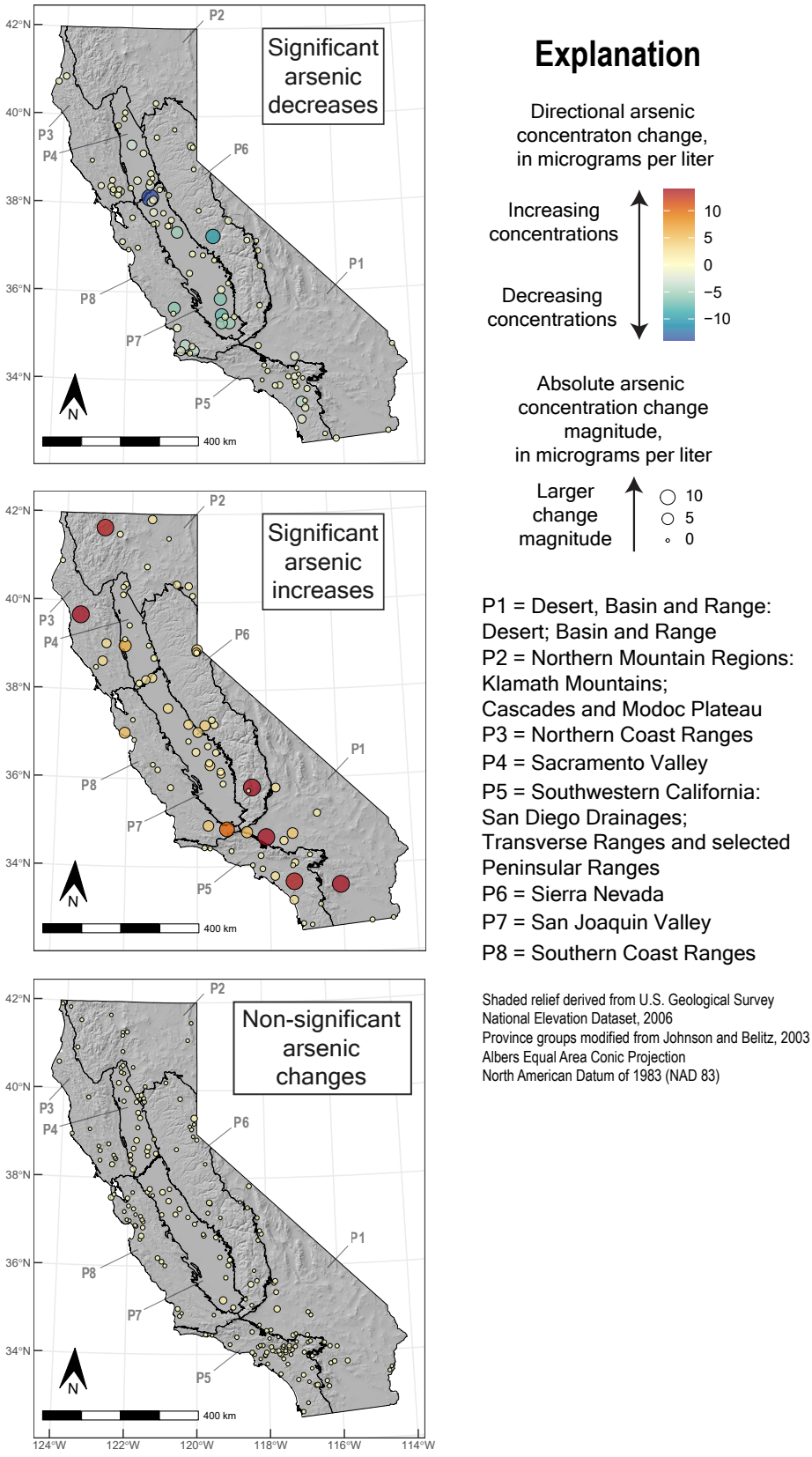

Figure 20. Maps of California showing study sites that had significant decreases (top), significant increases (middle), and non-significant changes (bottom) for decadal comparisons of arsenic. Change significance is indicated for initial and decadal concentration values with non-overlapping confidence intervals. Point sizes and colors are scaled to absolute and directional concentration changes, respectively. Directional differences ranged from -23 to 29 micrograms per liter, but scales were symmetrically saturated at value of ±14 micrograms per liter to prevent outliers (less than 2 percent of change values state-wide) from obscuring visualization of most change values. Data summarized from Levy and Soldavini (2026).

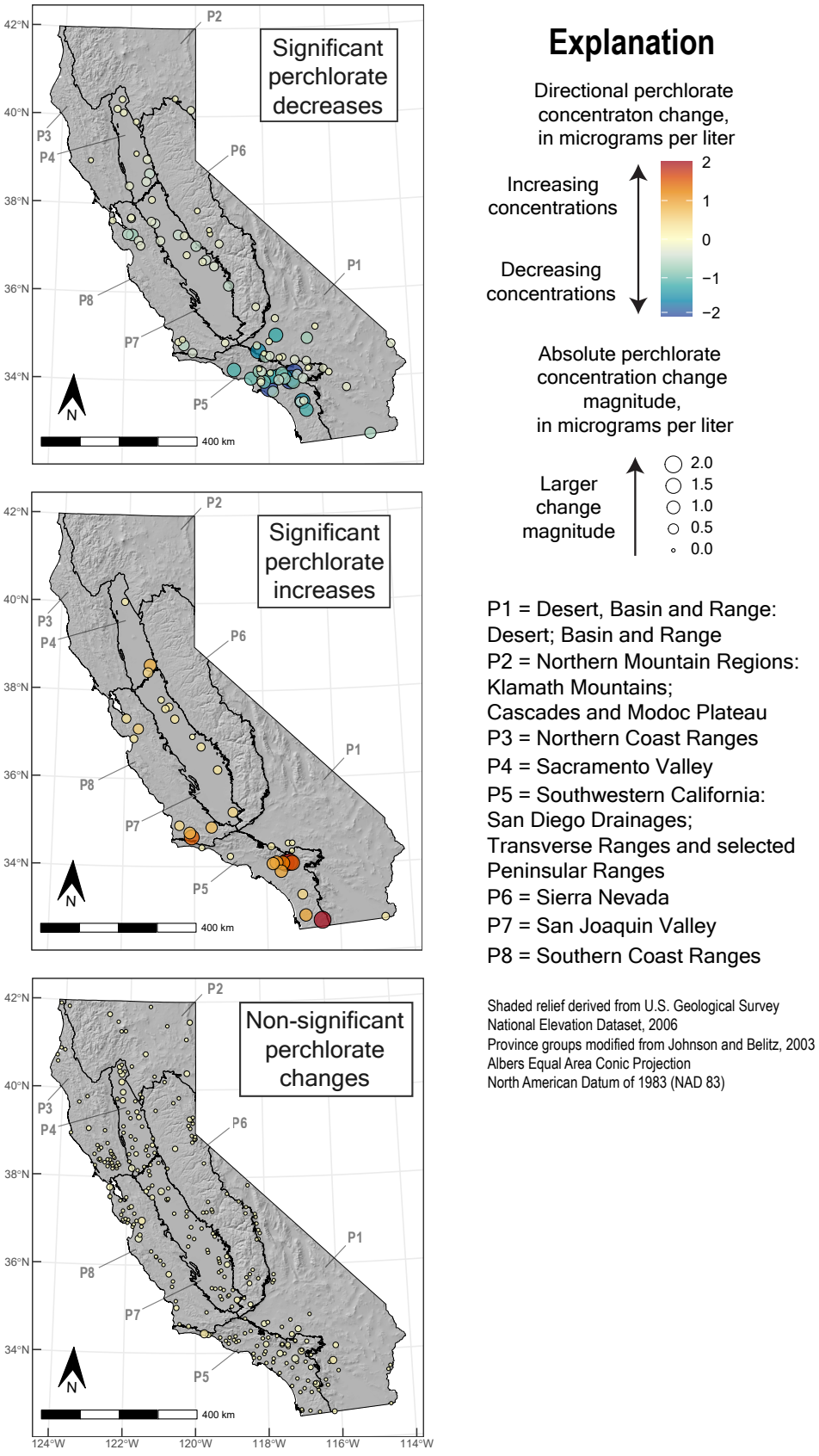

Figure 21. Maps of California showing study sites that had significant decreases (top), significant increases (middle), and non-significant changes (bottom) for decadal comparisons of perchlorate. Change significance is indicated for initial and decadal concentration values with non-overlapping confidence intervals. Point sizes and colors are scaled to absolute and relative concentration changes, respectively. Directional differences ranged from -4.3 to 3.5 micrograms per liter, but scales were symmetrically saturated at value of ±2 micrograms per liter to prevent outliers (less than 2 percent of change values statewide) from obscuring visualization of most change values. Data summarized from Levy and Soldavini (2026).

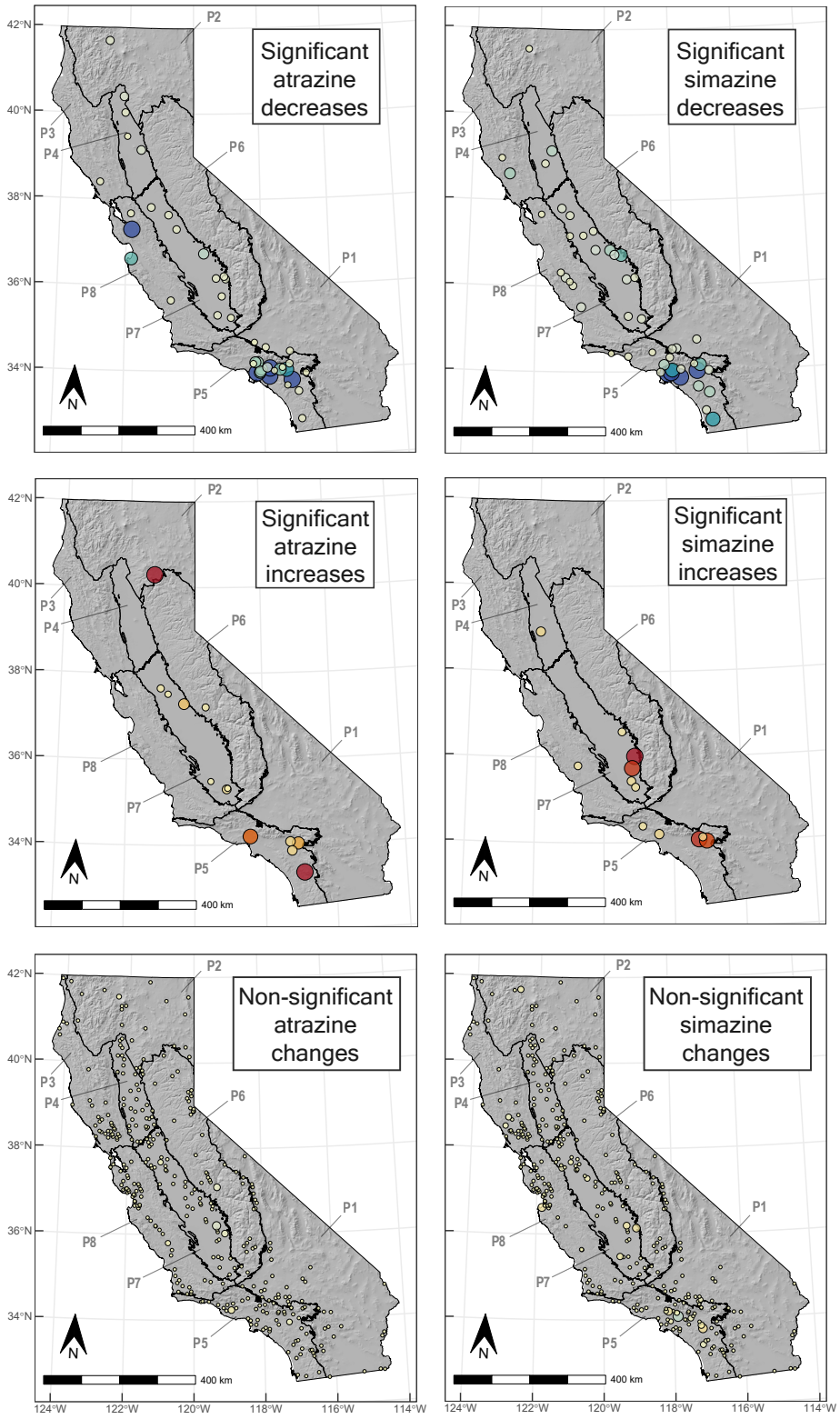

Explanation

Directional herbicide concentration change, in micrograms per liter

Increasing concentrations

Decreasing concentrations

0.02
0.01
0.00
−0.01
−0.02

Absolute herbicide concentration change magnitude, in micrograms per liter

Larger change magnitude

0.02
0.01
0.00

P1 = Desert, Basin and Range: Desert; Basin and Range
P2 = Northern Mountain Regions: Klamath Mountains; Cascades and Modoc Plateau
P3 = Northern Coast Ranges
P4 = Sacramento Valley
P5 = Southwestern California: San Diego Drainages; Transverse Ranges and selected Peninsular Ranges
P6 = Sierra Nevada
P7 = San Joaquin Valley
P8 = Southern Coast Ranges

Shaded relief derived from U.S. Geological Survey National Elevation Dataset, 2006
Province groups modified from Johnson and Belitz, 2003
Albers Equal Area Conic Projection
North American Datum of 1983 (NAD 83)

Figure 22. Maps of California showing study sites that had significant decreases (top), significant increases (middle), and non-significant changes (bottom) for decadal comparisons of atrazine (left) and simazine (right). Change significance is indicated for initial and decadal concentration values with non-overlapping confidence intervals. Point sizes and colors are scaled to absolute and directional concentration changes, respectively. Directional differences ranged from -0.13 to 0.04 micrograms per liter for atrazine and -0.15 to 0.04 micrograms per liter for simazine. Respective measurement scales for both atrazine and simazine were symmetrically saturated at values of ±0.03 micrograms per liter to prevent outliers (less than 2 percent of change values statewide) from obscuring visualization of most change values. Data summarized from Levy and Soldavini (2026).

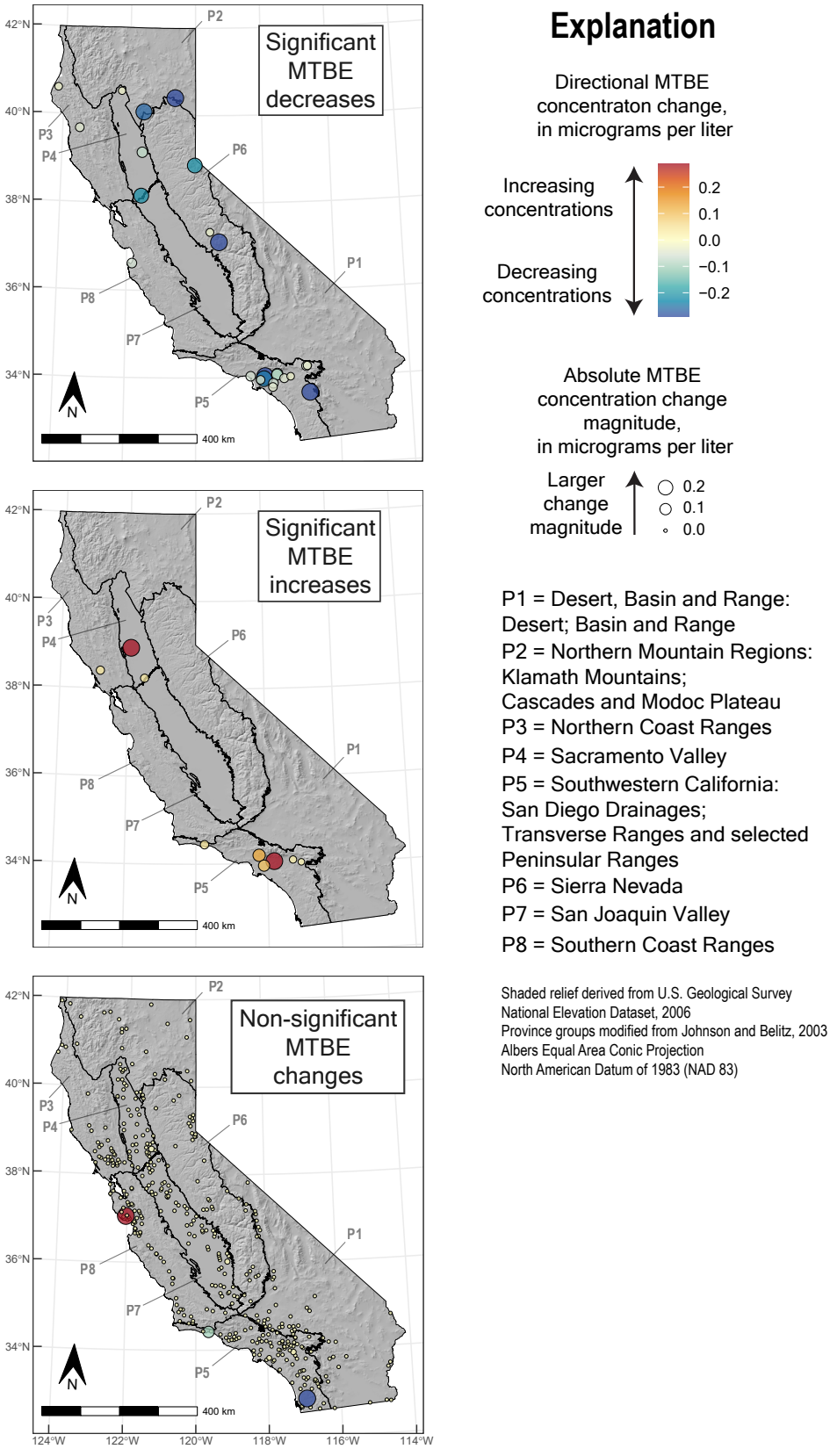

Figure 23. Maps of California showing study sites that had significant decreases (top), significant increases (middle), and non-significant changes (bottom) for decadal comparisons of methyl *tert*-butyl ether (MTBE). Change significance is indicated for initial and decadal concentration values with non-overlapping confidence intervals. Point sizes and colors are scaled to absolute and directional concentration changes, respectively. Directional differences ranged from -3.2 to 2.3 micrograms per liter, but scales were symmetrically saturated at value of ±0.29 micrograms per liter to prevent outliers (less than 2 percent of change values statewide) from obscuring visualization of most change values. Data summarized from Levy and Soldavini (2026).

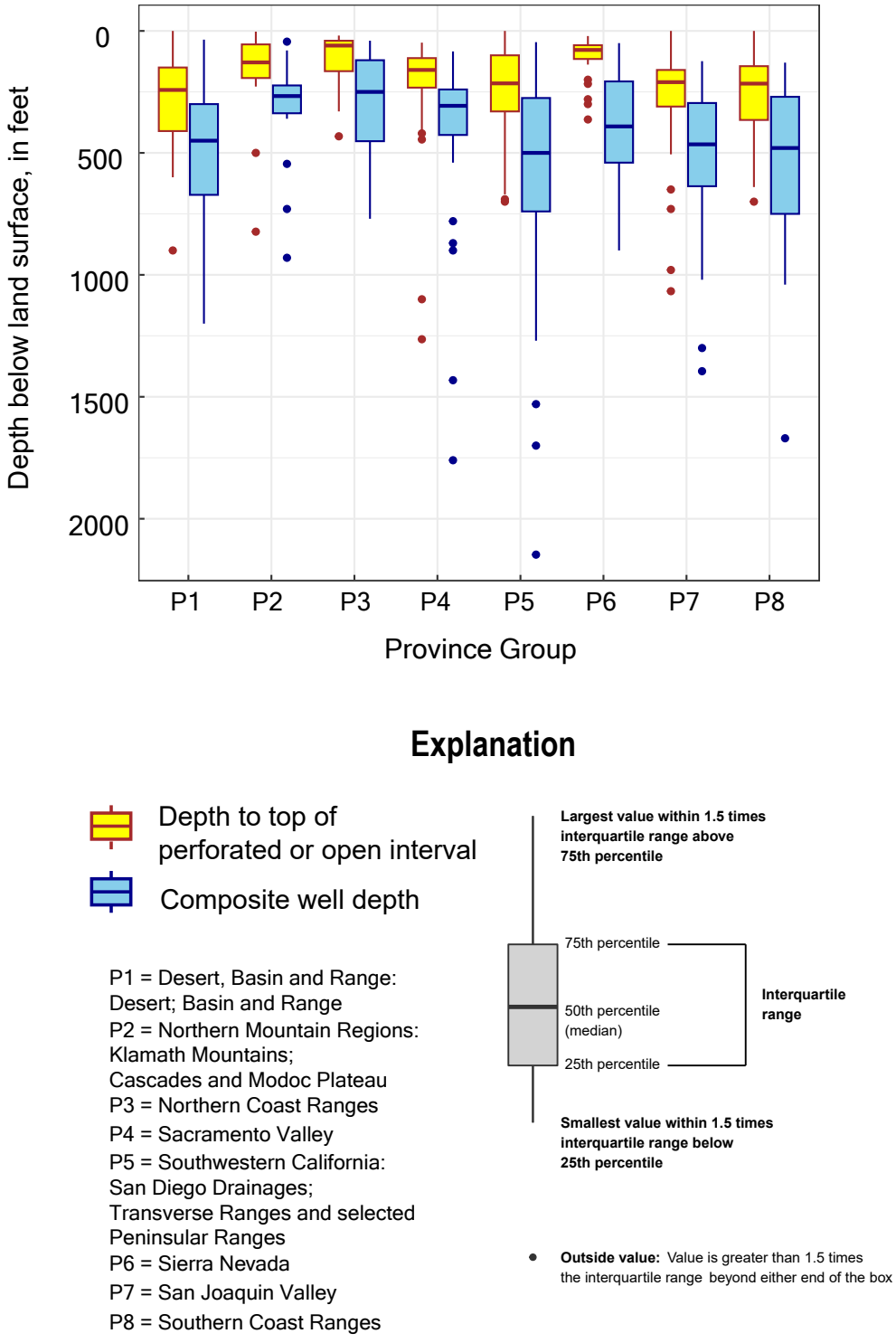

Figure 1.1. Boxplots showing depth to top of the open or perforated interval and composite well depth for public-supply well sites used to analyze decadal trends in this study by province group. Data summarized from Levy and Soldavini (2026).

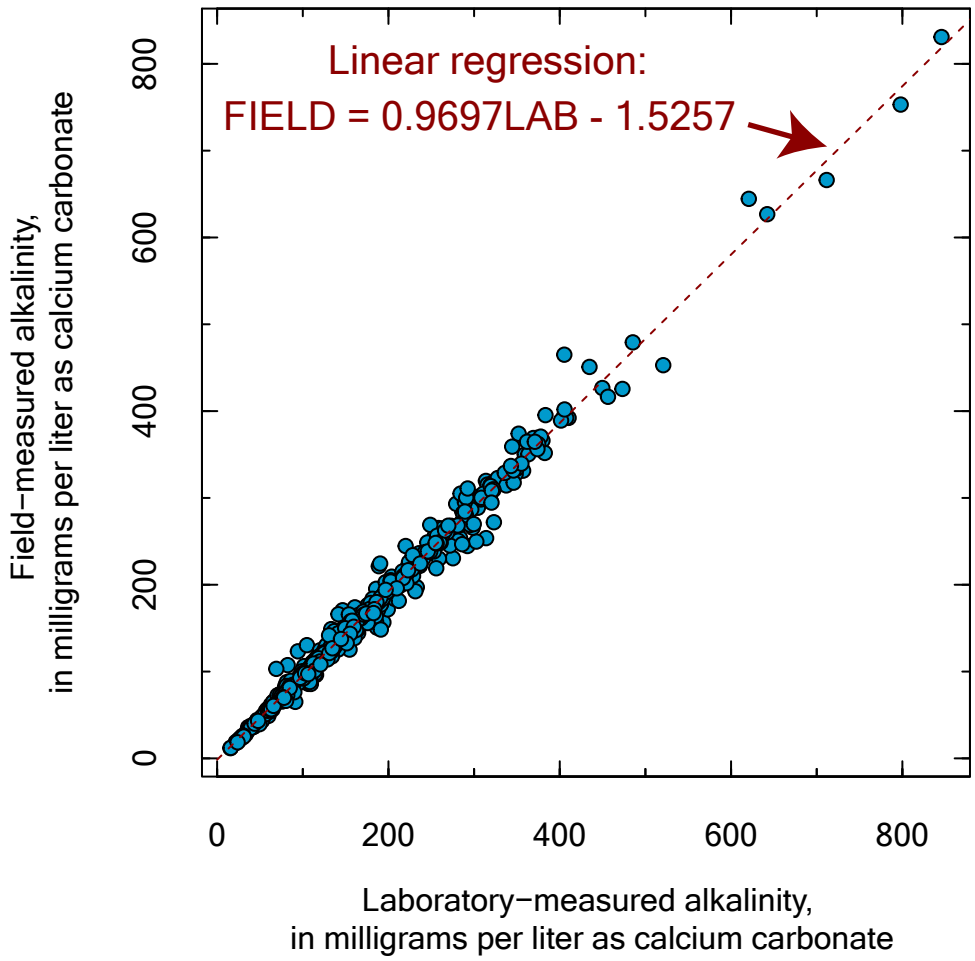

Figure 3.1. Comparison of laboratory to field measured alkalinity values analyzed by the Groundwater Ambient Monitoring and Assessment Program Priority Basin Project (GAMA-PBP) during 2005–2023 with regression line and equation. Data summarized from Levy and Soldavini (2026).

Table 1. Summary of constituents by class and benchmark type used to assess decadal trends in the quality of groundwater used for public drinking-water supply in California, 2004–2023.

[Data summarized from Levy and Soldavini (2026). HBB, health-based benchmark; MCL, maximum contaminant level; SMCL, secondary maximum contaminant level; VOCs, volatile organic compounds]

Constituent Class	Benchmark type			
	MCL	SMCL	HBB	No benchmark
Inorganic constituents and nutrients	12	6	5	10
VOCs	33	0	7	1
Pesticide constituents	3	0	26	34
Geochemical indicators	0	0	0	8

Table 2. Summary of sites used to assess the status of drinking-water quality in aquifers used for public drinking-water supply in California during 2004–2012 compared to those used to assess decadal trends during 2004–2023.

[Data summarized from Belitz and others (2015) and Levy and Soldavini (2026). VOC, volatile organic compounds]

	Status Assessment		Inorganic Constituent Trends			VOC Trends			Pesticide Constituent Trends		
Province Group	Number of sampled sites	Percent of sites in province group compared to total sampled in status assessment	Number of sampled sites	Percent of sites in province group compared to total sampled for inorganic trends	Percent of sites in province group sampled for inorganic trends compared to total sampled in status assessment	Number of sampled sites	Percent of sites in province group compared to total sampled for VOC trends	Percent of sites in province group sampled for VOC trends compared to total sampled in status assessment	Number of sampled sites	Percent of sites in province group compared to total sampled for pesticide trends	Percent of sites in province group sampled for pesticide trends compared to total sampled in status assessment
P1 (Desert, Basin and Range: Desert; Basin and Range)	278	14	46	13	17	55	12	20	52	13	19
P2 (Northern Mountain Regions: Klamath Mountains; Cascades and Modoc Plateau)	126	6	24	7	19	24	5	19	24	6	19
P3 (Northern Coast Ranges)	148	7	30	8	20	37	8	25	35	9	24
P4 (Sacramento Valley)	193	10	41	11	21	47	11	24	39	10	20
P5 (Southwestern California: San Diego Drainages; Transverse Ranges and selected Peninsular Ranges)	448	22	79	22	18	105	24	23	81	20	18
P6 (Sierra Nevada)	200	10	41	11	21	41	9	21	41	10	21
P7 (San Joaquin Valley)	330	16	58	16	18	70	16	21	67	17	20
P8 (Southern Coast Ranges)	284	14	45	12	16	63	14	22	60	15	21
Totals	**2007**		**364**		**18**	**442**		**22**	**399**		**20**

Table 3. Summary of statewide results for water-quality constituents showing at least 10 percent increasing or decreasing values or a significant directional step trend in assessment of decadal trends in the quality of groundwater used for public drinking-water supply in California, 2004–2023.

[Data summarized from Levy and Soldavini (2026). Statistical test significance was evaluated using an alpha value of 0.05. <, less than; n.s., not significant]

Constituent	Number of decadal pairs	Proportion increasing	Proportion decreasing	Proportion unchanging	Wilcoxon signed-rank test p-value	Hodges-Lehmann estimator, as relative concentration[1]	Test result	90th percentile of increases, as relative concentration[1]	90th percentile of absolute decreases, as relative concentration[1]
Inorganic constituents with regulatory benchmarks									
Arsenic	364	0.209	0.266	0.525	0.204	-0.0043	n.s.	0.529	0.372
Barium	365	0.397	0.351	0.252	0.369	0.0006	n.s.	0.043	0.036
Chromium	384	0.167	0.128	0.706	0.161	0.0030	n.s.	0.054	0.050
Fluoride	362	0.061	0.345	0.594	<0.001	-0.0280	decrease	0.157	0.096
Nitrate, as nitrogen	364	0.346	0.324	0.330	0.232	0.0076	n.s.	0.270	0.184
Perchlorate	410	0.085	0.217	0.698	<0.001	-0.0297	decrease	0.245	0.192
Selenium	364	0.176	0.231	0.593	0.191	-0.0003	n.s.	0.038	0.023
Uranium	364	0.473	0.225	0.302	<0.001	0.0092	increase	0.140	0.086
Organic constituents with regulatory benchmarks									
Atrazine	399	0.033	0.108	0.860	<0.001	-0.0029	decrease	0.033	0.028
Methyl *tert* -butyl ether (MTBE)	442	0.020	0.054	0.925	0.005	-0.0041	decrease	0.069	0.028
Simazine	399	0.030	0.115	0.855	<0.001	-0.0009	decrease	0.007	0.005
Trichloromethane (Chloroform)	442	0.179	0.133	0.688	0.115	0.0001	n.s.	0.008	0.017
Inorganic constituents with non-regulatory, health-based benchmarks									
Boron	365	0.384	0.197	0.419	<0.001	0.0020	increase	0.027	0.037
Molybdenum	364	0.245	0.368	0.387	0.004	-0.0038	decrease	0.107	0.079
Strontium	364	0.580	0.187	0.234	<0.001	0.0082	increase	0.064	0.043
Vanadium	364	0.327	0.223	0.451	0.007	0.0008	increase	0.010	0.013
Inorganic constituents with non-regulatory, aesthetic-based benchmarks									
Chloride	365	0.589	0.271	0.140	<0.001	0.0042	increase	0.063	0.052
Iron	375	0.229	0.093	0.677	<0.001	0.0727	increase	1.174	0.907
Manganese	363	0.303	0.204	0.493	0.007	0.0178	increase	1.977	1.098
Sulfate	364	0.588	0.308	0.104	<0.001	0.0036	increase	0.073	0.065
Total dissolved solids (TDS)	364	0.261	0.190	0.549	0.027	0.0178	increase	0.213	0.142

[1] Benchmarks used to compute relative concentrations (in other words, computed concentration change divided by the benchmark) are available in the data release of Levy and Soldavini (2026).

Table 4. Summary of statewide results for geochemical indicators used to assess drivers of decadal trends in the quality of groundwater used for public drinking-water supply in California, 2004–2023.

[Data summarized from Levy and Soldavini (2026). Statistical test significance was evaluated using an alpha value of 0.05. $\delta^{13}C$, carbon-13; $\delta^{18}O$, oxygen-18; <, less than; deuterium excess, d-excess; n.s., not significant]

Constituent	Measurement units	Number of decadal pairs	Proportion increasing	Proportion decreasing	Proportion unchanging	Wilcoxon signed-rank test p-value	Hodges-Lehmann estimator, in measurement units	Test result
Geochemical conditions								
Dissolved oxygen	milligrams per	405	0.279	0.343	0.378	0.021	-0.33	decrease
pH	standard units	370	0.030	0.049	0.922	0.256	-0.01	n.s
Groundwater source and age								
$\delta^{18}O$	per mille	424	0.271	0.184	0.545	0.006	0.07	increase
d-excess	per mille	424	0.050	0.090	0.861	0.019	-0.6	decrease
Carbon-14	percent modern carbon	306	0.296	0.272	0.432	0.433	0.5	n.s.
Salinity indicators								
$\delta^{13}C$	per mille	306	0.157	0.271	0.572	0.005	-0.2	decrease
Alkalinity	milligrams per liter as calcium carbonate	367	0.360	0.180	0.460	<0.001	10	increase
Calcium	milligrams per	364	0.569	0.212	0.220	<0.001	3	increase

Table 5. Summary of water-quality constituents with regulatory maximum contaminant level (MCL) benchmarks showing significant directional or high-magnitude decadal changes in aquifers used for public drinking-water supply statewide and in land-use and province-based network groups, California, 2004–2023.

[Data summarized from Levy and Soldavini (2026). Constituents displayed in red and blue fonts show significant increases and decreases in respective step-trend categories. Statistical test significance was evaluated using an alpha value of 0.05. n.s., not significant; MTBE; methyl *tert* -butyl ether; PCE, tetrachloroethene; TCE, trichloroethene]

Network group	Directional increases	Directional decreases	High-magnitude increases	High magnitude decreases	Directional and high-magnitude increases	Directional and high-magnitude decreases
Statewide	Uranium	Fluoride, perchlorate, atrazine, simazine	Arsenic, nitrate, uranium	Arsenic, nitrate, perchlorate	Uranium	Perchlorate
Land-use groups						
Agricultural	Uranium	Fluoride, perchlorate, atrazine	Arsenic, nitrate, uranium	Arsenic, nitrate, uranium	Uranium	Perchlorate
Urban	Uranium, chloroform, bromodichloromethane	Fluoride, perchlorate, atrazine, simazine, MTBE	Arsenic, nitrate, uranium, perchlorate	Arsenic, nitrate, fluoride, perchlorate, PCE	Uranium	Fluoride, perchlorate
Natural	Chromium, uranium	Fluoride, perchlorate	Arsenic, nitrate, uranium	Arsenic, fluoride, perchlorate	Uranium	Fluoride, perchlorate
Province groups						
P1 (Desert, Basin and Range: Desert; Basin and Range)	Uranium	Fluoride, perchlorate	Arsenic, nitrate, fluoride, uranium	Perchlorate, fluoride	Uranium	Fluoride, perchlorate
P2 (Northern Mountain Regions: Klamath Mountains; Cascades and Modoc Plateau)	Arsenic, barium, uranium	n.s.	Arsenic	n.s.	Arsenic	n.s.
P3 (Northern Coast Ranges)	n.s.	Selenium	Arsenic, barium, boron, chloride, iron, manganese, TDS	Arsenic	n.s.	n.s.
P4 (Sacramento Valley)	Uranium	Fluoride	Arsenic, uranium	Arsenic, nitrate	Uranium	n.s.
P5 (Southwestern California: San Diego Drainages; Transverse Ranges and selected Peninsular Ranges)	Uranium	Fluoride, perchlorate, atrazine, simazine	Arsenic, nitrate, perchlorate, uranium, PCE	Arsenic, nitrate, perchlorate, fluoride, uranium, PCE, TCE	Uranium	Fluoride, perchlorate
P6 (Sierra Nevada)	n.s.	Fluoride	Arsenic, uranium	Arsenic, fluoride	n.s.	Fluoride
P7 (San Joaquin Valley)	Barium, nitrate, uranium, chloroform	Fluoride	Arsenic, nitrate, uranium, PCE	Arsenic, nitrate	Nitrate, uranium	n.s.
P8 (Southern Coast Ranges)	n.s.	Fluoride	Arsenic, cadmium, chromium, nitrate, perchlorate, selenium	Arsenic, nitrate, chloroform	n.s.	n.s.

Table 6. Summary of water-quality constituents with non-regulatory benchmarks showing significant directional or high-magnitude decadal changes in aquifers used for public drinking-water supply statewide and in land-use and province-based network groups, California, 2004–2023.

[Data summarized from Levy and Soldavini (2026). Constituents displayed in red and blue fonts show significant increases and decreases in respective step-trend categories. Statistical test significance was evaluated using an alpha value of 0.05. n.s., not significant; TDS, total dissolved solids]

Network group	Directional increases	Directional decreases	High-magnitude increases	High magnitude decreases	Directional and high-magnitude increases	Directional and high-magnitude decreases
Statewide	Boron, strontium, vanadium, chloride, iron, manganese, sulfate, TDS	Molybdenum	Molybdenum, iron, manganese, TDS	Manganese, TDS	Iron, manganese, TDS	n.s.
Land-use groups						
Agricultural	Strontium, chloride, iron, manganese, sulfate, TDS	n.s.	Iron, manganese, TDS	Iron, manganese, TDS	Iron, manganese, TDS	n.s.
Urban	Boron, strontium, chloride, iron, sulfate	Molybdenum	Iron, manganese, TDS	Manganese, TDS	Iron	n.s.
Natural	Boron, strontium, vanadium, chloride, iron, sulfate	n.s.	Molybdenum, iron, manganese, TDS	Molybdenum, iron, manganese	Iron	n.s.
Province groups						
P1 (Desert, Basin and Range: Desert; Basin and Range)	Boron, strontium, sulfate	n.s.	Molybdenum, iron, manganese, TDS	Iron, manganese	n.s.	n.s.
P2 (Northern Mountain Regions: Klamath Mountains; Cascades and Modoc Plateau)	Arsenic, barium, uranium, boron, strontium	n.s.	Iron, manganese	Manganese	n.s.	n.s.
P3 (Northern Coast Ranges)	Strontium, chloride	n.s.	Boron, chloride, iron, manganese, TDS	Iron, manganese	Chloride	n.s.
P4 (Sacramento Valley)	Strontium, vanadium	n.s.	Manganese	Manganese, TDS	n.s.	n.s.
P5 (Southwestern California: San Diego Drainages; Transverse Ranges and selected Peninsular Ranges)	Boron, strontium, chloride, iron	n.s.	Chloride, iron, manganese, TDS	Manganese, TDS	Chloride, iron	n.s.
P6 (Sierra Nevada)	Strontium, sulfate	n.s.	Molybdenum, iron, manganese	Boron, molybdenum, manganese	n.s.	n.s.
P7 (San Joaquin Valley)	Strontium, chloride, manganese, sulfate, TDS	Molybdenum	Iron, manganese, TDS	Iron, TDS	Manganese, TDS	n.s.
P8 (Southern Coast Ranges)	Chloride	Molybdenum	Molybdenum, chloride, iron, manganese, sulfate, TDS	Molybdenum, chloride, iron, manganese, sulfate, TDS	Chloride	Molybdenum

Table 7. Summary of geochemical indicators showing significant directional decadal changes in aquifers used for public drinking-water supply statewide and in land-use and province-based network groups, California, 2004–2023.

[Data summarized from Levy and Soldavini (2026). Constituents displayed in red and blue fonts show significant increases and decreases in respective step-trend categories. Statistical test significance was evaluated using an alpha value of 0.05. $\delta^{13}C$, carbon-13; $\delta^{18}O$, oxygen-18; d-excess, deuterium excess; DO, dissolved oxygen; n.s., not significant]

Network group	Directional increases	Directional decreases
Statewide	$\delta^{18}O$, alkalinity, calcium	$\delta^{13}C$, d-excess, DO
Land-use groups		
Agricultural	Alkalinity, calcium	$\delta^{13}C$, d-excess
Urban	Alkalinity, carbon-14, calcium	DO
Natural	Calcium	n.s.
Province groups		
P1 (Desert, Basin and Range: Desert; Basin and Range)	Alkalinity, calcium	n.s.
P2 (Northern Mountain Regions: Klamath Mountains; Cascades and Modoc Plateau)	Calcium	n.s.
P3 (Northern Coast Ranges)	$\delta^{18}O$	n.s.
P4 (Sacramento Valley)	Alkalinity, calcium	$\delta^{13}C$
P5 (Southwestern California: San Diego Drainages; Transverse Ranges and selected Peninsular Ranges)	Calcium	n.s.
P6 (Sierra Nevada)	Calcium	DO
P7 (San Joaquin Valley)	Alkalinity, carbon-14, calcium	d-excess
P8 (Southern Coast Ranges)	$\delta^{18}O$, calcium	$\delta^{13}C$, d-excess

Table 8. Summary of groundwater age classifications based on tritium for initial compared to decadal sample pairs used to evaluate groundwater resources used for public drinking-water supply in California, 2004–2023.

[Data summarized from Levy and Soldavini (2026). Numbers displayed in blue font indicate decadal sample pairs with older groundwater ages. Numbers displayed in red font indicate decadal sample pairs with younger groundwater ages. Age classifications are consistent with those defined by Lindsey and others (2019).]

		Decadal		
		Premodern	**Mixed**	**Modern**
Initial	**Premodern**	59	33	1
	Mixed	18	117	32
	Modern	0	12	131